

Chapter 12**METEOROLOGY-CHEMISTRY INTERFACE PROCESSOR (MCIP) FOR
MODELS-3 COMMUNITY MULTISCALE AIR QUALITY (CMAQ) MODELING
SYSTEM****Daewon W. Byun* and Jonathan E. Pleim****Atmospheric Modeling Division
National Exposure Research Laboratory
U.S. Environmental Protection Agency
Research Triangle Park, NC 27711**Ruen Tai Tang**Dyntel Corporation
Research Triangle Park, NC 27711**Al Bourgeois**Lockheed Martin/U.S. EPA Scientific Visualization Center
Research Triangle Park, NC 27711**ABSTRACT**

The Meteorology-Chemistry Interface Processor (MCIP) links meteorological models such as MM5 with the Chemical Transport Model (CTM) of the Models-3 Community Multiscale Air Quality (CMAQ) modeling system to provide a complete set of meteorological data needed for air quality simulations. Because most meteorological models are not built for air quality modeling purpose, MCIP deals with issues related to data format translation, conversion of units of parameters, diagnostic estimations of parameters not provided, extraction of data for appropriate window domains, and reconstruction of meteorological data on different grid and layer structures. To support the multiscale generalized coordinate implementation of the CMAQ CTM, MCIP provides appropriate dynamic meteorological parameters to allow mass-consistent air quality computations. The current implementation of MCIP links MM5 meteorological data to CMAQ CTM. Because its code has a streamlined modular computational structure, adapting the system to other inputs only require inclusion of a reader module and coordinate related routines specific for the meteorological model.

* On assignment from the National Oceanic and Atmospheric Administration, U.S. Department of Commerce.
Corresponding author address: Daewon W. Byun, MD-80, Research Triangle Park, NC 27711. E-mail:
bdx@hpcc.epa.gov

** On assignment from the National Oceanic and Atmospheric Administration, U.S. Department of Commerce.

12.0 METEOROLOGY-CHEMISTRY INTERFACE PROCESSOR (MCIP) FOR MODELS-3 COMMUNITY MULTISCALE AIR QUALITY (CMAQ) MODELING SYSTEM

12.1 Introduction

Models-3 Community Multiscale Air Quality (CMAQ) modeling system is a next generation modeling system designed to handle research and application issues for multiscale (urban and regional) and multi-pollutant (oxidants, acid deposition, and particulates) air quality problems. Its Chemical Transport Model (CTM) uses a generalized coordinate system. To accommodate meteorological inputs from a variety of meteorological models using different coordinate systems, CMAQ CTM (CCTM) requires information about the coordinates and grid as well as the meteorological data. The Meteorology-Chemistry Interface Processor (MCIP) links a meteorological model with CCTM to provide a complete set of meteorological data needed for air quality simulation. Because most meteorological models are not built for air quality modeling purposes, MCIP takes care of many issues related to data format translation, conversion of units of parameters, diagnostic estimations of parameters not provided, extraction of data for appropriate window domains, and reconstruction of meteorological data on different horizontal and vertical grid resolutions through interpolations as needed. Considering these functions, it is not difficult to see that MCIP is a key processor in the Models-3 CMAQ system.

In the Models-3 CMAQ system, the role of MCIP is further expanded to enforce consistency among the meteorological variables. The consistency among meteorological parameters and the way they are utilized in a CTM greatly influence the success of air quality simulations. This issue becomes a dominant concern for the CCTM, which uses a generalized coordinate system, because it should be able to deal with data from different meteorological models that may or may not use fully compressible formulations (or assumptions on the atmospheric dynamics such as hydrostatic or nonhydrostatic approximation). Chapters 5 and 6 of this science document provide detailed descriptions on the generalized coordinate system.

CMAQ's MCIP provides similar functions as the meteorological preprocessor for Regional Acid Deposition Model (RADM) (Chang et al., 1987, 1990). MCIP's code has a streamlined computational structure, incorporating many of the physical and dynamical algorithms necessary to prepare meteorological inputs used by CMAQ. Some of the planetary boundary layer (PBL) parameterizations are extensively updated subroutines of the RADM's meteorological preprocessor which was described in Byun and Dennis (1995). MCIP is highly modularized to accommodate data from different meteorological models. This versatility is accomplished by allowing incorporation of a different set of input modules for a specific meteorological model. At present, two sets of input modules are available. One links to the output of Pennsylvania State University/National Center for Atmospheric Research (PSU/NCAR) Mesoscale Modeling System Generation 5 (MM5) with CCTM and the other links to meteorological data already in the Models-3 input/output applications programming interface (I/O API) format. MM5 can be run either in hydrostatic mode using a time dependent terrain-following hydrostatic pressure coordinate, or in nonhydrostatic mode using a time independent terrain-following reference pressure coordinate. For the details on how MM5 simulations are conducted and how the reference state is determined, refer to Seaman et al. (1995), Seaman and Stauffer (1993), Dudhia (1993), Grell et al. (1994), Stauffer and Seaman (1993), Tesche and McNally (1993), and Haagensohn et al. (1994). To

characterize past atmospheric conditions properly, MM5 is usually run with Four Dimensional Data Assimilation (FDDA) for air quality simulations. It incorporates the results of intensive meteorological observations into the model simulations so that the uncertainties associated with meteorological input for a CTM are minimized (Stauffer and Seaman, 1993; Seaman et al., 1995). Different output data generated by the different options, such as dynamics cloud parameterization and surface-PBL algorithms used for the operation of MM5 operation, can be handled by MCIP accordingly.

This chapter provides a detailed description of the functions and data flow of MCIP and formulations used for estimating parameters diagnostically. Although this chapter mainly describes the current implementation of MCIP written for MM5, it also provides key information necessary to build different MCIP versions for other meteorological models. It is hoped that developers of different MCIP versions can concentrate their efforts to read in data files from different meteorological models with minimal modifications for diagnostic routines and output processes. Section 12-1 describes basic functions and data dependency of MCIP. Section 12-2 deals with meteorological data types, coordinates, and grids. Section 12-3 contains descriptions of diagnostic algorithms used for estimating parameters necessary for air quality simulation and Section 12-4 describes additional parameters needed for the generalized coordinate system. Section 12-5 provides key operational details, such as building and executing MCIP including how to set up grids/domains and environmental variables for different runtime options. Refer to Figure 12-1 for the structure of the contents of the present chapter.

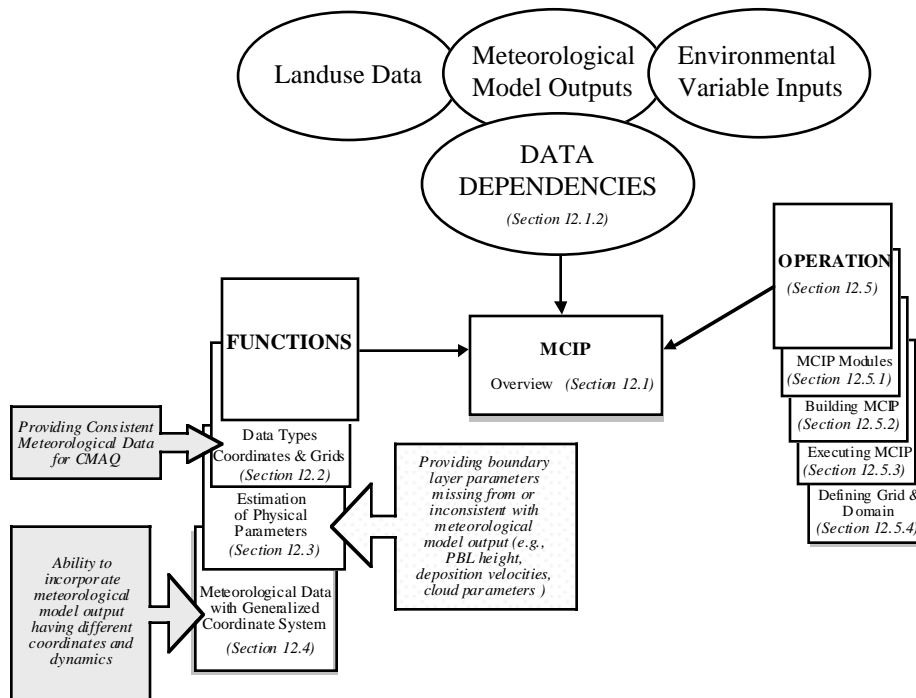


Figure 12-1. Contents and Structure of Chapter 12

12.1.1.1 MCIP Functions

One of MCIP's functions is to translate meteorological parameters from the output of a mesoscale model (e.g., MM5) to the Models-3 I/O API format (Coats, 1996), which is required for operations of Models-3 CMAQ processors. Some other necessary parameters not available from the meteorological model are estimated with appropriate diagnostic algorithms in the program. The key functions of MCIP are summarized below.

Reading in meteorological model output files:

The EPA-enhanced MM5 version (Pleim et al., 1997) generates not only the standard MM5 output but also several additional files that contain detailed PBL, cloud, and surface parameters. MCIP reads these files and stores the information in the memory for further processing. Essential header information is passed to the Models-3 I/O API file header.

Extraction of meteorological data for CTM window domain:

In general, the CCTM uses a smaller computational domain than MM5. Also, MM5 predictions in the cells near the boundary may not be adequate for use in air quality simulation. Therefore, MCIP extracts only the portion of the MM5 output data which falls within the CCTM's main domain and boundary cells.

Interpolation of coarse meteorological model output for finer grid:

When user requests meteorological data on a finer resolution grid than that simulated in the meteorological model, MCIP interpolates profile data using simple bilinear interpolation.

Collapsing of meteorological profile data if coarse vertical resolution data is requested:

MCIP performs a mass-weighted averaging of data in the vertical direction. For example, 30-layer meteorological data may be lumped into 15 layers, or 6 layers for the CCTM.

Computation or passing through surface and PBL parameters:

Depending on the user options, MCIP either passes through surface and PBL parameters simulated by the meteorology model directly or diagnoses them using the mean wind, temperature, and humidity profiles, surface data, and detailed landuse information available.

Diagnosing of cloud parameters:

When important parameters needed for processing cloud effects in the CCTM are not provided by the meteorological model, MCIP diagnoses cloud information (i.e., cloud top, base, liquid water content, and coverage) using a simple convective parameterization. The information can be used in the CCTM to process aqueous-phase chemistry and cloud mixing as well as to modulate photolysis rates that reflect the effects of cloud.

Computation of species-specific dry deposition velocities:

MCIP computes dry deposition velocities for important gaseous species using either diagnosed PBL parameters or the surface/PBL information passed through from the meteorological model.

Generation of coordinate dependent meteorological data for the generalized coordinate CCTM simulation:

Many of the coordinate-related functions traditionally treated in a CTM have been incorporated as a part of the MCIP functions. This change was necessary to maintain modularity of the CCTM regardless of the coordinates used and to eliminate many coordinate-dependent processor modules in the CCTM. By incorporating dynamically consistent interpolation methods and associated subroutines in the CCTM, the dynamic and thermodynamic consistencies among the meteorological data can be maintained even after the temporal interpolations.

Output meteorological data in Models-3 I/O API format:

MCIP writes the bulk of its two- and three-dimensional meteorological and geophysical output data in a transportable binary format using the Models-3 input/output applications program interface (I/O API) library.

12.1.2 MCIP's Data Dependency

MCIP processes meteorological model output files in order to provide environmental data needed for the other computational subsystems in Models-3 CMAQ. Landuse data is also required to generate additional meteorological information needed for air quality simulations. MCIP utilizes this and profiles of temperature, moisture, and wind components to estimate parameters for the turbulence and surface exchange characteristics. When the meteorological model computes all the necessary information, it can be passed through the MCIP as well. The inputs for MCIP consist of operational inputs and meteorological model output files. These inputs are described below.

12.1.2.1 Environmental Variable Inputs

The user can select a computational path among the internal process options and define parameters in MCIP output files by specifying several UNIX environmental variables. These settings allow MCIP to be configured to fit a particular meteorological model simulation and to follow process steps requested by the user. First, it defines the mode of meteorological model run to check if the meteorology data linked have been generated using options compatible with the MCIP. Then it assigns filenames of meteorology model output files, defines CTM model window domain offset coordinates in terms of the meteorological model grid definition, determines simulation time and duration of the MCIP, and assigns appropriate landuse data file type. Refer to Section 12-5 and Table 12-10 for the details of the UNIX environmental variables used in MCIP for these settings.

12.1.2.2 Meteorology Model Outputs

It is anticipated that MCIP will include a unique set of reader modules for a variety of meteorological models. Most of the idiosyncrasies of meteorological data from a specific meteorological model should be resolved in this module. They include the number of files, information on the data such as where they are stored and in what format, etc. In the following, we provide a description of the output files from MM5 as an example.

Standard MM5 output

The standard MM5 time-stepped grid-domain output contains most of the key meteorological data written by the MM5 subroutine OUTTAP. Each time-step includes a header record. This header is read by MCIP at each time-step, but only the header from the first time-step is used and the subsequent headers are ignored. Data following each header consist of two- and three-dimensional arrays. The time-step interval for the meteorological data is taken from the header record on the first time-step.

EPA-added MM5 output

EPA and MCNC added two more output files for additional information to facilitate air quality modeling. One includes additional two-dimensional boundary layer parameters and flux values and the other contains the detailed Kain-Fritsch (Kain and Fritsch, 1993) cloud data file, which describes locations and cloud lifetimes of convective clouds. Currently, only the first file is used to process CMAQ dry deposition module options and the second file is not actively used because

the CCTM does not yet support a corresponding aqueous-phase Kain-Fritsch cloud mixing module.

12.1.2.3 Landuse Data

MCIP requires landuse data that define surface characteristics in order to compute dry deposition velocities and other PBL parameters. Depending on the PBL and dry deposition modules desired, the needs for landuse data vary. The RADM dry deposition algorithm (Wesely, 1989) needs 11-category fractional landuse data. On the other hand, the new CMAQ deposition algorithm requires cell-averaged parameters defining surface exchange characteristics (i.e., landuse dependent parameters). The latter algorithm assumes that the landuse dependent subgrid effects are processed in the meteorology modeling system. To avoid incorrect averaging of the land-surface parameters, it distinguishes a dominant water cell from other landuse types.

Table 12-1. Relations Among MM5, CMAQ/RADM, and USGS Landuse Categories

MM5	MM5 Category	MCIP	CMAQ/RADM Category	USGS	USGS Category
1	Urban Land	1	Urban Land	1	Urban/built up
2	Agriculture Land	2	Agriculture	2	Dry cropland & pasture
				3	Irrigated cropland & pasture
				4	Mixed dryland/irrigated pasture
3	Range-Grassland	3	Range	7	Grassland
				8	Shrubland
				9	Mixed shrubland/grassland
				10	Chaparral
4	Deciduous Forest	4	Deciduous Forest	12	Broadleaf deciduous forest
				16	Deciduous coniferous forest
5	Coniferous Forest	5	Coniferous Forest	13	Evergreen coniferous forest
				14	Sub alpine forest
				17	Evergreen broadleaf
6	Mixed Forest/Wet Land	6	Mixed Forest and Wet Land	6	Woodland/cropland mosaic
				15	Mixed forest
7	Water	7	Water	18	Water
8	Marsh or Wet Land	9	Nonforest Wet Land	19	Herbaceous
				20	Forested wetlands
9	Desert	11	Rock, Open Shrub	21	Barren or sparsely vegetated
10	Tundra	8	Barren Land	22	Shrub & brush tundra
				23	Herbaceous tundra
				24	Bare ground tundra
				25	Wet tundra
				26	mixed tundra
11	Permanent Ice	7	Water	27	Perennial snowfields or glaciers
12	Tropical Forest	3*	Range*		
13	Savannah	3	Range	11	Savannah
None		10	Mixed Agriculture/Range Land	5	Grassland/cropland mosaic

* Mapping "Tropical Forest" to "Range" is not appropriate in most locations.

Currently, MCIP accepts four different types of landuse data. Two types of landuse input (one from MM5 directly, or the other from TERRAIN, a preprocessor for MM5 system) contain 13-category data. The third one is a preprocessed landuse data set in an ASCII file. Recently, we added a landuse processor (LUPROC) for the USGS vegetation information (described below) to improve landuse data quality. For the case of MM5, the percentages of MM5's 13 landuse category are transformed into the CMAQ/RADM's 11-category fractions in the landuse reader module. The USGS vegetation category is also transformed into the 11-category fractions. Table 12-1 provides the conversion rules for landuse types from MM5 13-category, and USGS 27 (http://edcwww.cr.usgs.gov/landdaac/glcc/nadoc1_1.html) category to CMAQ/RADM's 11-category. The USGS North America land cover characteristics data base has 1-km nominal spatial resolution and is based on 1-km AVHRR data spanning April 1992 through March 1993. This data base has been adapted to the CMAQ's base map projection which uses Lambert conformal projection with origins at latitude 40° N and longitude 90° W.

Landuse Processor (LUPROC)

CMAQ's Landuse Processor (LUPROC) is a special processor that provides a high-resolution landuse data base for the system. MCIP requires landuse data that define surface characteristics to compute dry deposition and other PBL parameters. Depending on the PBL and dry deposition modules desired, the needs for the landuse data are somewhat different.

LUPROC windows out the landuse data for the user-defined domain and converts percentages of 27 vegetation categories in the database into the fractional landuse data in RADM's 11-category. The output of the LUPROC should have the same resolution as the CCTM domain and the LUPROC domain should include the boundary cells in addition to the CCTM's computational domain. In the near future, MM5 will be upgraded to allow use of the USGS land cover characteristic data as an option. When the CMAQ dry deposition algorithm is used and necessary PBL parameters are provided by the MM5 directly, LUPROC will not be needed.

12.1.3 Computational Structure

The MCIP data flow diagram, Figure 12-2, shows the key processing sequences. First, MCIP executes the one-time processes such as: reading the header, processing other operational information for the meteorological output, reading appropriate landuse data, and generating time independent MCIP output files. Then, MCIP loops through the time stepped (hourly or sub-hourly depending on the meteorology data) input data from a meteorology model performing the functions described above. The processing sequence of MCIP is summarized below:

- GETMET: reads and extracts meteorology data from standard MM5 output for the CCTM window domain, converts variables into SI units and process special files (e.g., two-dimensional surface/PBL data and Kain-Fritsch cloud files);
- PBLPKG/PBLSUB: computes PBL parameters using diagnostic method if desired;
- BCLDPRC_AK: computes diagnostic convective cloud parameters if needed;
- SOLAR: computes solar radiation parameters;
- RADMDRY/M3DDEP: computes dry deposition velocities; and

- METCRO_OUT & METDOT_OUT: computes additional meteorology data required for the generalized CTM, interpolates mean profile data into finer grid resolution if needed, and output Models-3 I/O API meteorology files.

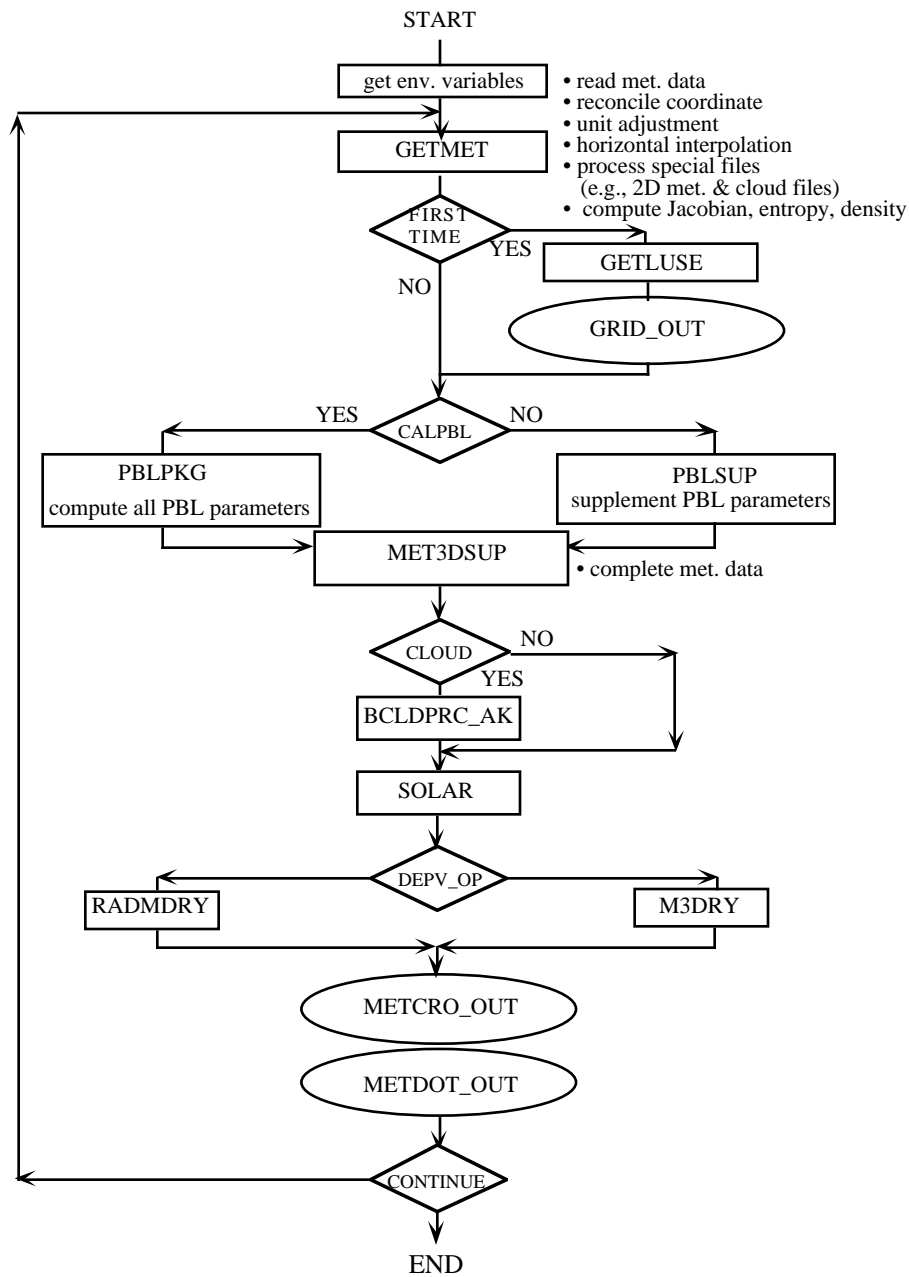


Figure 12-2. Flow Chart of MCIP Showing Key Data Processing Sequence.

12.2 Data Types, Coordinates, and Grids

MCIP's essential role is to provide consistent meteorological data for the CMAQ modeling system. Therefore, it is very important to understand the vertical coordinate used in the meteorological modeling system. For example, MM5 can be used either in hydrostatic mode, in which the hydrostatic pressure (time dependent) is used to define the terrain-influenced vertical coordinate, or in nonhydrostatic mode, where a reference hydrostatic pressure (time independent) in a normalized height form is used as the vertical coordinate. Many parts of current MCIP code deal with these differences in the vertical coordinate specifically. In the following we provide technical information related with coordinates and grids used in MCIP.

12.2.1 Meteorological Data Types

Many different combinations of approximations are used for describing the atmosphere in meteorological models. Therefore, classification of MCIP output parameters based on detailed classification of vertical coordinate types (such as geometric height, pressure, terrain-following coordinates, etc.), and their application approximations (such as hydrostatic and nonhydrostatic), can be exceedingly complex for the CTM with generalized coordinate implementation. Unlike previous use of detailed classification of meteorological coordinates for determining meteorological data type, we classify the coordinate types mainly based on the temporal dependency of the Jacobians (explained later). The benefit of this distinction is obvious. For example, a height coordinate which is time independent may require only a time constant file for describing the vertical coordinate while a dynamic pressure coordinate requires several parameters related with the coordinate description that needs to be stored in a time dependent file.

A similar distinction is made based on the need for describing data in different horizontal positions, such as flux-point data for horizontal wind components and cross-point for most other scalar parameters. For MM5, two horizontal wind components are defined at so-called 'dot' points while all other scalar values are at 'cross' points, following Arakawa-*E* grid definition. Refer to Figure 12-3 for the definitions of Arakawa *C*-grid and *E*-grid (Mesinger and Arakawa, 1976). For the CCTM, certain flux data are defined on the Arakawa *C*-grid in which the flux points are not collocated in \hat{x}^1 - and \hat{x}^2 -directions. Therefore, MCIP interpolates MM5's dot-point wind components linearly and multiplies the result with the two-point averaged density to provide the flux-point momentum component data. Both the flux-point and dot point data require array sizes larger than the cross-point data by one cell in each horizontal direction.

CMAQ utilizes contravariant wind components, instead of the regular wind components, to advect tracer species. Figure 12-4 shows that the east-west component of the contravariant wind field, \hat{u} , is placed at the \hat{x}^1 -direction flux points (marked with the square symbol) and the north-south (\hat{x}^2 -direction) component of the contravariant wind field, \hat{v} , is placed at the \hat{x}^2 -direction flux points (marked with the triangle symbol). The vertical wind component is defined at the full-layer height.

The Models-3 I/O API requires individual data components to have exactly the same temporal and spatial dimensions in a file. Because the flux-point data and dot-point data both need additional column or row positions, we can combine them together in a so-called DOT file, which is larger than the CRO file by one cell for each horizontal direction. It is important to note that because the

flux points are different from the dot-points, they must be shifted by a half cell east or north (depending on whether they are square-point or triangle-point flux values) for graphical visualization of the flux-point parameters.

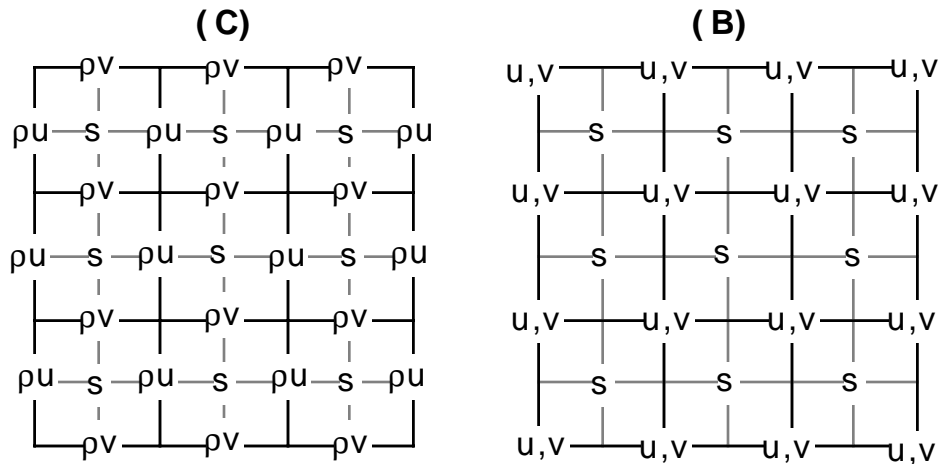


Figure 12-3. Two Different Grid Point Definitions, Arakawa C- and B-grids, Used in MCIP. u and v are horizontal wind components, s represents a scalar quantity, and ρ is density of air. For MM5, p^* is used instead of ρ .

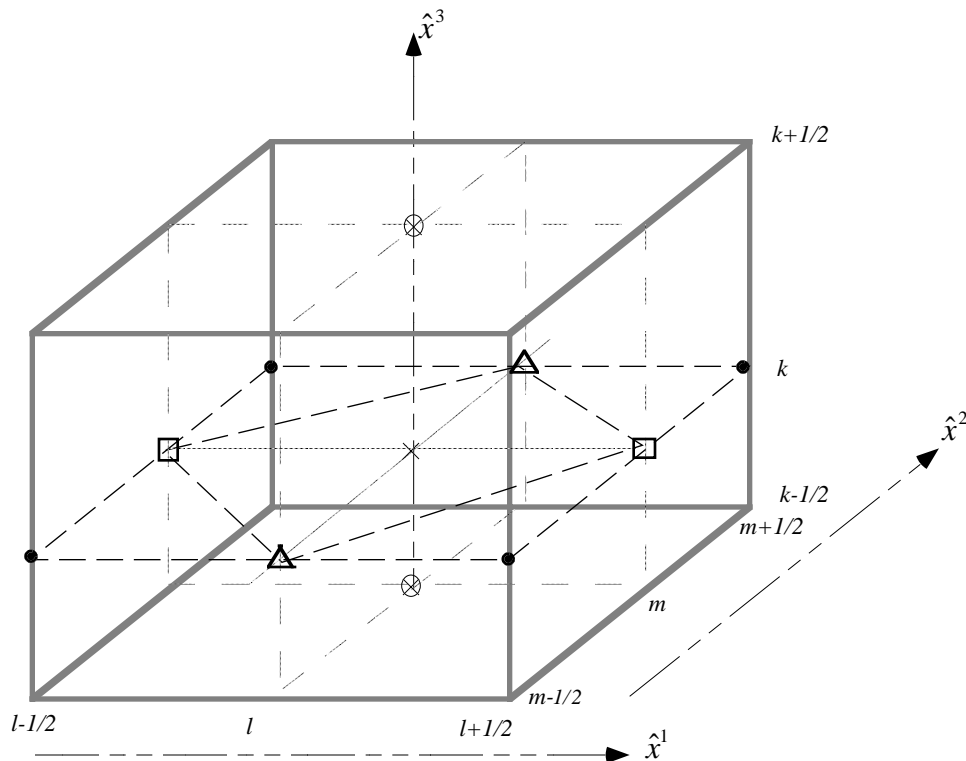
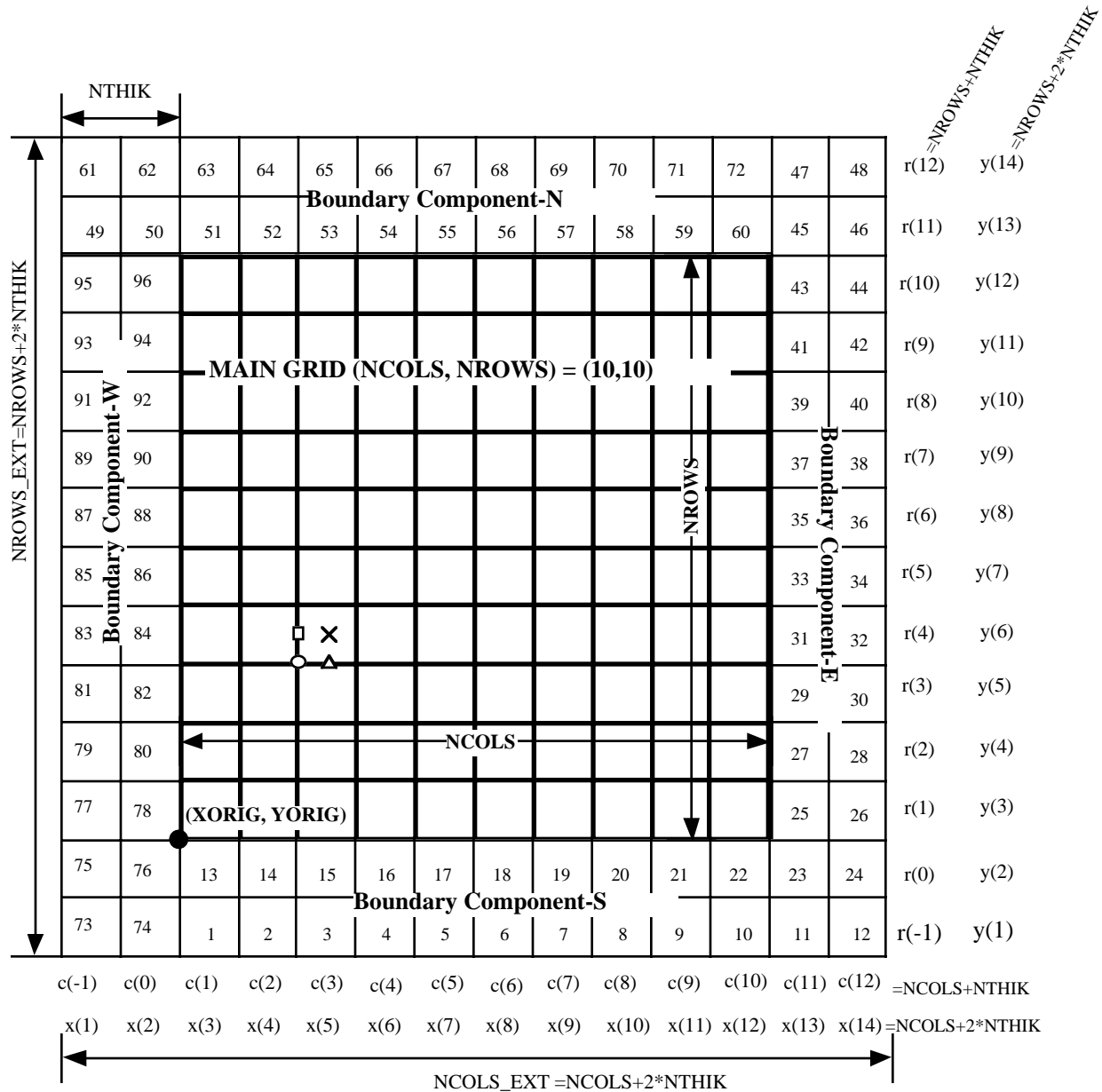


Figure 12-4. Computational Grid Points and Corresponding Indices Used in MCIP. Markers are for dot points (●), cross points (×), x-direction flux points (□), y-direction flux points (Δ), and vertical cross point at layer interface (⊗).

Furthermore, when these two flux components are assigned to form vectors in a visualization program like PAVE (Thorpe, 1996), the starting points of the vectors in the visualization are relocated at the dot-points although the two components are actually not collocated there.

Data for the boundary cells are defined with a special I/O API boundary data type. Depending on the need to describe boundary mass flux accurately, one may want to have a boundary domain with *NTHIK* cells (see Figure 12-5). The boundary grid is represented as the external perimeter to the main grid. This perimeter is *NTHIK* cells wide (where you may use a negative *NTHIK* to indicate an internal perimeter as used by such air quality modeling systems ROM and RADM). The boundary array is dimensioned in terms of the sizes of the arrays surrounding the main domain. Current Models-3 CMAQ system uses *NTHIK*=1 throughout the system components.

Finally, the dimensionality of the parameters (i.e., whether they contain three-dimensional or two-dimensional information) is used to distinguish the data type of meteorological parameters. In vertical direction, we define half and full layer positions based on the values of the generalized vertical coordinate, (\hat{x}^3). Vertical wind component and flux values are examples of the full-layer parameters. Although full-layer data require one more data point vertically, often the flux values at the bottom boundary (i.e., at the lowest full-layer) are zero. Therefore, we do not need to use additional data types for these, as long as we save the non-zero lowest full-layer data in a corresponding two-dimensional data type file separately. (Refer to Table 12-2 for dimensions used for each grid points.) Because a file represents a set of data with the same data type (with only a few exceptions) in the Models-3 system, locating meteorological parameters from an appropriate I/O API file is relatively easy. Table 12-3 summarizes the possible data types for the meteorological parameters. Depending on the choice of coordinates and grids, some of data types may not be relevant. For example, the current version of MCIP does not use *GRID_DOT_3D* and *MET_DOT_2D* data types. Appendix 12A provides the list of MCIP output parameters in each data file.



Note: Individual boundary component grids are treated as a I/O API 2-D file
 S(1:NCOLS+NTHIK, 1-NTHIK:0)
 E(NCOLS+1:NCOLS+NTHIK, 1:NROWS+NTHIK)
 N(1-NTHIK:NCOLS, NROWS+1:NROWS+NTHIK)
 W(1-NTHIK:0, 1-NTHIK:NROWS)

Figure 12-5. Grid Data Structure for Models-3/CMAQ Showing Main Grid and Boundary Components. Here $NTHIK=2$, $NCOLS=10$, $NROWS=10$ are used for the illustration.

Table 12-2. Dimensions and Indices for Grid Points used in MCIP and CCTM

	Dot-Point <i>(start: end)</i> <i>dimension</i> <i>index</i>	Cross-Point <i>(start: end)</i> <i>dimension</i> <i>index</i>	\hat{x}^1 - direction Flux Point	\hat{x}^2 -direction Flux Point	Full-Layer <i>(start: end)</i> <i>dimension</i> <i>index</i>	Half-Layer <i>(start: end)</i> <i>dimension</i> <i>index</i>
\hat{x}^1	(1:NCOLS+1) NCOLS+1 $l \pm 1/2$	(1:NCOLS) NCOLS l	(1:NCOLS+1) NCOLS+1 $l \pm 1/2$	(1:NCOLS) NCOLS l	N/A	N/A
\hat{x}^2	(1:NROWS+1) NROWS+1 $m \pm 1/2$	(1:NROWS) NROWS m	(1: NROWS) NROWS m	(1: NROWS +1) NROWS+1 $m \pm 1/2$	N/A	N/A
\hat{x}^3	N/A	N/A	N/A	N/A	(0:NLAYS) NLAYS+1 $k \pm 1/2$	(1:NLAYS) NLAYS k

Table 12-3. Classification of Meteorological Data Types in the CMAQ System.

Data types GRID_DOT_3D and MET_DOT_2D (in gray color) are not used in CMAQ currently.

Time Independent		Time Dependent	
GRID_CRO_2D	GRID_CRO_3D	MET_CRO_2D	MET_CRO_3D
GRID_DOT_2D	GRID_DOT_3D	MET_DOT_2D	MET_DOT_3D
GRID_BDY_2D	GRID_BDY_3D	MET_BDY_2D	MET_BDY_3D

12.2.2 Coordinates

12.2.2.1 Horizontal Coordinates and Grid

MCIP can be configured with horizontal coordinates based on conformal map projections, such as Lambert Conformal, Polar Sterographic, and Mercator. Table 12-4 summarizes the necessary information for the description of the conformal map projections as defined in Models-3 I/O API. To generate I/O API files, which require exact definitions of the grid and coordinate system, users need to provide all the necessary map projection information in addition to vertical coordinate and layering definitions. The Models-3 CMAQ system uses square cells for the horizontal grid representation. A modeling domain is defined with the integer multiples of the square cells in E-W (column-wise) and N-S (row-wise) directions. Although a rectangular cell shape can be handled by the I/O API, the fractional time splitting approach used for the modularization of CTM processes requires use of square grid to maintain the accuracy of the finite differencing algorithms consistently. The effect of different horizontal coordinate is reflected in the values of the map scale

factor. Because of the need to couple the map scale factor (m) with other state variables and wind components, MCIP provides map scale factor for both the dot- and cross-points.

Table 12-4. Map Scale Factors and Parameters Defining Horizontal Coordinates in Models-3 I/O API (Coats, 1996)

Coordinate	ID in Models-3 I/O API	Map Parameters	Map Scale (m)	Note
lat.-long.	LATGRD3=1	N/A	N/A $m = 1$	$(\hat{x}^1, \hat{x}^2) = (\text{long}, \text{lat})$ are in degrees
Lambert	LAMGRD3=2	$P_\alpha = \phi_1 \leq P_\beta = \phi_2$ two latitudes that determine the projection cone. $P_\gamma = \lambda_o$, central meridian	$m = \frac{\sin(\pi/2 - \phi_1) \left[\frac{\tan(\pi/4 - \phi/2)}{\tan(\pi/4 - \phi_1/2)} \right]^n}{\sin(\pi/2 - \phi) \left[\frac{\tan(\pi/4 - \phi/2)}{\tan(\pi/4 - \phi_1/2)} \right]^n}$ $n = \ln \left[\frac{\sin(\pi/2 - \phi_2)}{\sin(\pi/2 - \phi_1)} \right]$ $\bullet \left[\ln \left(\frac{\tan(\pi/4 - \phi_2/2)}{\tan(\pi/4 - \phi_1/2)} \right) \right]^{-1}$	$(\hat{x}^1_{cent}, \hat{x}^2_{cent}) = (\lambda_o, \phi_o)$ for the center of coordinate system. (\hat{x}^1, \hat{x}^2) are in meters
Mercator	MERGRD3=3	$P_\alpha = \phi_o, P_\beta = \lambda_o$: latitude longitude of coordinate origin within the tangent circle. P_γ : angle between cylinder axis and the North polar axis	$m = \frac{\cos \phi_o}{\cos \phi}$	$(\hat{x}^1_{cent}, \hat{x}^2_{cent}) = (\lambda_o, \phi_o)$ for the center of coordinate system. (\hat{x}^1, \hat{x}^2) are in meters
Stereo-graphic	STEGRD3=4	$P_\alpha = \phi_o, P_\beta = \lambda_o$: latitude and longitude of the point of tangency. P_γ : angle from true north to \hat{x}^2 -axis	$m = \frac{1 + \sin \phi_o}{1 + \sin \phi}$	$(\hat{x}^1_{cent}, \hat{x}^2_{cent}) = (\lambda_o, \phi_o)$ for the center of coordinate system. (\hat{x}^1, \hat{x}^2) are in meters
UTM	UTMGRD3=5	P_α is the UTM zone P_β, P_γ not used	$m = 1$	$(\hat{x}^1_{cent}, \hat{x}^2_{cent})$ are offset from the UTM coordinate origin. (\hat{x}^1, \hat{x}^2) are in meters

12.2.2.2 Vertical Coordinates and Grid

The Models-3 CMAQ system allows many popular vertical coordinates used in meteorological models. We expect that the Models-3 I/O API will be extended to include several other vertical coordinates. The I/O API follows the definitions of vertical coordinates as used in meteorological models. However, in CMAQ the vertical coordinates are redefined to increase monotonically with height. This precaution is needed because the CMAQ code is expected to handle generalized coordinate system. We found that this constraint in the vertical coordinate is extremely useful for

the implementation of CTM in the generalized coordinate system by removing possible sign errors wherever vertical differentiations are involved. For example, the Jacobian information for a coordinate can be directly used to replace some of the derivatives involved with the generalized vertical coordinate. This internal change does not require redefinition of the vertical coordinates in the MCIP output files. The impact of this constraint is limited to an include file that defines the coordinates and vertical layers. In a typical Models-3 operation, this include file is automatically generated by the system framework through the use of the coordinate/grid manager. In the following two typical application examples are presented; one for the time dependent coordinate and the other for time independent coordinate.

Time dependent hydrostatic sigma-pressure coordinate

For the MM5 system, this coordinate is used when the hydrostatic option is chosen. In general, this coordinate can be used not only for the hydrostatic atmosphere simulations but also for nonhydrostatic cases. For example, when a regional scale hydrostatic meteorological model provides hydrostatic values, the same coordinate can be used in a nonhydrostatic nested model as described by Jaung (1992). In MCIP implementation, we should view this coordinate as an example of processing meteorological data with a dynamic vertical coordinate definition rather than an example of a hydrostatic coordinate.

The CCTM utilizes a generalized coordinate system that allows construction of the vertical layering consistent with the meteorological coordinate used. However, to maintain the vertical coordinate definition monotonically increasing with height, the coordinate definition for the CCTM has been modified as:

$$\hat{x}^3 = \xi \equiv 1 - \sigma_{\tilde{p}}; \sigma_{\tilde{p}} = \frac{\tilde{p} - p_T}{\tilde{p}_s - p_T} = \frac{\tilde{p} - p_T}{\tilde{p}^*} \quad (12-1)$$

where $\tilde{p}(\hat{x}^1, \hat{x}^2, \hat{x}^3, t)$ is the hydrostatic pressure, p_T is the pressure at the model top which is held constant, $\tilde{p}_s(\hat{x}^1, \hat{x}^2, t)$ is the surface pressure, and $\tilde{p}^* = \tilde{p}_s - p_T$. Because the pressure used in the definition of the vertical coordinate is in hydrostatic balance, we have:

$$\frac{\partial \tilde{p}}{\partial z} = -\tilde{\rho}g \quad (12-2)$$

The Jacobian is then defined as:

$$J_{\hat{x}^3} \equiv \left| \frac{\partial \hat{x}^3}{\partial z} \right|^{-1} = \left| -\frac{1}{\tilde{\rho}^*} \frac{\partial \tilde{p}}{\partial z} \right|^{-1} = \frac{\tilde{p}^*}{\tilde{\rho}g}, \quad (12-3)$$

and it is time dependent because the surface pressure and air density are time dependent.

Time independent reference hydrostatic sigma-pressure coordinate

In MM5 this coordinate is specifically used for the simulation of the nonhydrostatic atmosphere. The layer structure is entirely different from the case when hydrostatic option is used. The

coordinates defined with this option are time independent and have very similar characteristic to those of the normalized geometric height coordinates. The only difference is that the vertical layer thickness is defined with a nonlinear function of the geometric height. Here, we should view this coordinate as an example of processing meteorological data with time independent vertical coordinate.

The terrain-following reference hydrostatic pressure (σ_{p_o}) coordinate, again in a monotonically increasing form, is given as:

$$\hat{x}^3 = \xi \equiv 1 - \sigma_{p_o} ; \sigma_{p_o} = \frac{P_o - P_T}{P_{os} - P_T} = \frac{P_o - P_T}{P_{os}^*} \quad (12-4)$$

where $p_o(\hat{x}^1, \hat{x}^2, \hat{x}^3)$ is the hydrostatic pressure of the reference atmosphere, p_T is the pressure at the model top, $p_{os}(\hat{x}^1, \hat{x}^2)$ is the reference surface pressure which is determined by the topographic height z_s , and $p_o^* = p_{os} - p_T$.

Because the reference atmosphere is in hydrostatic balance, we have:

$$\frac{\partial p_o}{\partial z} = -\rho_o g \quad (12-5)$$

The Jacobian is then defined as:

$$J_{\hat{x}^3} \equiv \left| \frac{\partial \hat{x}^3}{\partial z} \right|^{-1} = \left| -\frac{1}{p_o^*} \frac{\partial p_o}{\partial z} \right|^{-1} = \frac{p_o^*}{\rho_o g} \quad (12-6)$$

and it is time independent because it is a function of the time-independent surface pressure and the density of the reference atmosphere. Here, the vertical coordinate z represents a height above the lowest point in a modeling domain, or the mean sea level (MSL) height if there is no place lower than the MSL. Usually, this type of vertical coordinate accompanies with a simple description of reference temperature profile of the base state. For example, in MM5 the base temperature profile is defined with a simple expression:

$$T_o(z) = T_{os} + A \ln \left(\frac{p_o(z)}{p_{oo}} \right) \quad (12-7)$$

where the reference values are chosen such that T_{os} is a sea level reference temperature in K , $p_{oo} = 1000 \text{ mb} = 10^5 \text{ Pascal}$, and A , which is set to be 50 K , is a measure of atmospheric lapse rate represented in temperature difference for the e -folding depth. With Equations 12-5 and 12-7 and the Equation of State, we could relate the reference pressure in terms of height z in a differential equation:

$$\frac{d \ln p_o(z)}{dz} = -\frac{g}{R} \frac{1}{[T_{os} - A \ln(p_{oo})] + A \ln(p_o(z))} \quad (12-8)$$

which can be readily solved for $p_o(z)$ by the separation-of-variables technique. The solution is a quadratic equation in terms of $\ln p_o$. For typical tropospheric conditions, the base pressure can be related with the geometric height by taking the positive square root term:

$$p_o(z) = \exp\left[\frac{-b + \sqrt{b^2 - 2Ac}}{A}\right] \quad (12-9)$$

where $b = T_{os} - A(\ln p_{oo})$, and $c = \frac{g}{R}z - [\frac{1}{2}A(\ln p_{oo})^2 + b(\ln p_{oo})]$.

Equation 12-9 shows that $p_o(z)$ is a monotonic, but nonlinear, function of z .

12.2.3 Modification of Grid Structure

In CMAQ, the horizontal and vertical coordinate information (such as the map projection parameters) for CTM simulation domains are required to be exactly the same as (or a derivative of) the master coordinates used in the meteorological model simulation. However, the horizontal grid structures of the CTM domains can be redefined depending on the need for air quality simulations. Here, the concept of grid family is introduced. It is as a set of grid domain specifications with the following properties:

1. the same coordinate origin and map projection;
2. a window domain for the parent domain; or
3. a nest (multi-stage) domain from a window or the parent domain.

The Models-3 I/O API file header helps to describe the horizontal grid and coordinates unambiguously to position the background map correctly and to provide relations among the members (multi-stage nesting domains) of the grid family. Only with a limited manner, the user is allowed to modify the grids in the vertical directions because of the concern that *ad hoc* interpolation may destroy the integrity of the meteorological data.

12.2.3.1 Windowing

The windowing functions in MCIP extract MM5 output for a CCTM window domain. As a rule of thumb, a CCTM uses a smaller computational domain than the domain used by meteorological models, because predictions in the cells near the boundaries may not be suitable for use in air quality simulation. Therefore, MCIP extracts only the portion of the MM5 output data which falls within the CTM's main domain and boundary cells. The CTM domain should be located at least four or five cells inside the MM5 domain to minimize the boundary effects. MCIP can, however, generate output for the CMAQ domain as large as 2 cells smaller than the meteorology domain, because it generates files for the boundary cells with $NTHIK=1$. (Note in MM5 terminology, it

may seem like the CMAQ domain is smaller by three because a DOT point concept is used in MM5 system for the grid definition.)

Limitation on the number of horizontal cells (to 120 cells) of the meteorology grid is coming from the MCIP's parameters defined in MCIPPARM.EXT:

```
PARAMETER ( MAXI      = 120,          ! MET domain size in N-S dir.
&           MAXJ      = 120 )        ! MET domain size in E-W dir.
```

When the meteorology data has larger dimensions, MAXI and MAXJ should be modified accordingly. Also, there could be some limitations with reader routines specific for meteorology models. Because these reader modules are essentially foreign codes, there is no easy way to generalize the input process of the meteorological data. Refer to Figure 12-6, which shows the relation among the meteorology domain, the window domain for meteorological data extraction, and the CTM main and boundary domains.

Relations among MM grid, extended-CTM grid, and CTM grid for NDX=3

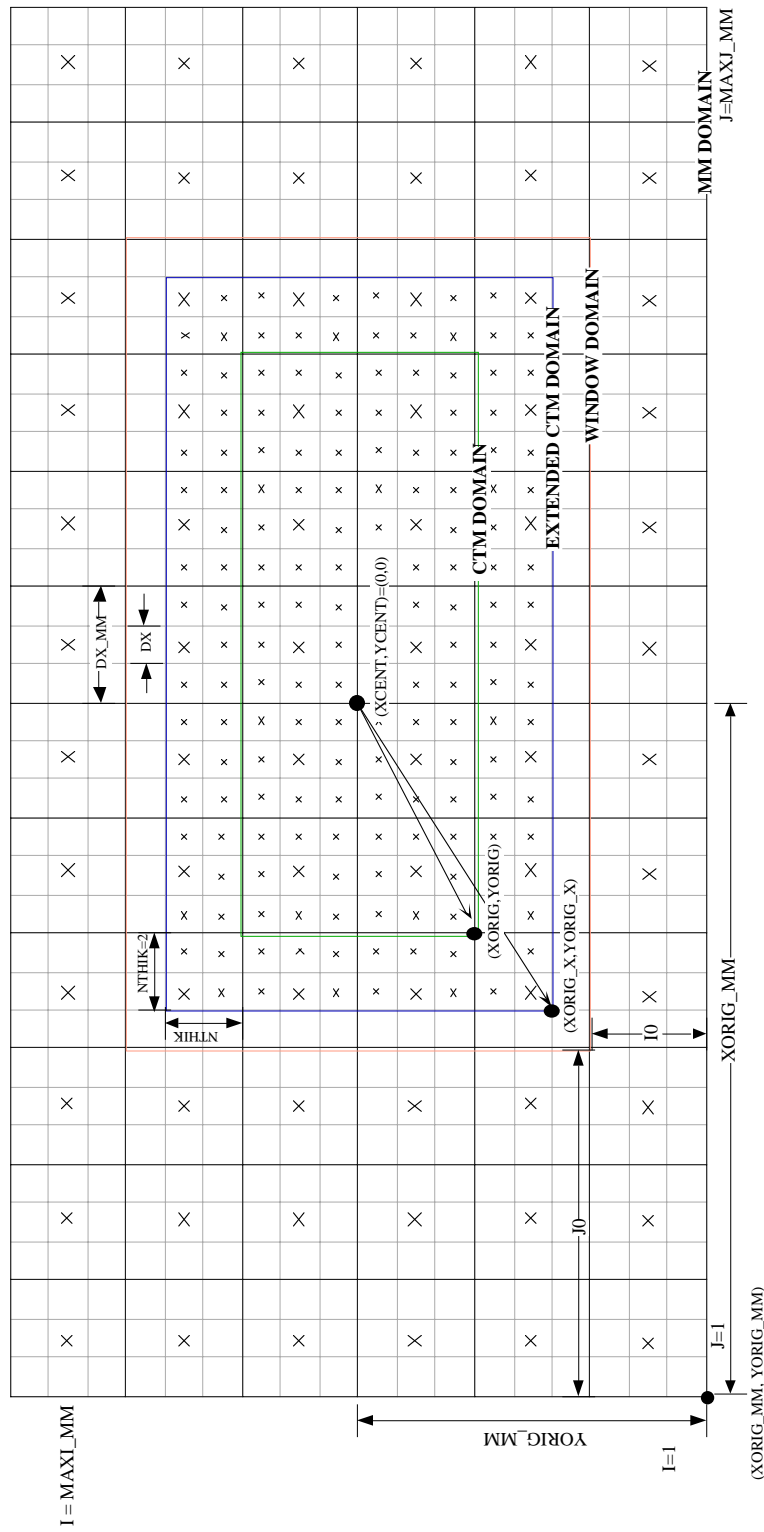


Figure 6. Relations among the meteorology domain, window domain for data extraction, and CTM's main and boundary domains.

12.2.3.2 Horizontal Interpolation

A horizontal interpolation function is provided to help users generate higher resolution data than the input meteorological data. This function is used when higher resolution emissions data is available but the detailed variations in meteorological fields can be neglected. This option is useful only when the surface and PBL parameters are diagnosed in MCIP. If interpolation is desired, *NDX* (defined in MCIPPARM.EXT) must be modified before the MCIP is compiled so that data arrays are dimensioned properly. When interpolation is desired, MCIP copies contiguous grid cell values from the coarse grid to the fine grid and then performs a two-dimensional bilinear interpolation on the three-dimensional data. The interpolated temperature profile is updated using fine resolution landuse data to reflect land-sea boundaries in the profile appropriately. The interpolated temperature, moisture, and wind components profiles, together with the detailed landuse data, are used to estimate surface and PBL parameters for the finer resolution. The user should be reminded that this procedure generates higher resolution meteorological data without enhanced physics, thus the newly generated data may have consistency problems. Therefore, such interpolation should be used sparingly for cases such as testing higher resolution emissions data with a finer resolution CTM. The procedure is never meant to replace or minimize the need for higher resolution meteorological model runs. It should be noted that the interpolated temperature and moisture profiles result in different estimations of cloud parameters (such as cloud bottom and top heights, fractions, liquid water contents) as determined by the diagnostic Anthes-Kuo cloud routine.

12.2.3.3 Vertical Layer Collapsing

A vertical collapsing function is supplied to generate a smaller data set for testing CTM in a smaller computer system. If desired, MCIP collapses MM5 profile data for the coarse vertical resolution data as defined by the user. MCIP performs a mass-weighted averaging of data in the vertical direction. For example, 30-layer MM5 data may be averaged into 15 or 6 CTM layers. During the collapsing procedure, the layer description is modified accordingly. The resulting profile may have consistency problems. This option is usually used to generate meteorology data for a system test-run for code debugging and development purposes. It is also appropriate to study the effects of the vertical resolution in air quality simulation such as presented in Byun and Dennis (1995). Refer to Table 12-5 as an example for the layer collapsing.

Defining the vertical layering structure for the CMAQ system requires consideration of several factors. Depending on the layer definitions used, the model results will be affected considerably. The implications of the layer definition are pervading across the entire system. For example, to determine mass exchange between the boundary layer and free troposphere, a good resolution near the boundary layer top is preferable. Also, different cloud parameterizations may perform differently, depending on the layering structure. Aerodynamic resistance, which influences dry deposition velocities, is a function of layer thickness and the boundary layer stability. For emissions processing, the layer thickness affects the plume rises from major stacks. Also, the vertical extent of the area emission effects is limited by the thickness of the lowest model layer for the CCTM. Although 6-layer vertical grid definition is provided with the tutorial simulation examples, we do not recommend it to be used for regulatory applications because of the difficulties in simulating certain processes, such as dry deposition under stable atmospheric conditions.

Current limitation on the number of vertical layers to 30 comes from one of the MCIP's parameters defined in MCIPPARM.EXT:

```
PARAMETER ( MAXK      = 30 )      ! MET number of layers
```

When a meteorological data has more number of layers, the parameter MAXK should be increased accordingly. Collapsing is done automatically when the COORD.EXT file (see Models-3 CMAQ User's Guide for the details) for the output grid has smaller number of layers than the input grid.

Table 12-5. An example of layer collapsing from 15 to 6 σ -layers. Full and half σ -levels and standard heights are provided to show relations between the two vertical grid systems. (adapted from Byun and Dennis, 1995)

Level Index(15)	Level Index(6)	σ -Level		Standard Height (m)	
		Full(15)	Half(15)	Full(15)	Half(15)
15	6	0.0	0.05	16069	13712
14		0.1	0.15	11998	10649
13		0.2	0.25	9512	8513
12	5	0.3	0.35	7621	6813
11		0.4	0.45	6073	5390
10		0.5	0.55	4754	4159
9		0.6	0.65	3600	3071
8	4	0.7	0.74	2570	2187
7		0.78	0.81	1818	1550
6		0.84	0.865	1289	1077
5	3	0.89	0.91	868	705
4		0.93	0.945	544	425
3		0.96	0.97	307	230
2	2	0.98	0.985	152	114
1		0.99	0.995	76	38
0		1.0		0	

12.3 Estimation of Physical Parameters

MCIP's essential role is to provide consistent meteorological data for the CMAQ modeling system. However, the meteorological models used for air quality study may not provide important boundary layer parameters at all, or may predict those at very coarse temporal resolution, or may only compute a subset of the needed parameters. In such a case, it becomes necessary to estimate remaining meteorological parameters using certain diagnostic methods. MCIP allows either the direct pass through of the PBL parameters provided by MM5, or they can be computed from the mean profiles of temperature, humidity and momentum together with the surface landuse data. In the following, we explain the diagnostic methods used in MCIP. Note that the approaches introduced here may not be consistent with MM5 directly and therefore may produce somewhat different spatial distribution patterns for certain parameters. Basically, the diagnostic routines treat meteorological model outputs as the pseudo radiosonde observations.

When desired, MCIP estimates key parameters for cloud distributions based on Anthes-Kuo parameterization. They include precipitation rate, cloud fraction, and cloud base and top heights. MCIP also provides estimated dry deposition velocities for various chemical species in the RADM and carbon bond 4 (CB-4) mechanisms.

12.3.1 PBL Parameters

Depending on the user option, MCIP either passes through MM5 predicted surface and PBL parameters or estimates them us the MM5 profile data and detailed landuse information. The algorithms used for the diagnostic computation of PBL parameters are provided below.

12.3.1.1 Surface Flux Related Parameters

We utilize a diagnostic method based on similarity theory to estimate the turbulence flux related parameters. When the meteorological model uses very high vertical resolution and the thickness of lowest model layer is less than 20 m, we can utilize the surface similarity theory to determine turbulence parameters for both stable and unstable atmosphere.

For the computation of the surface layer parameters, MCIP utilizes analytical solutions suggested by Byun (1990) to minimize the needs for numerical iterations in solving the flux-profile relations. The method has been reviewed and successfully applied in several surface layer studies (e.g., Hess, 1992; Lo, 1993 and 1995). Also, a weather research model, the Advanced Regional Prediction System (ARPS) (Xue et al., 1995) utilizes it in the description of the surface layer. The algorithm is summarized below.

The nondimensional surface layer profile functions for momentum (ϕ_m) and potential temperature (ϕ_h) are defined as:

$$\frac{kz}{u_*} \frac{\partial U}{\partial z} = \phi_m \left(\frac{z}{L} \right) \quad (12-10a)$$

$$\frac{kz}{\theta_*} \frac{\partial \Theta}{\partial z} = \phi_h \left(\frac{z}{L} \right) \quad (12-10b)$$

where U and Θ are the horizontal wind speed and potential temperature in the boundary layer, respectively, u_* is the friction velocity, and θ_* is the temperature scale representing the surface heat flux (covariance of potential temperature and wind fluctuations) divided by the friction velocity. L is the Monin-Obukhov length defined as:

$$L = \frac{\Theta_o u_*^2}{kg\theta_*} \quad (12-11)$$

The similarity functional forms proposed by Businger et al. (1971) are used in MCIP as follows: For moderately stable conditions ($1 \geq z/L \geq 0$) we have:

$$\phi_m = 1 + \beta_m \frac{z}{L} \quad (12-12a)$$

$$\phi_h = \text{Pr}_o \left(1 + \beta_h \frac{z}{L} \right), \quad (12-12b)$$

where Pr_o is the Prandtl number for neutral stability and β_m and β_h are the coefficients determined through field experiments. Refer to Table 12-6 for the values of these coefficients used in MCIP. For unstable conditions ($z/L < 0$), we have:

$$\phi_m = \left(1 - \gamma_m \frac{z}{L} \right)^{-1/4} \quad (12-13a)$$

$$\phi_h = \left(1 - \gamma_h \frac{z}{L} \right)^{-1/2} \quad (12-13b)$$

where γ_m and γ_h are coefficients of the profile functions. In addition, we added a function for the very stable condition ($z/L \geq 1$) to extend the applicability of the surface layer similarity following Holtslag et al. (1990):

$$\phi_m = \beta_m + \frac{z}{L} \quad (12-14a)$$

$$\phi_h = \text{Pr}_o \left(\beta_h + \frac{z}{L} \right) \quad (12-14b)$$

To estimate surface turbulence fluxes with the layered data from a meteorological model, we utilize the integrated flux-profile relationships: For ($z/L < 1$) we have profile functions represented as a modified logarithmic functions, when integrated from the height of the roughness length (z_o),

$$U(z) = \frac{u_*}{k} \left[\ln \frac{z}{z_o} - \psi_m \left(\frac{z}{L}, \frac{z_o}{L} \right) \right] \quad (12-15a)$$

$$\Delta\Theta(z) = \frac{\text{Pr}_o \theta_*}{k} \left[\ln \frac{z}{z_o} - \psi_h \left(\frac{z}{L}, \frac{z_o}{L} \right) \right] \quad (12-15b)$$

and for strongly stable conditions, ($z/L \geq 1$), we use direct integration of the profile functions:

$$U(z) = \frac{u_*}{k} \left[\beta_m \ln \frac{z}{z_o} + \frac{z - z_o}{L} \right] \quad (12-16a)$$

$$\Delta\Theta(z) = \frac{\text{Pr}_o \theta_*}{k} \left[\beta_h \ln \frac{z}{z_o} + \frac{z - z_o}{L} \right] \quad (12-16b)$$

The ψ functions are given by (e.g., Paulson 1970), for moderately stable conditions ($1 \geq z/L \geq 0$):

$$\psi_m \left(\frac{z}{L} \right) = -\beta_m \frac{z - z_o}{L} \quad (12-17a)$$

$$\psi_h \left(\frac{z}{L} \right) = -\beta_h \frac{z - z_o}{L} \quad (12-17b)$$

and for unstable conditions:

$$\psi_m \left(\frac{z}{L} \right) = 2 \ln \left(\frac{1+x}{1+x_o} \right) + \ln \left(\frac{1+x^2}{1+x_o^2} \right) - 2 \tan^{-1}(x) + 2 \tan^{-1}(x_o) \quad (12-18a)$$

$$\psi_h \left(\frac{z}{L} \right) = 2 \ln \left(\frac{1+y}{1+y_o} \right), \quad (12-18b)$$

where $x = (1 - \gamma_m \frac{z}{L})^{1/4}$, $x_o = (1 - \gamma_m \frac{z_o}{L})^{1/4}$, and

$$y = (1 - \gamma_h \frac{z}{L})^{1/2}, \quad y_o = (1 - \gamma_h \frac{z_o}{L})^{1/2}.$$

One important fact to note here is that although the similarity functions for stable conditions, Equations 12-12a-b and 12-14a-b, are continuous at $z/L=1$, their integrated profiles are not continuous.

The flux profile relations described above are used to relate the Monin-Obukhov stability parameters with the readily computable bulk Richardson number Ri_b :

$$Ri_b = \frac{g(z - z_o)}{\Theta_o} \frac{\Delta\Theta}{U^2} \quad (12-19)$$

For moderately stable conditions ($I > z/L \geq 0$), we have:

$$\zeta = \frac{\left(\frac{z}{z - z_o}\right) \ln \frac{z}{z_o}}{2\beta_h(\beta_m Ri_b - 1)} \left[-(2\beta_h Ri_b - 1) - \left(1 + \frac{4(\beta_h - \beta_m) Ri_b}{Pr_o}\right)^{1/2} \right] \quad (12-20)$$

and for strongly stable conditions, ($z/L \geq I$), we can derive a similar solution following the same procedure as described in Byun (1990) to give:

$$\zeta = \frac{\beta_m \left(\frac{z}{z - z_o}\right) \ln \frac{z}{z_o}}{Pr_o - Ri_b} \left[-\left(\frac{1}{2} - Ri_b\right) + \left(\left(\frac{1}{2} - Ri_b\right)^2 + (Pr_o - Ri_b) Ri_b\right)^{1/2} \right] \quad (12-21)$$

Given a positive bulk Richardson number, one should use both Equations 12-20 and 12-21 to compute ζ and choose the value in the correct range between the moderately stable and strongly stable conditions.

For unstable conditions, we use an efficient analytical approximation by Byun (1990), for $(Q_b^3 - P_b^2) \geq 0$,

$$\zeta \approx \left(\frac{z}{z - z_o}\right) \ln \left(\frac{z}{z_o}\right) \left[-2\sqrt{Q_b} \cos\left(\frac{\theta_b}{3}\right) + \frac{1}{3\gamma_m} \right] \quad (12-22)$$

and for $(Q_b^3 - P_b^2) < 0$,

$$\zeta \approx \left(\frac{z}{z - z_o}\right) \ln \left(\frac{z}{z_o}\right) \left[-\left(T_b + \frac{Q_b}{T_b}\right) + \frac{1}{3\gamma_m} \right] \quad (12-23)$$

where $s_b = \frac{Ri_b}{Pr_o}$;

$$Q_b = \frac{1}{9} \left[\frac{1}{\gamma_m^2} + 3 \frac{\gamma_h}{\gamma_m} s_b^2 \right];$$

$$P_b = \frac{1}{54} \left[-\frac{2}{\gamma_m^3} + \frac{9}{\gamma_m} \left(-\frac{\gamma_h}{\gamma_m} + 3\right) s_b^2 \right];$$

$$\theta_b = \arccos\left(\frac{P_b}{\sqrt{Q_b^3}}\right); \text{ and}$$

$$T_b = \left[\sqrt{P_b^2 - Q_b^3} + P_b\right]^{1/3}.$$

The above equations are used to estimate friction velocity, u_* , by estimating the bulk Richardson number using the layered meteorological data:

$$u_* = \frac{kU(1)}{\ln(z/z_o) - \Psi_m(z/L) + \Psi_m(z_o/L)} \quad (12-24)$$

Heat flux can be found by using the temperature scale estimated with:

$$H = -\rho C_p u_* \theta_* \quad (12-25)$$

where

$$\theta_* = \frac{k[\Theta_1 - \Theta_s]}{\text{Pr}_o[\ln(z_1/z_o) - \Psi_h(z_1/L) + \Psi_h(z_o/L)]} \quad (12-26)$$

There have been several suggestions for the coefficients of the surface layer profile functions. For example, Businger et al. (1971) suggested:

$$\beta_m = 4.7, \beta_h = 6.35, \gamma_m = 15.0, \gamma_h = 9.0, \text{Pr}_o = 0.74$$

with the von Karman constant value of 0.35. On the other hand, Högström (1988) reanalyzed the experimental data used for the determination of the similarity functions and suggested use of:

$$\beta_m = 6.0, \beta_h = 8.21, \gamma_m = 19.3, \gamma_h = 11.6, \text{Pr}_o = 0.95$$

with the von Karman constant value of 0.40. In the current version of MCIP, the latter set of coefficient values are used (refer to Table 12-6).

Moisture flux is found by using similar method as the potential temperature:

$$E = -\rho u_* q_*, \quad (12-27)$$

where mixing ratio scale, q_* , is determined with an equation similar to Equation 12-26 for given $\Delta q = q_1 - q_s$ (q_1 and q_s are the mixing ratios at the lowest model layer and at the surface, respectively).

12.3.1.2 Estimation of Surface Fluxes Using PBL Profile Functions

Occasionally meteorological models use the lowest model layer thicker than 40 m or so. Under this condition, it becomes difficult to believe that the lowest layer always belongs to the surface layer all the time, especially for very stable conditions. To avoid this limitation, MCIP estimates surface heat, momentum and moisture flux transfer parameters from MM5 surface wind and temperature by using the boundary layer similarity profiles proposed by Byun (1991). In this section, we describe the methods used in MCIP for estimating surface fluxes when the thickness of the lowest model layer is too thick to rely on the surface layer similarity. The intention is to provide a diagnostic method that can estimate the surface fluxes even when the lowest model layer extends above the surface layer. It is difficult to expect that a layer with 40 m thick, for example, continuously belongs to the surface layer though out a day.

Table 12-6. Parametric Constants Used to Describe the PBL in MCIP

Parameter	Symbol	Value
von Karman constant	K	0.4
Coefficient in stable profile function for momentum	β_m	6.0
Coefficient in stable profile function for heat (scalar)	β_h	8.21
Coefficient in unstable profile function for momentum	γ_m	19.30
Coefficient in unstable profile function for heat (scalar)	γ_h	11.60
Prandtl number for neutral stability	Pr_o	0.95
Critical Richardson Number	Ri_{cr}	0.25
Maximum bulk Richardson number	$\max(Ri_B)$	0.70
Minimum bulk Richardson number	$\min(Ri_B)$	-4.75
Minimum magnitude of Monin-Obukhov length	$\text{abs}(L)$	4.0
Scale height ratio for neutral stability	λ_o	0.07
Zilitinkevich c_h	c_h	0.80
Neutral value of similarity function for wind component parallel to surface stress	$A(0)$	1.70
Neutral value of similarity function for wind component normal to surface stress	$B(0)$	4.50
Reference height	z_r	10 m

The wind and temperature predicted by a meteorological grid model represent layer averaged values. In order to simplify computation of the surface fluxes, we apply the assumption that the predicted wind for the lowest model layer has the same direction as the surface stress (i.e., $u_m^2 + v_m^2 \approx U_m^2$, where u_m and v_m are latitudinal and longitudinal components of the first layer mean wind on the map and U_m is the layer mean wind speed in the direction of surface stress). Applying the PBL momentum profile functions of Byun (1991) and integrating them vertically from z_o (roughness length) to the top of the lowest CTM layer ($z_{F1} \leq h$), one can obtain wind and potential temperature profiles in the form:

$$U_m = \frac{u_*}{k} P_u(\mu, \eta_o, \eta_F), \quad (12-28)$$

$$\Theta_m - \Theta_o = \frac{\text{Pr}_o \theta_*}{k} P_\theta(\mu, \eta_o, \eta_F) \quad (12-29)$$

where $\eta_o = \frac{z_o}{h}$, $\eta_F = \frac{z_{F1}}{h}$, and $\mu = \frac{h}{L}$. For a detailed description of the notation used, refer to Byun (1991) and Byun and Dennis (1995). Initially, the atmospheric stability (μ) is approximated by the analytical solutions of flux-profile relationships described earlier. Then, we compute μ , u_* , and θ_* using Equations 12-28 and 12-29, with the Newton-Raphson iteration. Equation 12-29 is then used to estimate temperatures at heights 1.5 m and 10 m in MCIP.

12.3.1.3 Utilization of Sub-grid Scale Landuse Information

Accurate description of atmospheric turbulence is one of the important elements in modeling the deposition of pollutants. For Eulerian air quality models, grid-average surface roughness based on sub-grid scale landuse information has played an important role in the characterization of the surface condition, which in turn determines intensity of turbulence in the atmosphere. To represent the atmospheric deposition process utilizing the available sub-grid landuse information, Walcek et al. (1986) introduced a method to estimate friction velocity for each landuse patch, which is used in the calculation of the subgrid-scale aerodynamic resistance. Also, several estimation methods have been proposed for the effective roughness length for use in meteorological grid models. Compared with the latter methods that estimate the representative grid values for the given sub-grid information, Walcek et al. (1986) emphasized the description of the sub-grid flux estimation by introducing a somewhat *ad hoc*, but useful assumption. They assumed that the quantity Uu_* is constant both for the cell averaged parameters and for the individual landuse patches, i.e.:

$$Uu_* = U_j u_{*j} = \text{constant}, \quad (12-30)$$

where the non-subscripted variables refer to grid-averaged values while the j -subscripted values refer to the corresponding quantities over individual landuse types. Equation 12-30 is an intuitive expression of the often observed condition that where wind speed is high, the turbulence is low, and vice versa, under similar pressure gradient forcing. Strict validity of Equation 12-30 could be controversial, however, this approach is more realistic than those that assume constant wind or constant friction velocity. In the dimensional analysis point of view, the condition is a statement about the conservation of kinematic energy in the presence of surface friction. A derivation leading to Equation 12-30 is provided below using a combination of the surface layer similarity and the mixing length theories.

The momentum flux is related with mean wind gradient as:

$$-\overline{(u''w'')} = u_*^2 = K_m \frac{\partial U}{\partial z} \quad (12-31)$$

and the eddy diffusivity for momentum is given by:

$$K_m = \frac{ku_*z}{\phi_m(z/L)} \quad (12-32)$$

When we apply assumptions such as steady state flow and horizontal homogeneity of the each landuse patch, the momentum conservation equation can be simplified to give:

$$U \frac{\partial U}{\partial z} + \frac{\partial \overline{u''w''}}{\partial z} = -\frac{1}{\rho} \nabla_z p \quad (12-33)$$

Coriolis forcing is neglected in deriving Equation 12-33 because we are dealing with only the sub-grid scale variation of momentum field.

The right hand side of Equation 12-33 represents the pressure gradient forcing imposed over the grid and is therefore not dependent on sub-grid representation. Within the surface layer, which is treated as a constant flux layer, Equation 12-33 is further simplified to give:

$$U \frac{\partial U}{\partial z} = -\frac{1}{\rho} \nabla_z p = \text{const.} \quad (12-34)$$

Combining Equations 12-31, 12-32 and 12-34, one obtains

$$Uu_* \frac{\phi_m(z/L)}{kz} = \text{const.} \quad (12-35)$$

For the atmosphere at neutral stability, $\phi_m = 1$, and the same expression should be applicable for each landuse patch. Then, Equation 12-35 becomes identical to Equation 12-30 at a given reference height $z = z_r$.

In addition to Equation 12-30, Walcek et al. (1986) assumed that the surface roughness length can be averaged as

$$z_o = \exp\left[\sum f_j \ln z_{oj}\right], \quad (12-36)$$

where f_j 's are fractions of different landuse types in a grid cell. Walcek et al. (1986) stated that Equation 12-36 conforms to a logarithmic wind profile. In reality, however, Equation 12-36 can be derived from a simple geometric averaging and it does not produce a logarithmic wind profile. On the other hand, Mason (1987) suggest an averaging method based on the logarithmic wind profile by introducing a blending height (l_b) concept:

$$\left(\frac{\ln \frac{l_b}{z_o}}{z_o}\right)^2 = \left[\sum \frac{f_j}{\ln(l_b/z_{oj})^2}\right]^{-1} \quad (12-37)$$

Although this approach is a practical averaging method of the roughness length, this by itself cannot be used to estimate landuse-dependent friction velocities. Therefore, here we compare several other roughness length averaging schemes that satisfy both Equation 12-30 and the logarithmic wind profile function for the neutral condition:

$$U(z_r) = \frac{u_*}{k} \ln \frac{z_r}{z_o} \quad (12-38a)$$

and

$$U_j(z_r) = \frac{u_{*j}}{k} \ln \frac{z_r}{z_{oj}} \quad (12-38b)$$

where z_r is the reference height. The objective is to compute landuse specific friction velocities from the cell average wind and friction velocity values while providing a consistent averaging scheme for the roughness length. The simplest method for estimating the grid average values from the sub-grid scale information is using the linear summation with the fractional weight:

$$\langle x \rangle = \sum_j f_j x_j, \quad (12-39)$$

where x_j is a physical quantity and $\sum f_j = 1$. Because $U_j u_{*j} = \text{constant}$, one can rewrite Equation 12-30 with Equation 12-39 as follows:

$$U u_* = U_j u_{*j} = \sum_j f_j U_j u_{*j} = \langle U u_* \rangle \quad (12-40)$$

If the surface wind is a quantity that follows Equation 12-39, a relation between the grid average and sub-grid landuse dependent roughness lengths can be found as:

$$z_o = z_r \exp \left[- \frac{(\sum_j f_j u_{*j} \ln(z_r / z_{oj}))^2}{\sum_j f_j u_{*j}^2 \ln(z_r / z_{oj})} \right] \quad (12-41)$$

In order for the expression to be useful, u_{*j} in Equation 12-41 should be eliminated. From Equations 12-38a-b and 12-40, a simple relation for u_{*j} is found in terms of known quantities:

$$u_{*j} = u_* \left[\frac{\ln(z_r / z_o)}{\ln(z_r / z_{oj})} \right]^{1/2} \quad (12-42)$$

Substituting Equation 12-42 into Equation 12-41, we obtain a simple relation for the effective roughness length that satisfies both the logarithmic wind profile and the linearly-additive wind speed assumptions under the approximation, Equation 12-30:

$$z_o = z_r \exp \left[- \left(\sum f_j \sqrt{\ln(z_r / z_{oj})} \right)^2 \right] \quad (12-43)$$

The reference height z_r needs to be within the regime where the log-linear wind profile can be satisfied. This means that it should be far away from z_o , but still within the surface layer. In the current MCIP, we are using $z_r=10\text{m}$. The new method conserves wind speed and $U_j u_{*j}$ under the linear summation (Equation 12-39). With this assumption the turbulence momentum flux (u_*^2) can be summed linearly when it is scaled with the factor $\left[\ln(z_r / z_o) / \ln(z_r / z_{oj}) \right]$. Depending on the degree of inhomogeneity, this factor can be substantially different from unity, making less consistent with the expectation that fluxes from different patches can be summed up. One may expect that Equation 12-43 is sensitive to the choice of reference height z_r ; however, the average roughness length is not strongly sensitive to the reasonable value of z_r between 1 to 10 m.

An alternative approach to the linearly-additive wind speed assumption is to assume that the sub-grid scale momentum flux can be summed linearly:

$$u_*^2 = \sum_j f_j u_{*j}^2 = \langle u_*^2 \rangle \quad (12-44)$$

Using Equation 12-39 and the logarithmic wind profiles, one can find:

$$\frac{1}{\left[\ln(z_r / z_o) \right]^2} = \sum_j f_j \frac{(U_j / U)^2}{\left[\ln(z_r / z_{oj}) \right]^2} \quad (12-45)$$

In order that Equation 12-45 to be useful, (U_j / U) should be expressed in terms of z_o , z_{oj} , and z_r . This is accomplished by dividing Equation 12-38a with Equation 12-38b and substituting (u_* / u_{*j}) with Equation 12-30 to get:

$$\frac{U_j}{U} = \left[\frac{\ln(z_r / z_{oj})}{\ln(z_r / z_o)} \right]^{1/2} \quad (12-46)$$

This leads to an averaging method for the sub-grid scale roughness length:

$$z_o = z_r \exp \left[- \left(\sum_j \frac{f_j}{\ln(z_r / z_{oj})} \right)^{-1} \right] \quad (12-47)$$

Another popular assumption is that at the reference height (or blending height) the drag coefficients representing the individual landuse patches in a cell can be summed linearly, i.e.:

$$C_D \equiv \frac{u_*^2}{U^2} = \sum_j f_j C_{Dj} = \langle C_D \rangle \quad (12-48)$$

Unlike the two other assumptions introduced, this assumption does not depend on Equation 12-30. The resulting equation for average roughness length is then identical to Equation 12-37.

$$z_o = z_r \exp \left[- \left(\sum_j \frac{f_j}{[\ln(z_r / z_{oj})]^2} \right)^{-1/2} \right] \quad (12-37')$$

Although the assumption in Equation 12-48 has been used often in the literature, it is not intuitive that the sub-grid drag coefficients can be added linearly. The drag coefficient simply quantifies the turbulence exchange characteristic of a landuse patch. By using this assumption together with the Equation 12-30, one can readily show that:

$$C_D = \sum_j f_j C_{Dj} = \sum_j f_j \frac{u_{*j}^2}{U_j^2} = \frac{1}{u_*^2 U^2} \sum_j f_j u_{*j}^4 = \frac{\langle u_*^4 \rangle}{u_*^2 U^2} \quad (12-49)$$

It is difficult to expect that u_*^4 is a physical quantity that can be added linearly. In MCIP, we have implemented both Equations 12-43 and 12-47 as a user option. Results of the comparison of the two recommended methods should be available as the model evaluation project progresses.

12.3.1.4 Boundary Layer Heights

Boundary layer height is a key parameter that determines the domain of atmospheric turbulence in which pollutants disperse. It is used as a fundamental scaling parameter for the similarity theory in the description of atmospheric diffusion characteristics. Estimating PBL height has been one of the key functions of meteorological pre-processors for air quality models. Below, we summarize PBL height estimation algorithms used in MCIP.

Unstable conditions

MCIP estimates the PBL height using the vertical profiles of potential temperature and the bulk Richardson number with an algorithm similar to the one reported in Holtslag et al. (1995). The bulk Richardson number of each model layer with respect to the surface is given as:

$$(Ri_B)^k = g \frac{z_H^k (\Theta_H^k - \Theta_o)}{\Theta_o (U_H^k)^2} \quad (12-50)$$

where subscript H represents values at the layer middle (i.e., half sigma level).

First, the index of the PBL top (k_{PBL}) is determined at the layer when Ri_B first becomes larger than $\max(Ri_B)$. Then the proration factor of the bulk Richardson number relative to $\max(Ri_B)$ is computed with:

$$f_{Ri_B} = \min \left\{ 1, \frac{\max(Ri_B) - (Ri_B)^{k_{PBL}-1}}{(Ri_B)^{k_{PBL}} - (Ri_B)^{k_{PBL}-1}} \right\} \quad (12-51)$$

where $\max(Ri_B)=0.7$ (refer to Table 12-6). Depending on the value of f_{Ri_B} , the index k_{PBL} and f_{Ri_B} are modified as follows:

$$\text{for } f_{Ri_B} > 0.5, f'_{Ri_B} = f_{Ri_B} - 0.5; k'_{PBL} = k_{PBL}, \text{ and}$$

$$\text{for } f_{Ri_B} < 0.5, f'_{Ri_B} = f_{Ri_B} + 0.5; k'_{PBL} = k_{PBL} - 1.$$

Once the fraction and index for the PBL top are determined, we estimate the initial PBL height with:

$$h_{PBL} = f'_{Ri_B} z_F^{k'_{PBL}-1/2} + (1 - f'_{Ri_B}) z_F^{k'_{PBL}-3/2} \quad (12-52)$$

The above proration procedure ensures gradual increase of PBL height. Without the procedure, the resolution of PBL height is limited by the layer thickness of the model. In the RADM preprocessor, the PBL height is determined simply at the layer where the potential temperature first becomes warmer than the surface temperature for convective conditions. Compared with the RADM method, the present method takes into account effects of the wind shear as well.

Stable conditions

For stable conditions, the PBL height is determined by the maximum of the PBL height computed with above method and the stable boundary layer height given by the Zilitinkevich's (1989) formula:

$$h_{PBL} = \frac{1}{2} \left[-\frac{kc_h^2 L}{\lambda_o} + \sqrt{\left(\frac{kc_h^2 L}{\lambda_o}\right)^2 + 4ku_* c_h^2 \frac{L}{f}} \right] \quad (12-53)$$

Limiting PBL heights

Unlike the PBL height estimation algorithms based on temporal integration of surface heat flux (e.g., Carson, 1973; Betts, 1973; Driedonks, 1981), the above diagnostic algorithm could predict temporally disconnected PBL heights when the hourly meteorological data change abruptly. To minimize this effect, following limits on the PBL height are imposed.

1. Compare with PBL height for neutral conditions, and take maximum except for the tropical areas:

$$h'_{PBL} = \max\{h_{PBL}, \lambda_o \frac{u_*}{f}\} \quad (12-54)$$

2. Compare with the urban boundary layer height, which is approximated with:

$$h_{UBL} = (1 - f_{urban}) h_{PBLmin} + f_{urban} h_{UBLmin} \quad (12-55)$$

where f_{urban} is the fraction of urban landuse in a cell. In MCIP, the minimum PBL height for urban area and other landuse types are set to be $h_{UBLmin}=300$ m and $h_{PBLmin}=50$ m. Then, take a maximum of the two to reflect the effect of urban landuse:

$$h'_{PBL} = \max\{h_{PBL}, h_{UBL}\} \quad (12-56)$$

This step is introduced to apply the urban landuse classification, which is consistent with the one used for the emission processing, for the determination of the PBL height.

3. Limit the PBL height with a maximum value ($h_{PBLmax}=3000$ m) in case the temperature profile does not have a capping inversion:

$$h'_{PBL} = \min\{h_{PBL}, h_{PBLmax}\}. \quad (12-57)$$

12.3.1.5 Aerodynamic Resistances

Aerodynamic resistance describes the ability of the atmospheric turbulence to transport pollutant to the surface for the deposition. In this regard, it may well be described with the probability concept. If 100 particles, say, are at height 20m, how many of them can reach the surface to be available for deposition during a given time interval? Or, what is the transport rate of particles in the air to the surface? The ratio represents the maximum potential deposition rate of particles subjected to atmospheric turbulence. However, even those particles which arrive at the surface may not all be deposited because of other resistances, which usually are parameterized using characteristics of surface and gaseous elements.

There have been many efforts to compare different formulations for dry deposition velocities. While there are a lot of uncertainties in describing atmospheric processes, the different aerodynamic resistance formulas in the literature are mainly originated from the differences in the applications and approximations of the same PBL theories and formulas. Among the components involved in atmospheric resistance computation, formulations for aerodynamic resistance have the least controversy. To compute the aerodynamic resistance, the parameterization of the eddy diffusivity for the PBL should be known. The eddy-diffusivity formulations used in the derivation of aerodynamic resistance are discussed below.

Eddy diffusivity formulations

The similarity theory suggests that eddy diffusivity in the surface layer for heat flux is given by:

$$K_h = \frac{ku_*z}{\phi_h(z/L)} \quad (12-58)$$

The profile function ϕ_h is defined in Equations 12-12b and 12-13b. Eddy diffusivity in the PBL (above the surface layer) (Brost and Wyngaard 1978) is given as:

$$K_h = \frac{ku_*z(1 - z/h_{PBL})^{3/2}}{\phi_h(z/L)} \quad (12-59a)$$

for stable atmosphere ($z/L > 0$), and as:

$$K_h = kw_*z\left(1 - \frac{z}{h_{PBL}}\right) \quad (12-59b)$$

for unstable atmosphere ($z/L \leq 0$), where the convective velocity scale w_* is defined as

$$w_* = \left[-\frac{g}{\Theta_o} h_{PBL} u_* \theta_* \right]^{1/3} \quad (12-60)$$

Aerodynamic resistance formulations

We often characterize the ability of turbulent atmosphere to carry pollutants to the vegetation or other surface elements using the aerodynamic resistance concept. Certain meteorological models may use the resistance representation of surface exchange processes in lieu of the conventional bulk aerodynamic methods and the aerodynamic resistance is available as a part of meteorological data with other PBL parameters. Conversely, there are models that do not predict resistances and related parameters needed. In such cases, we need to estimate it using PBL parameters and profiles of state variables.

The aerodynamic resistance (R_a) and sub-layer resistance (R_b) are parameterized in terms of friction velocity and surface roughness (Walcek, 1987; Chang et al., 1987 and 1990; Wesely, 1989; Wesely and Hicks, 1977). Although some consider the estimation of aerodynamic resistance as an integral part of the dry deposition velocity computation, we treat the aerodynamic resistance as an independent element that characterizes the effects of atmospheric turbulence. Here, we provide a set of integrated equations, which allow robust estimation of aerodynamic resistance compared with the method based on the nonintegrated form, which sometimes provides negative fluxes for unstable conditions. Refer to Byun and Dennis (1995) for details.

General formulation for the aerodynamic resistance at the deposition height z_{dep} (where concentration is represented) is divided into two components; the resistance in the surface layer (whose top is at z_{SL} , height of the surface layer) and the resistance in the PBL above the surface layer:

$$R_a = \int_{z_o}^z \frac{dz}{K_z(z)} = \int_{z_o}^{z_{SL}} \frac{dz}{K_z(z)} + \int_{z_{SL}}^{z_{dep}} \frac{dz}{K_z(z)} = R_{aSL} + R_{aPBL} \quad (12-61)$$

(a) For stable conditions:

$$R_{aSL} = \frac{\text{Pr}_o}{ku_*} \left[\ln\left(\frac{z_{SL}}{z_o}\right) + \beta_h \frac{z_{SL} - z_o}{L} \right] \quad (12-62a)$$

$$R_{aPBL} = \frac{\text{Pr}_o}{ku_*} \left[\frac{2(\beta + 1)}{\sqrt{1 - \eta_{dep}}} - \frac{2(\beta + 1)}{\sqrt{1 - \eta_{SL}}} + \ln \left| \frac{(-1 + \sqrt{1 - \eta_{dep}})(1 + \sqrt{1 - \eta_{SL}})}{(1 + \sqrt{1 - \eta_{dep}})(-1 + \sqrt{1 - \eta_{SL}})} \right| \right], \quad (12-62b)$$

where $\beta = \beta_h \frac{h_{PBL}}{L}$, $\eta_{dep} = \frac{z_{dep}}{h_{PBL}}$ and $\eta_{SL} = \frac{z_{SL}}{h_{PBL}}$.

(b) For unstable conditions:

$$R_{aSL} = \frac{\text{Pr}_o}{ku_*} \left[\ln \left| \frac{(-1 + \sqrt{1 + \gamma_h z_{SL}/L})(1 + \sqrt{1 + \gamma_h z_o/L})}{(1 + \sqrt{1 + \gamma_h z_{SL}/L})(-1 + \sqrt{1 + \gamma_h z_o/L})} \right| \right] \quad (12-63a)$$

$$R_{aPBL} = \frac{1}{kw_*} \ln \left[\frac{\eta_{dep}(1 - \eta_{SL})}{\eta_{SL}(1 - \eta_{dep})} \right]. \quad (12-63b)$$

12.3.2 Dry Deposition Velocities

The term dry deposition represents a complex sequence of atmospheric phenomena resulting in the removal of pollutants from the atmosphere to the surface of the earth. The rate of transfer of pollutants between the air and exposed surfaces is controlled by a wide range of chemical, physical, and biological factors, which vary in their relative importance according to the nature and state of the surface, characteristics of the pollutant, and the strength of turbulence in the atmosphere. The complexity of the individual processes involved and the variety of possible interactions among them prohibits simple generalization of the process. Nevertheless, a "deposition velocity," analogous to a gravitational falling speed is of considerable use. In practice, the knowledge of dry deposition velocities enables fluxes to be estimated from airborne concentrations. Two dry deposition estimation methods, that from Wesely (1989) currently as implemented in CMAQ, and the new Models-3/CMAQ approach are presented.

12.3.2.1 RADM Method

The RADM dry deposition module in MCIP calculates deposition velocities of sixteen chemical species (Table 12-7). It requires various ancillary 2-D meteorology fields such as the PBL height, mixing scale velocities, Monin-Obukov length, etc. They are usually estimated from horizontal wind components, temperature and humidity profiles. The dry deposition flux of each chemical species from the atmosphere to surface is calculated in the CCTM by multiplying the concentration in the lowest model layer with the dry deposition velocity. The dry deposition velocity (V_d) is computed from the resistance-in-series method;

$$V_d = (R_a + R_b + R_c)^{-1} \quad (12-64)$$

where R_a is the aerodynamic resistance, R_b is the quasi-laminar boundary layer resistance, and R_c is the canopy (surface) resistance. Refer to Figure 12-7. V_d is usually estimated from a series of resistances to vertical transfer and surface uptake. Aerodynamic resistance (R_a) is a function of turbulent transfer in the atmospheric surface layer and can be estimated in several ways depending on the instrumentation used or parameterizations provided.

The canopy resistances (R_c) for SO_2 and O_3 are estimated from available measurements as a function of season, insolation, surface wetness, and land type (Walcek et al., 1986; Shieh et al., 1979; Fowler, 1978). The surface resistances for all other gaseous species, due to the lack of extensive measurements, are qualitatively scaled to the SO_2 and O_3 surface resistances according to their reactivity and solubility. The surface resistance for particulate sulfate is parameterized in terms of stability and friction velocity in the surface layer (Wesely, 1989), based on limited studies that do not include water surfaces. In CMAQ this method only applies to the treatment of surrogate gas-phase representation of sulfate species. Size dependent deposition velocities for particle depositions are estimated inside the CCTM's aerosol module. See Chapter 10 of this document and Binkowski and Shankar (1995) for details.

The laminar sub-layer resistance (R_b) depends on the landuse specific friction velocity and molecular characteristics of gases. Using the landuse dependent friction velocity or the cell average friction velocity, R_b 's for heat (R_{bh}) and trace gases (R_{bx}) are estimated with the Schmidt number (Sc):

$$R_{bh} = \frac{2}{ku_*} Sc^{2/3} \quad (\text{for heat}) \quad (12-65a)$$

$$R_{bx} = \frac{2}{ku_*} Sc_x^{2/3} \quad (\text{for trace gas species}) \quad (12-65b)$$

where Schmidt number is defined as the kinematic viscosity of air ($\nu = 0.146 \text{ cm}^2\text{s}^{-1}$) divided by molecular diffusivity (i.e., $Sc = \nu / D_g$ for heat and $Sc_x = \nu / D_{gx}$ for trace gases). Here, ν is kinematic viscosity of air; D_g is molecular diffusivity of air (heat); and D_{gx} is molecular diffusivity of trace species. For heat, the molecular thermal diffusivity (D_g) is $0.206 \text{ cm}^2\text{s}^{-1}$; for water vapor, molecular diffusivity (D_{gw}) is $0.244 \text{ cm}^2\text{s}^{-1}$; and, for ozone molecular diffusivity (D_{gO_3}) is $0.159 \text{ cm}^2\text{s}^{-1}$ (molecular diffusivities of other chemical species are included in the model).

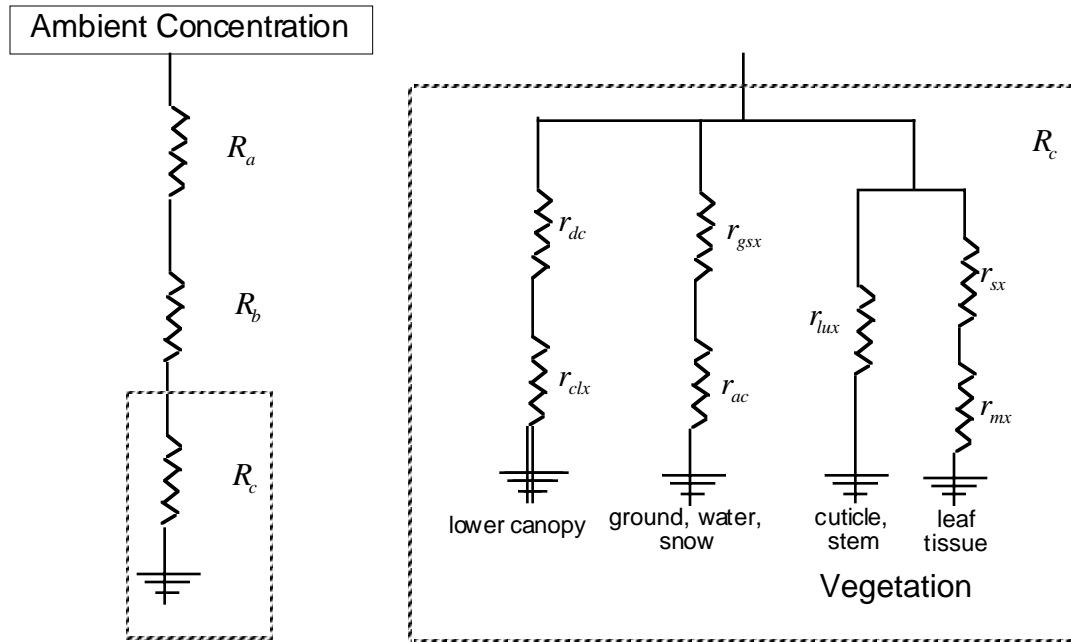


Figure 12-7. Schematic Diagram of Pathway Resistances Used in RADM Dry Deposition Model Resistances with subscript x are for different chemical species.

R_c represents the canopy resistance defined as:

$$R_c = \left(\frac{1}{r_{sx} + r_{mx}} + \frac{1}{r_{lux}} + \frac{1}{r_{dc} + r_{clx}} + \frac{1}{r_{ac} + r_{gsx}} \right)^{-1} \quad (12-66)$$

where r_{sx} = stomatal resistance;

r_{mx} = mesophyl resistance;

r_{lux} = resistance of the outer surface of leaves in the upper canopy;

r_{dc} = resistance for the gas transfer affected by buoyant convection in canopy;

r_{clx} = lower canopy resistance (uptake pathways at the leaves, twig, etc.);

r_{ac} = resistance that depends on the canopy height; and

r_{gsx} = resistance of soil, leaf litter, and other ground materials.

Stomatal resistance for water is obtained using following equation:

$$r_{sw} = r_{s \min} \left(1 + \left[\frac{200}{0.1 + G_{sw}} \right]^2 \right) \left(\frac{400}{T_c(40 - T_c)} \right) \quad (12-67)$$

where r_{sw} = stomatal resistance for water;

$r_{s \min}$ = minimum stomatal resistance for water, specified in Table 12-7;

T_c = surface air temperature in the canopy in Celsius temperature; and
 G_{sw} =- solar radiation reaching at the canopy in W/m² unit.

Then stomatal resistance for trace gas species is obtained with:

$$r_{sx} = r_{sw} \frac{D_{gw}}{D_{gx}} \quad (12-68)$$

where D_{gw} is the molecular diffusivity of water. Ratio of molecular diffusivity of water to that of each trace species is provided in Table 12-7.

The mesophyl resistance is parameterized as:

$$r_{mx} = \left(\frac{H_{*x}}{3000} + 100f_{ox} \right)^{-1} \quad (12-69)$$

where H_{*x} is Henry's gas constant (in mole atm⁻¹) for the species, and f_{ox} is the reaction intensity factor.

Both the Henry's gas constants and reaction intensity factors are provided in Table 12-7 as well. r_{lux} is related with the upper canopy resistance for water (r_{lu}) which is provided in Table 2 of Wesely (1989) as:

$$r_{lux} = r_{luw} (10^{-5} H_{*x} + f_{ox})^{-1} \quad (12-70)$$

r_{dc} is parameterized in terms of the available solar radiation and the slope of local terrain:

$$r_{dc} = 100[1 + 1000(G_{sw} + 10)^{-1}](1 + 1000\theta)^{-1} \quad (12-71)$$

where θ is the slope of local terrain in radians. r_{clx} and r_{gsx} are estimated based on the respective resistance values for SO_2 and O_3 as follows:

$$r_{clx} = \left(\frac{H_{*x}}{10^5 r_{clS}} + \frac{f_{ox}}{r_{clO}} \right)^{-1} \quad (12-72a)$$

$$r_{gsx} = \left(\frac{H_{*x}}{10^5 r_{gsS}} + \frac{f_{ox}}{r_{gsO}} \right)^{-1} \quad (12-72b)$$

where subscript S and O are for SO_2 and O_3 , respectively. All of these values, and r_{ac} (the resistance that depends on the canopy height) are landuse dependent and listed in Table 2 of Wesely (1989).

Table 12-7. Gaseous Species Treated in RADM Dry Deposition Module and Their Properties Relevant to Estimating Resistance Components as Implemented in MCIP (Modified from Wesely, 1989.)

Gaseous species	Symbol	D_{gw} / D_{gx}	H_{*x} (mole atm ⁻¹)	f_{ox}
Sulfur dioxide	SO_2	1.9	1.0×10^5	0.0
Sulfate	SO_4	-	-	-
Nitrogen dioxide	NO_2	1.6	0.01	0.1
Nitric oxide	NO	1.3	0.002	0.0
Ozone	O_3	1.6	0.01	1.0
Nitric acid vapor	HNO_3	1.9	1.0×10^{14}	0.0
Hydrogen peroxide	H_2O_2	1.4	1.0×10^5	1.0
Acetaldehyde	ALD	1.6	15.0	0.0
Formaldehyde	$HCHO$	1.3	6.0×10^3	0.0
Methyl hydroperoxide	OP	1.6	240.0	0.1
Peroxyacetic acid	PAA	2.0	540.0	0.1
Formic acid	ORA	1.6	4.0×10^6	0.0
Ammonia	NH_3	1.0	2.0×10^4	0.0
Peroxyacetyl nitrate	PAN	2.6	3.6	0.1
Nitrous acid	$HONO$	1.6	1.0×10^5	0.1
Carbon monoxide	CO	1.2	0.001	0.0

12.3.2.2 Models-3/CMAQ Dry Deposition Model

The Models-3/CMAQ dry deposition (M3DDEP) module estimates dry deposition velocities according to the same electrical resistance analog represented by Equation 12-64. M3DDEP uses common components with the new land-surface model that has recently been added to MM5. Specifically, the aerodynamic resistance and the canopy or bulk stomatal resistance are the same as those used in the modified MM5 (MM5PX) for computing evapotranspiration. Since the land surface scheme includes soil moisture and has an indirect nudging scheme for improving soil moisture estimates, the resulting stomatal resistance estimates should be better than those achieved with a stand alone dry deposition model. Pleim and Xiu (1995) give a description of an early prototype of the land surface model which is now coupled to MM5. Pleim et al (1996) and Pleim et al. (1997) briefly describe the dry deposition model and some studies comparing model results to field measurements of surface fluxes and PBL heights. The description which follows here is partially drawn from these sources.

When using the M3DDEP option in the CMAQ system the aerodynamic resistance, as well as the bulk stomatal resistance (r_{stbw} ; discussed below) is provided to MCIP from the MM5PX. Note that these parameters are computed as part of the land surface model in the MM5PX and are not available from the standard MM5. In MM5PX the aerodynamic resistance R_a is computed assuming similarity with heat flux such that:

$$R_a = \rho C_p (\Theta_g - \Theta_1) / H - R_{bh} \quad (12-73)$$

where R_{bh} is the quasi-laminar resistance for heat (defined in Equation 12-65a), Θ_g and Θ_1 are potential temperature of the ground surface and the air, respectively, in the lowest model layer, and H is the sensible heat flux defined in Equation 12-25. If the sensible heat flux is very small (as during transition periods) the surface layer theory for neutral conditions is used as follows:

$$R_a = \frac{\text{Pr}_o}{ku_*} \ln\left(\frac{z_1}{z_o}\right) \quad \text{for } |H/(\rho C_p)| < 10^{-15} \text{ [K m s}^{-1}\text{]} \quad (12-74)$$

where z_1 is the height of model layer 1 and z_o is the roughness length. The heat and momentum fluxes are derived from flux-profile relationships as in the MM5 (see Grell et al., 1995). The quasi-laminar boundary layer resistance accounts for diffusive transfer across a thin laminar layer adjacent to surfaces. Because of the no-slip condition, turbulent eddies cannot penetrate to a surface. Therefore, there exists a thin layer of non-turbulent air where molecular diffusion is the primary mechanism for transfer. While this concept is not relevant for momentum, it is relevant for any quantity that directly interacts with the surface such as heat, moisture, and chemical deposition. Therefore, for these quantities, the addition of a resistance based on molecular diffusion is necessary. Deposition layer resistance varies by the transported quantity because of differences in molecular diffusivity, which is defined earlier in Equations 12-65a and b.

The total surface resistance to dry deposition (R_s) has several components including bulk stomatal resistance (r_{stb}), dry cuticle resistance (r_{cut}), wet cuticle resistance (r_{cw}), ground resistance (r_g), and in-canopy aerodynamic resistance (r_{lc}):

$$R_s = \left[\frac{f_v}{r_{stb}} + LAI \left(\frac{f_v(1-f_w)}{r_{cut}} + \frac{f_v f_w}{r_{cw}} \right) + \frac{1-f_v}{r_g} + \frac{f_v}{r_{lc} + r_g} \right]^{-1} \quad (12-75)$$

Bulk stomatal resistance (r_{stb}), vegetation fractional coverage (f_v), leaf area index (LAI) and fractional leaf area wetness (f_w) are all provided by MM5PX since the same parameters are used in the land surface scheme. Figure 12-8 shows a schematic representation of Equation 12-75. Note that r_{stb} , as output from MM5PX, is already a combination of stomatal resistance on a leaf area basis r_{st} , mesophyll resistance r_m , and LAI as described below. A key component of the land surface model in the MM5PX is the parameterization of the bulk stomatal resistance that is used to compute evapotranspiration. The bulk stomatal resistance for water vapor is read in to MCIP from MM5PX and adjusted for chemical dry deposition in the M3DDEP model by weighting with the ratio of molecular diffusivities for water vapor and the chemical species:

$$r_{stbc} = \frac{D_{gw}}{D_{gx}} r_{stbw} \quad (12-76)$$

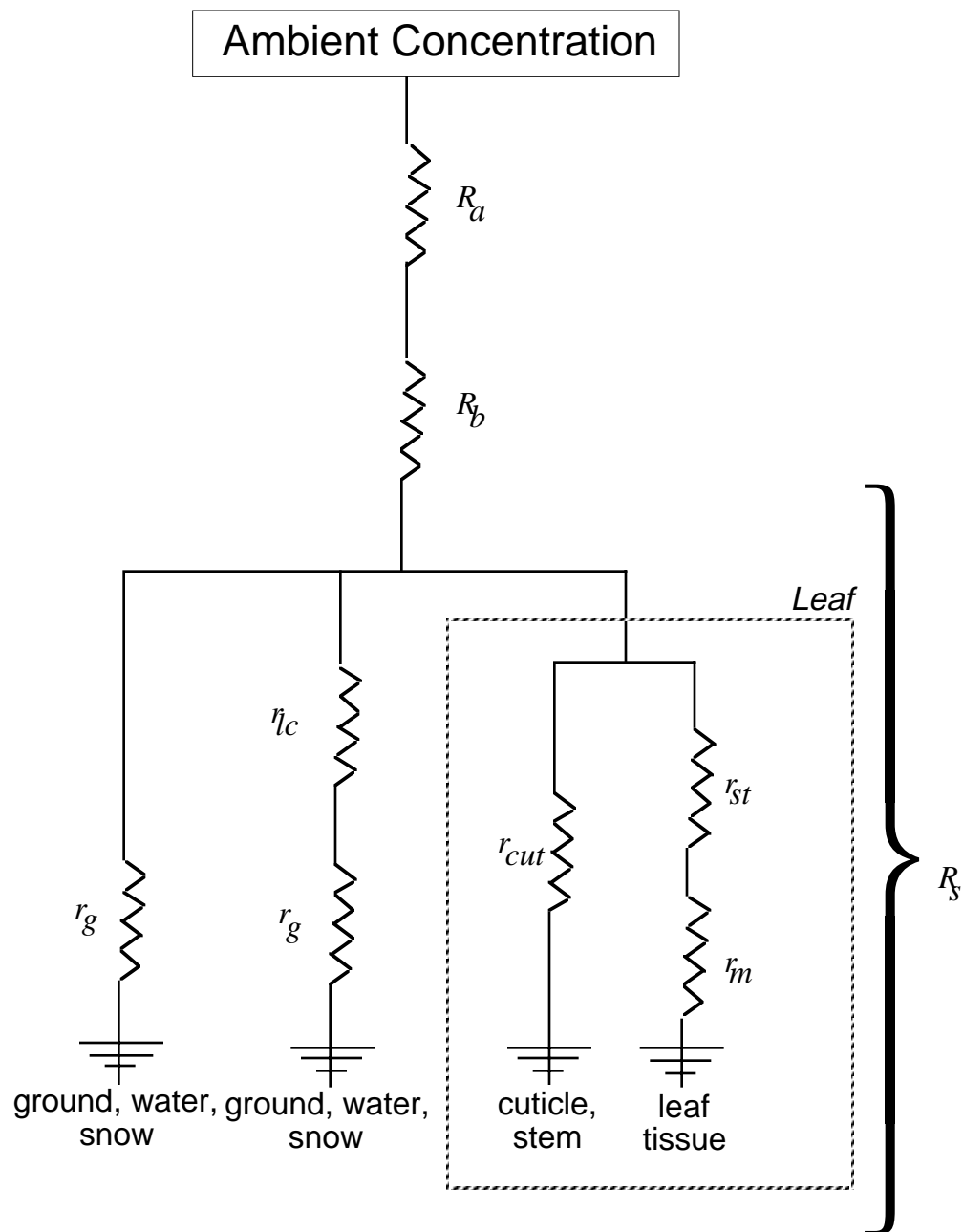


Figure 12-8. Schematic Diagram of Pathway Resistances Used in Models-3/CMAQ Dry Deposition Model.

In general, the bulk stomatal resistance is related to leaf based stomatal resistance as:

$$r_{stb} = \frac{P_s}{LAI} (r_{st} + r_m) \quad (12-77)$$

where P_s is a shelter factor to account for shading in denser canopies. For water vapor and many chemical species, such as O_3 and SO_2 , r_m is assumed to be zero, however, for many less soluble

species a non-zero value should be used. The shelter factor is given by: $P_s = 0.3 LAI + 0.7$ with a minimum of $P_s = 1.0$. Leaf scale stomatal resistance, computed as:

$$r_{st} = \frac{r_{st \min}}{F_1(PAR)F_2(w_2)F_3(RH_s)F_4(T_a)} \quad (12-78)$$

depends on four functions of environmental factors which influence stomatal function, and the minimum stomatal resistance ($r_{st \min}$) which depends on vegetative species. The minimum stomatal resistance is a bulk parameter which reflects the maximum conductance of a leaf per unit area under unstressed conditions (well watered, full sunlight, and optimal temperature and humidity). This parameter is specified in the model according to vegetation type. The key to the model's ability to simulate stomatal conductance in real world conditions is the four environmental stress functions, F_{1-4} in Equation 12-78. This kind of stomatal model, with independent empirical stress functions, is often called a Jarvis-type model after Jarvis (1976). Specifically, the land surface model in MM5PX is based on Noilhan and Planton (1989) (hereafter referred to as NP89) with many subsequent modifications. The radiation stress function is:

$$F_1 = \frac{1 + f}{f + r_{st \min} / r_{st \max}} \quad (12-79)$$

with $f = 0.55 \frac{2R_G}{R_{GL}}$ where $r_{st \max}$ is maximum stomatal resistance which is an arbitrarily large number (5000 s/m), R_G is solar radiation at the surface and the 0.55 factor is an approximation for the photosynthetically active portion, and R_{GL} is a limit value of 30 W/m² for forest and 100 W/m² for crops according to NP89. The only difference from the F_1 in NP89 is that the dependence on LAI has been removed since the effects of leaf shading within the canopy are now accounted for by the shelter factor in Equation 12-77. Therefore, the F_1 as defined here represents the effects of sunlight on an individual leaf rather than the integrated effect on a canopy. The functions of root zone soil moisture and air temperature (F_2 and F_4) were modified to follow the form of logistic curves as suggested by Avissar et al. (1985). Logistic curves are "S"-shaped and therefore good for representing a smooth transition from one state to another. Also, logistic curves can be defined with varying degrees of abruptness, from an almost linear transition to an almost threshold behavior, and can be altered while maintaining differentiability. The function of root zone soil moisture (w_2) is:

$$F_2 = 1 / \left(1 + \exp \left[-5.0 (w_{af} + b_w) \right] \right) \quad (12-80)$$

where the available soil moisture fraction is:

$$w_{af} = \frac{w_2 - w_{wlt}}{w_{fc} - w_{wlt}}$$

and the half point of the function (where $F_2 = 0.5$) is:

$$b_w = (w_{fc} - w_{wlt})/3 + w_{wlt}$$

where w_{wlt} is the wilting point and w_{fc} is the field capacity. All soil moisture values (w) are in volumetric fraction. In many previous models, including NP89, Jacquemin and Noilhan (1990), Wetzal and Chang (1988), Mihailovic et al. (1993), Sellers et al. (1986), and Avissar et al (1985), the function of air humidity (F_3) is expressed in terms of vapor pressure deficit between the inside of the leaf, assumed to be saturated at leaf temperature, and ambient air humidity ($vpd = e_s(T_s) - e_a$). However, recent advances in plant physiology research have led to a new generation of stomatal models based on leaf photosynthesis (Sellers et al., 1997) in which stomatal conductance ($g_{st} = 1/r_{st}$) is a linear function of relative humidity at the leaf surface (Collatz et al., 1991):

$$g_{st} = g'_{st}RH_s + b \quad (12-81)$$

where g'_{st} is the stomatal conductance at $RH_s = 1$ and b is the minimum stomatal conductance at $RH_s = 0$. Clearly, it makes more sense that stomata react to the humidity at the surface of the leaf rather than the ambient air humidity at some height above the canopy. Although, a physical mechanism for this linear relationship to leaf surface RH has not been determined, experimental data shows it to be a very good fit (Ball et al., 1987). Since leaf surface relative humidity is neither an easily measured nor a modeled quantity, it must be computed from other parameters. According to the electrical analog, the humidity at the leaf surface (q_l) is an intermediate potential between the ambient air humidity (q_a) and the leaf interior humidity, $q_s(T_s)$, where T_s is surface temperature and q_s is saturation humidity (see Figure 12-9 for the schematics of the derivation). Assuming constant flux from the ambient air to the leaf interior, the relative humidity at the leaf surface ($RH_s = q_l/q_s(T_s)$) can be represented as:

$$RH_s = \frac{q_a g_a + q_s g_{st}}{(g_{st} + g_a)q_s} \quad (12-82)$$

where g_a is the air conductance ($1/(R_a + R_{bw})$) and q_s is short hand for $q_s(T_s)$. If we assume that b in Equation 12-81 is small compared to g_{st} , which will be true in all but the driest conditions, and g'_{st} is the result of Equation 12-78 without the effects of humidity ($g'_{st} = F_3/r_{st}$), then RH_s is the solution of a quadratic equation which can be computed, once all the other components of Equation 12-78 have been determined. F_3 is equal to RH_s but with a minimum imposed at 0.25.

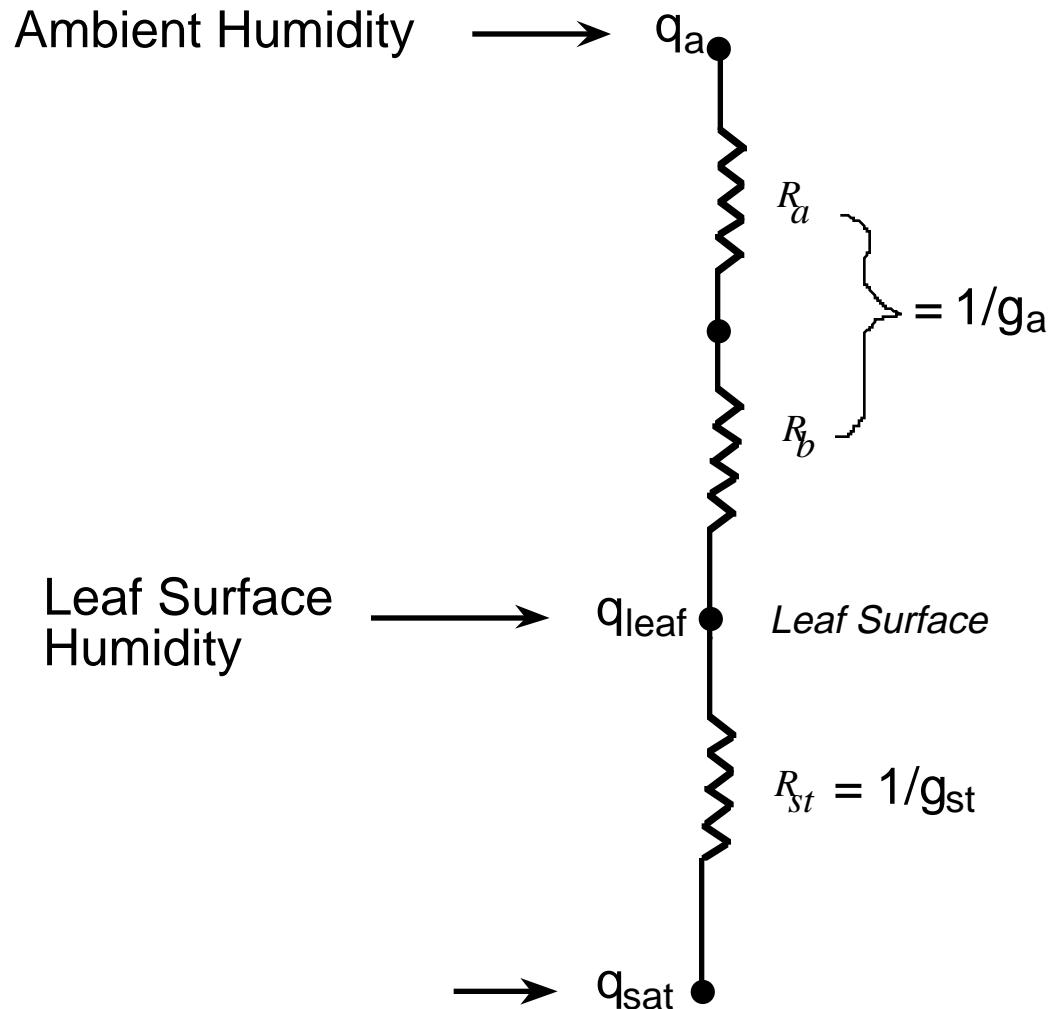


Figure 12-9. Derivation of Leaf Surface Relative Humidity

The fourth environmental stress function (F_4) is related to ambient temperature. Again, we deviate from the NP89 formulation which used a quadratic function peaking at the optimal temperature of 298 K. Instead, we followed the method of Avissar et al. (1985) which results in a function with a plateau over a range of optimal temperatures, the idea being that temperature (T_a) inhibits stomatal function only at extremes of heat or cold. F_4 is defined as:

$$F_4 = 1 / (1 + \exp[a_T(T_a - b_T)]) \quad (12-83)$$

where $a_T = -0.41$ and $b_T = 282.05$ K for $T_a \leq 302.15$ K and $a_T = 1.18$ and $b_T = 314$ K for $T_a > 302.15$ K. Note that the high side of the function extends into higher temperatures than suggested by Avissar et al. (1985) who used a $b_T = 307.95$. The current function is very similar to the function used by Rochette et al. (1991) and is close to the high side of the NP89 F_4 function.

Resistances for all of the non-stomatal dry deposition pathways in the M3DDEP module of MCIP are similar to the dry deposition model developed for the Acid Deposition and Oxidant Model

(ADOM) by Pleim et al. (1984) and later evaluated and modified by Padro et al. (1991). As in ADOM, surface resistances to ground and leaf cuticles are scaled relative to the most well measured chemical species such as SO_2 and O_3 . The term used for the scaling factor: *relative reactivity* has caused considerable confusion since many users try to find a chemical definition for this parameter. This factor has no chemical definition but is simply meant to be a relative scaling factor for the removal rate of different species at the ground or cuticle surfaces. It is assumed that the relative propensity to deposit to different surfaces is similar, so that the same scaling factor can be used for ground and cuticles:

$$r_g = r_{go} A_o/A \quad (12-84a)$$

$$r_{cut} = r_{cuto} A_o/A \quad (12-84b)$$

where r_{go} and r_{cuto} are the ground and cuticle resistances, respectively, for the reference chemical species (usually SO_2 or O_3) and A_o and A are the relative reactivities for the reference species and the modeled species, respectively.

One improvement from the original ADOM model is the inclusion of an in-canopy aerodynamic resistance which is added in series to the ground resistance for the vegetated portion of the modeled area (f_v) according to Erissman et al. (1994):

$$r_{lc} = 14 LAI h_c / u_* \quad (12-85)$$

where h_c is the height of the canopy. For wet or partially wet canopies (f_w), the surface resistance to wet cuticle is estimated as:

$$r_{cw} = r_{cwo} K_H / \alpha^* \quad (12-86)$$

where K_H is the nondimensional Henry's law constant and α^* is an aqueous dissociation factor. The empirical factor (r_{cwo}) is set to $2.4 \times 10^8 \text{ s m}^{-1}$, which is similar to Wesely (1989). For O_3 , r_{cw} is set to 1250 s m^{-1} based on field measurements. The pH of the canopy water can be specified to compute α^* for species such as SO_2 and NH_3 which readily dissociate. The canopy wetness fraction (f_w) is provided by the surface model in MM5PX. For deposition to open water, the ground resistance is replaced by a water surface resistance according to Slinn et al. (1978):

$$r_{gw} = K_H / (4.8e-4 \alpha^* u_*) \quad (12-87)$$

The parameters needed for the non-stomatal part of this model are quite uncertain for many chemical species. Our latest estimation of these parameters for the species in the RADM2 chemical mechanism for which dry deposition is considered to be an important process are presented in Table 12-8. The Henry's law coefficients in Table 12-8 are in non-dimensional form as the ratio of gas- to aqueous-phase.

Molecular diffusivity and Henry's law have the least amount of uncertainty since these have definite chemical definitions and can be experimentally determined. Relative reactivity, however,

is less well defined and is estimated according to experimental and modeling studies in the published literature. The only organic species for which dry deposition is considered significant are the aldehydes, peroxides, and acids, all of which are soluble in water. For these organic lumped species the numbers for reactivity are merely educated guesses.

Table 12-8. Chemical Dependent Parameters for M3DDEP

<i>Species</i>	<i>Diff</i> (<i>cm</i> ² / <i>s</i>)	α^* (<i>dimensionless</i>)	<i>Reactivity</i> (<i>dimensionless</i>)	<i>Henry's law</i> ^{&} (K_H) (<i>dimensionless</i>)
<i>SO</i> ₂	0.1509	1000.0	8.00	0.04
<i>NO</i> ₂	0.1656	1.0	2.00 [@]	3.5
<i>O</i> ₃	0.1594	10.0	16 [@]	2.0
<i>H</i> ₂ <i>O</i> ₂	0.2402	1.0	30 [@]	4.e-7
<i>HNO</i> ₃	0.1628	1.0e9	800 [@]	2.7e-7
<i>NH</i> ₃	0.2626	1.0e5	10.0	6.6e-4
<i>PAN</i>	0.0938 [#]	1.0	4.0	0.01
<i>NO</i>	0.1877 [#]	1.0	2.0 ⁺	23.
<i>HCHO</i>	0.1877 [#]	1.0	10.0 ⁺	4.E-6
<i>ALD</i>	0.1525 [#]	1.0	10.0 ⁺	2.7e-3 [#]
<i>OP</i>	0.1525 [#]	1.0	10.0 ⁺	1.7e-4 [#]
<i>PAA</i>	0.1220 [#]	1.0	20.0 ⁺	7.6e-5 [#]
<i>ORA</i>	0.1525 [#]	1.0	20.0 ⁺	1.0e-8 [#]
<i>HONO</i>	0.1525 [#]	1.0	20.0 ⁺	4.1e-7 [#]
<i>CO</i>	0.2033 [#]	1.0	5.0	40.

[@] Updates based on literature review

[#] Diff and H based on Wesely (1989) same as RADM

⁺ Estimated

[&] gaseous phase value/aqueous phase value

The dissociation factor (α^*) is simply defined as the ratio of the effective Henry's law coefficient to the actual Henry's law coefficient. In this case, the effective coefficient is meant to include both aqueous dissociation and aqueous reactions. The α^* s for *SO*₂ and *NH*₃ are particularly important since their solubilities are greatly effected by dissociation, which is a strong function of *pH* for both species. Therefore, the model enables the user to specify the *pH* of the rainwater wetting the canopy and let the model compute α^* rather than use the default values in Table 12-7. The α^* for *O*₃ is also important since *O*₃ is only slightly soluble so any enhancement can have a large effect. The value of 10 for *O*₃ is meant to account for, very approximately, aqueous reactions such as the oxidation of *S(IV)* to *S(VI)*. Clearly, all of these parameters are quite uncertain and subject to revision.

The main advantage of the M3DDEP model over the many similar models previously used in air quality modeling is the coupling to the land surface model for description of the stomatal pathway. This is a very important feature for certain chemical species, particularly *O*₃ and *SO*₂, which have

been shown experimentally to have a strong stomatal pathway components. Several studies with this model have demonstrated its ability to realistically simulate both latent heat flux, with a large fraction from evapotranspiration, and ozone dry deposition, over corn and soybeans (Pleim et al., 1996; Pleim et al., 1997). These studies are continuing and are being extended to other chemical species (SO_2), and land-use types (deciduous and coniferous forests).

12.3.3 Cloud Parameters and Solar Radiation

Cloud information is developed and used in many different ways throughout the Models-3 CMAQ system. For example, MM5 includes parameterizations related with subgrid convective clouds, grid resolved cloud water and microphysics, and cloud effects on radiation. The CCTM needs cloud information for photolysis, convective transport, and aqueous chemistry. Therefore, MCIP has an important role in providing cloud information to CTMs by either propagating information from upstream processors (MM5) or by parameterization.

MCIP has multiple cloud parameterizations and functions depending on the options selected. There are currently two main options related to MM5 runs, either the standard MM5 version 2.6 which does not include cloud cover and radiation parameters in its output, and MM5PX which does. Later versions of MM5 (2.7, 2.8, and 2.9) also output these additional parameters. However, when MM5v2.6 or earlier versions are used, it is necessary to compute these parameters in MCIP. Incident solar radiation at the surface is an important output from MCIP since it is used to estimate biogenic emissions in the emissions processor.

Another cloud function in MCIP is to diagnose cloud information (such as cloud top, cloud base, liquid water content, and cloud coverage) which is passed to the CCTM to adjust actinic fluxes for computation of photolysis rates. This function is executed regardless of the choice of the MM5 version used. In addition, grid resolved cloud water and rain water are propagated through MCIP from the MM5 output to CMAQ for use in aqueous chemistry and for photolysis calculations at the 4 km grid resolution.

12.3.3.1 Cloud Coverage

The fractional cloud coverage scheme currently used in MCIP is the same as used in MM5PX and similar to the scheme used in the standard MM5. Cloud cover fraction (f_c^k) above the boundary layer is computed at each vertical model level k , according to Geleyn et al. (1982), as:

$$f_c^k = \left[\frac{RH^k - RH_c}{1 - RH_c} \right]^2 \quad (12-88)$$

where RH_c is the critical relative humidity defined as a function of σ as:

$$RH_c = 1 - 2\sigma_c(1 - \sigma_c)[1 + 1.732(\sigma_c - 0.5)]$$

where $\sigma_c = p^k / p^{k_{PBL}}$.

We have modified the Geleyn scheme to avoid the overprediction of clouds in well-mixed boundary layers. Within the convective boundary layer (CBL) when $RH > RH_c$ the cloud cover is estimate by:

$$f_c^k = 0.34 \frac{RH^k - RH_c}{1 - RH_c} \quad (12-89)$$

where the critical relative humidity (RH_c) within the CBL is set to be 0.98. The factor 0.34 is from the suggestion that convective mixing induced clouds within the CBL should not exceed the fractional area of the updrafts at top of CBL, which large eddy simulations estimate to be about 34% (Schumann, 1989; Wyngaard and Brost, 1984) when inactive clouds are disregarded. The resulting layered cloud fractions, from Equations 12-88 and 12-89, are used for both functions; namely, to be used in the surface radiation calculation when these parameters are not read from MM5, and to derive the cloud parameters needed for the photolysis calculations.

For the surface radiation calculation, the layered cloud cover fractions are aggregated into the same three broad vertical cloud layers (low, middle, and high) as in MM5, assuming maximum overlap. Each layer is defined by pressure such that the low layer is between 97 and 80 kPa, the middle layer is between 80 and 45 kPa and the high layer is above 45 kPa. These three cloud layer fractions are then used in the radiation calculation described in this section (12.3.3.2).

The photolysis model requires cloud information in a different form. For the sake of consistency, these parameters are estimated from the same layer resolved fractional coverage described above (Equations 12-88 and 12-89). The photolysis model assumes a single uniform, vertically mixed cloud layer. Therefore, the required parameters are; cloud top, cloud base, cloud fractional coverage, and average liquid water content. Cloud top and base layers (k_{top} and k_{base}) are determined by looking up and down from level of maximum coverage to where the fractional coverage first becomes 50% of the maximum. The layer average cloud cover is then computed from the volume averaging of layer cloud fractions between k_{top} and k_{base} :

$$f_c^{Tot} = \sum_{k_{base}}^{k_{top}} f_c^k \Delta z_F^k / \sum_{k_{base}}^{k_{top}} \Delta z_F^k \quad (12-90)$$

Once the base, top, and fraction of the cloud layer are determined, the average liquid water content of the cloud is computed assuming convective characteristics as described by Walcek and Taylor (1986), Chang et al. (1987), and Chang et al. (1990). The lifted condensation level is assumed to be at the cloud base, defined as the bottom boundary of cloud layer k_{base} , where the air is saturated at the model's ambient temperature. The in-cloud liquid water profile (q_c) is then computed as a fraction of the adiabatic liquid water profile (q_{ad}):

$$q_c = \alpha q_{ad} \quad (12-91)$$

where $\alpha = 0.7 \exp\left[\frac{(p - p_{lcl})}{8}\right] + 0.2$ and p_{lcl} is the pressure (in KPa) at the lifting condensation level according to Warner (1970). The layer liquid cloud water values are then vertically averaged in the same way as fractional coverage (Equation 12-90).

12.3.3.2 Computation of Solar Radiation Components

To meet air quality modeling needs, MCIP outputs several parameters related with radiation at the surface including: incident surface shortwave radiation (R_{gnd}), absorbed surface shortwave radiation (G_{sw}), net long wave radiation at the ground (G_{lw}), total net radiation at the ground (R_{net}), and surface albedo (A). These radiation components are used in several CMAQ processors. For example, photosynthetically active radiation (PAR), which is needed for the biogenic emissions processing, is estimated with $PAR = 0.55R_{gnd}$. Depending on which version of MM5 is used, surface radiation parameters are either passed through from MM5 or computed in MCIP. The computation of surface radiation parameters in MCIP is identical to the surface radiation option in MM5, as described in Grell et al. (1995), except that the dependence on zenith angle is added to the land use specified albedo (A_{lu}) such that:

$$A = A_{lu} + 0.1 \left[\exp(0.00386Z^{3/2}) - 1.0 \right] \quad (12-92)$$

where Z is zenith angle in degrees.

Note that MCIP computations of surface radiation parameters, which essentially replicate MM5, are a stop gap measure for use with MM5v2.6 which does not output these values. All later versions of MM5 do output these parameters which will be read and passed through by MCIP as is now done for the MM5PX option. It will be preferable in future applications of Models-3 to directly propagate the radiation parameters from MM5 to CMAQ so that the more sophisticated radiation models now available in MM5 can be used. The currently used surface radiation option includes effects of clouds, aerosols, and water vapor on radiation but neglects radiation effects on the atmosphere. Therefore, many future applications may utilize either the Dudhia radiation scheme (Dudhia, 1989) or the CCM2 scheme (Hack et al., 1993) which include atmospheric radiation effects. See Chapter 3, section 3.3.4.1, for description of MM5 radiation options.

12.4 Meteorological Data for CCTM with Generalized Coordinate System

One feature of the CMAQ system that is distinct from other Eulerian air quality modeling systems is its ability to incorporate meteorological models with various different coordinates and dynamics. This functionality is achieved by recasting meteorological parameters in terms of the variables used in the governing set of equations for the fully compressible atmosphere in generalized coordinate system (Byun, 1999a). Key dynamic and thermodynamic parameters are estimated for the given coordinates in such a way to ensure consistencies among the meteorological data. The consistency can be maintained throughout CCTM simulations when appropriate temporal interpolation methods are used.

12.4.1 Thermodynamic Variables: Pressure, Density and Entropy

To facilitate mass-consistent interpolation among the thermodynamic variables, the governing set of equations for the fully compressible atmosphere is used in the CMAQ system. The system includes prognostic equations for entropy and air density as suggested by Ooyama (1990). The algorithms used for estimating the thermodynamic parameters are presented below. For a detailed discussion on the governing set of equations and mass-consistent interpolation algorithm, refer to Byun (1999a and b).

12.4.1.1 Pressure, Density of Air and Density of Water Vapor

Like most of the other meteorological models, MM5 does not use a predictive equation for air density. Instead, air density is estimated with the equation of state using predicted pressure and temperature. For a terrain-influenced pressure coordinate, when it is applied for hydrostatic atmosphere, the hydrostatic pressure (\tilde{p}) can be computed with \tilde{p}^* available from MM5.

$$p = \tilde{p} = p_T + \sigma_{\tilde{p}} \tilde{p}^* \quad (12-93)$$

The total pressure (p) in the terrain-influenced reference pressure coordinate (applied for a nonhydrostatic atmosphere in MM5) is the sum of the reference pressure and perturbation pressure:

$$p = p_o + p_p = \sigma p_o^* + p_T + p_p \quad (12-94)$$

Once p is known, virtual temperature (T_v) and density of the (moist) air are computed with:

$$T_v = \frac{T}{1 + \left(\frac{m_w}{m_d} - 1\right) \frac{p_w}{p}}, \quad (12-95)$$

where m_w and m_d are the molecular weights of water vapor and dry air, respectively, and

$$\rho = \frac{p}{R_d T_v}. \quad (12-96)$$

The water vapor partial pressure (p_v) can be found from the vapor mixing ratio (r) supplied by MM5 using the following equation:

$$p_v = r \frac{R_v}{R_d} p_d. \quad (12-97)$$

Then, the density of water vapor is simply given as:

$$\rho_v = \frac{r}{1+r} \rho. \quad (12-98)$$

12.4.1.2 Entropy

In the CMAQ system, entropy is treated as one of the key thermodynamic parameters. Because its conservation equation follows similar continuity equation for air density, entropy can be interpolated using the same interpolation scheme as air density. Then, we can reconstruct temperature and pressure for the intermediate time steps from the interpolated densities (for air and water) and entropy. This type of interpolation will maintain mass consistency among the thermodynamic variables for air quality applications. Using the density of moist air and density of water vapor obtained above, the entropy for moist air can be computed with:

$$\zeta = (\rho_d C_{vd} + \rho_v C_{vv}) \ln\left(\frac{T}{T_{oo}}\right) + \rho_v \Lambda_{oo} - \rho_d R_d \ln\left(\frac{\rho_d}{\rho_{doo}}\right) - \rho_v R_v \ln\left(\frac{\rho_v}{\rho_{v*o}}\right), \quad (12-99)$$

where $\rho_d = \rho - \rho_v$, $p_{oo} = 10^5$ Pascal, Λ_{oo} is the specific entropy of saturated vapor, ρ_{doo} is the density of reference dry air, and ρ_{v*o} is the density of reference state water vapor saturated over water at reference temperature T_{oo} , 273.15 K. The integral constants are computed following Ooyama (1990):

$$\rho_{doo} = \frac{p_{oo}}{R_d T_{oo}} \quad (12-100)$$

$$\Lambda_{oo} = \Lambda(T_{oo}) = R_v T_{oo} \left. \frac{d \ln E(T_c)}{dT_c} \right|_{T_{oo}} \quad (12-101)$$

$$\rho_{v*o} = \rho_{v*}(T_{oo}) = \left. \frac{E(T_c)}{R_v T} \right|_{T_{oo}}, \quad (12-102)$$

where $T_c = T - 273.15$.

For the basic formulation of the saturation vapor pressure approximation, we use the AERK formula recommended by Alduchov and Eskridge (1996):

$$E(T_c) = ae^{bT_c/(c+T_c)} \quad (12-103a)$$

$$\frac{d \ln E(T_c)}{dT_c} = \frac{bc}{(c + T_c)^2}, \quad (12-103b)$$

where $a=610.94$, $b=17.625$, $c=243.04$ and $E(T_c)$ is in Pascal. With this information we can evaluate the integration constants, and thus the entropy using Equation 12-99.

12.4.2 Vertical Jacobian and Layer Height

In the CCTM, Jacobian is used for the definition of vertical and horizontal coordinates/grid system at every model synchronization time step. The Jacobian characterizes the coordinate transformation and is treated as one of the fundamental parameters defining grid structure of the CTM. Depending on the horizontal map projections and vertical coordinates, the physical characteristics of the Jacobian change.

12.4.2.1 Jacobian for Coordinate Transformation

The vertical Jacobian defines the coordinate transformation rules. For a vertical coordinate $\hat{x}^3 = \xi$, where ξ is a monotonically increasing function of height, the Jacobian is related with the geopotential height, $\Phi = gz$, as:

$$J_\xi = \frac{1}{g} \left| \frac{\partial \Phi}{\partial \xi} \right| = \frac{1}{g} \frac{\partial \Phi}{\partial \xi} \quad (12-104)$$

Sigma- \tilde{p} , time dependent coordinate

For hydrostatic application of MM5, the vertical coordinate is the same as the terrain-influenced sigma- \tilde{p} coordinate, whose vertical Jacobian is defined as

$$J_{\sigma_{\tilde{p}}} = \frac{\tilde{p}^*(x, y, t)}{\tilde{\rho}g} \quad (12-105)$$

Note that Equations 12-3 and 12-105 are identical although CMAQ uses monotonically increasing coordinate ξ and MM5 uses monotonically decreasing sigma- \tilde{p} coordinate.

Using the Equation of State and the definition of the sigma- \tilde{p} coordinate, the vertical Jacobian can be obtained using the temperature and surface pressure from MM5.

Jacobian at half sigma-level is estimated for $1 \leq k \leq K$ with:

$$\left(J_{\sigma_{\tilde{p}}} \right)_H^k = \frac{R_{air} \tilde{p}^* \bullet T_{vH}^k}{g(\sigma_H^k \tilde{p}^* + p_T)}, \quad (12-106)$$

where K is the number of model layer (i.e., $NLAYS$ in Models-3 I/O API), and Jacobian at full sigma-level is computed for $1 \leq k \leq K-1$ with:

$$\left(J_{\sigma_{\tilde{p}}}\right)_F^{k+1/2} = \frac{R_{air} \tilde{p}^* \bullet (T_{vH}^{k+1} + T_{vH}^k)}{2g(\sigma_F^{k+1/2} \tilde{p}^* + p_T)} \quad (12-107)$$

and, at the surface ($k=1/2$) with:

$$\left(J_{\sigma_{\tilde{p}}}\right)_F^{k=1/2} = \frac{R_{air} \tilde{p}^* \bullet T_{vs}}{g(\sigma_F^{k=1/2} \tilde{p}^* + p_T)}, \quad (12-108)$$

where we have used T_{vs} to represent the virtual air temperature at the surface.

For the thirty layer MM5 sigma- \tilde{p} coordinate, whose sigma value for the top of first layer is set 0.995 (i.e., about 38 m in the standard atmosphere), the reference temperature is estimated from the average between the skin temperature (T_g) and air temperature at the lowest model layer. The virtual air temperature at the surface is computed with the assumption that the relative humidity at the surface is the same as the relative humidity at the middle of first layer.

Time independent coordinate

For the nonhydrostatic application of MM5, we use the terrain-following sigma- p_o coordinate whose vertical Jacobian is defined as:

$$J_{\sigma_{p_o}} = \frac{p_o^*(x, y)}{\rho_o g} \quad (12-109)$$

Again, Equations 12-6 and 12-109 are identical although CMAQ uses monotonically increasing coordinate ξ and MM5 uses monotonically decreasing coordinate. Using the Equation of State for the reference hydrostatic atmosphere and the definition of the sigma- p_o coordinate, the vertical Jacobian can be obtained using the temperature and surface pressure from MM5. Jacobian at half σ -height is estimated for $1 \leq k \leq K$ with:

$$\left(J_{\sigma_{p_o}}\right)_H^k = \frac{R_{air} p_o^* \bullet \left[T_{os} + A \ln\left(\frac{\sigma_H^k p_o^* + p_T}{p_{oo}}\right) \right]}{g(\sigma_H^k p_o^* + p_T)} \quad (12-110)$$

and Jacobian at full σ -height is computed for $0 \leq k \leq K$ with:

$$\left(J_{\sigma_{p_o}}\right)_F^{k+1/2} = \frac{R_{air} p_o^* \bullet \left[T_{os} + A \ln\left(\frac{\sigma_F^{k+1/2} p_o^* + p_T}{p_{oo}}\right) \right]}{g(\sigma_F^{k+1/2} p_o^* + p_{oT})} \quad (12-111)$$

The Jacobian does not depend on MM5 data except for the topographic height and sigma-layer definition.

Total Jacobian

The total Jacobian ($\sqrt{\hat{\gamma}} \equiv J_{\xi} / m^2$) is used in the governing equations for the CCTM. The trace species concentrations are coupled with the total Jacobian. Because of the need to couple with both the trace species concentrations (defined at the layer middle) and vertical flux variables (defined at the layer interface), total Jacobians at the half and full level values are stored in the MET_CRO_3D file. The total Jacobian at the surface, $\left(J_{\sigma_{\bar{p}}}\right)_F^{k=1/2}$ divided by the map scale factor squared, is stored in the MET_CRO_2D file. For hydrostatic applications of MM5 the Jacobian varies with time and for nonhydrostatic applications it is constant with time. Although we could have saved some file space by distinguishing this feature, the Jacobians are stored in MET_CRO_3D and MET_CRO_2D files to maintain the compatibility of data structure for both time-dependent and time-independent coordinate systems.

For use in the mass-conserving temporal interpolation, Jacobian weighted densities at the half-levels defined for $1 \leq k \leq K$ as:

$$(J_{\xi} \rho / m^2)_H^k = (J_{\xi} / m^2)_H^k \bullet (\rho)_H^k \quad (12-112a)$$

$$(J_{\xi} \rho_v / m^2)_H^k = (J_{\xi} / m^2)_H^k \bullet (\rho_v)_H^k \quad (12-112b)$$

are stored in the MET_CRO_3D file. Like density, the Jacobian weighted entropy at the layer middle is obtained for $1 \leq k \leq K$ with:

$$(J_{\xi} \zeta / m^2)_H^k = (J_{\xi} / m^2)_H^k \bullet (\zeta)_H^k \quad (12-113)$$

They are stored in the MET_CRO_3D file as the Jacobian-weighted total air density and water vapor density, and entropy, respectively.

12.4.2.2 Layer Heights

In CMAQ, layer heights are computed using the basic definition of the geopotential height in terms of Jacobian instead of relying on the coordinate-specific analytic equations, such as a hypsometric equation for a hydrostatic coordinate. The height above mean sea level (MSL) is defined in terms of the vertical Jacobian as:

$$\hat{z} = \Phi / g = \hat{z}_s + \int_{\xi_s}^{\xi} J_{\xi} d\xi \quad (12-114)$$

The layer heights at the interface and middle of the layers above the ground level (AGL) are computed with:

$$z_F^{k+1/2} = \hat{z}_F^{k+1/2} - \hat{z}_s = \int_{\xi_s}^{\xi_F^{k+1/2}} J_\xi d\xi \cong \sum_{j=1}^k J_{\xi_H}^j (\xi_F^{j+1/2} - \xi_F^{j-1/2}) \quad (12-115a)$$

for $1 \leq k \leq K+1$, where

$$z_F^{k+1/2} \Big|_{k=0} = 0 \quad (12-115b)$$

and for $2 \leq k \leq K$ with:

$$\begin{aligned} z_H^k &= \hat{z}^k - \hat{z}_s = \int_{\xi_s}^{\xi_H^k} J_\xi d\xi \\ &\cong z_H^1 + \sum_{j=2}^k \frac{1}{2} (J_{\xi_H}^j + J_{\xi_H}^{j-1}) (\xi_H^j - \xi_H^{j-1}) \end{aligned} \quad (12-116a)$$

where

$$z_H^1 = \frac{1}{2} (J_{\xi_H}^1 + J_{\xi_F}^{1/2}) (\xi_H^1 - \xi_F^{1/2}) \quad (12-116b)$$

Note that both $z_F^{k+1/2}$ and z_H^k are stored either in the GRID_CRO_3D file for the time independent vertical coordinate, or in the file MET_CRO_3D for time dependent one. Because $z_F^{k+1/2} \Big|_{k=0}$ is always zero for the terrain-influenced coordinates, it is not stored in any of MCIP files.

12.4.3 Contravariant Velocity Components

The generalized CCTM requires a set of contravariant velocity components to simulate numerical advection. Contravariant velocity components are scaled components of the wind vectors for the transformed coordinates. When the true velocity components (i.e., wind components for earth-tangential coordinates) are predicted in a meteorological model, they need to be transformed accordingly.

12.4.3.1 Horizontal Wind Components

MM5 predicts horizontal wind velocity components defined on the spherical earth in the coupled form with the surface pressure scale p^* . First, we need to de-couple the surface pressure scale as follows:

$$U^{l+1/2, m+1/2} = (p^* U)^{l+1/2, m+1/2} / (p^*)^{l+1/2, m+1/2} \quad (12-117a)$$

$$V^{l+1/2, m+1/2} = (p^* V)^{l+1/2, m+1/2} / (p^*)^{l+1/2, m+1/2} \quad (12-117b)$$

for $0 \leq l \leq L$ and $0 \leq m \leq M$, where L is the number of columns and M is the number of rows for the rectangular modeling domain. In the expression, p^* represents either \tilde{p}^* or p_o^* depending on the hydrostatic/nonhydrostatic option in MM5. The value p^* at the dot-point is approximated with:

$$(p^*)^{l+1/2, m+1/2} = \frac{1}{4} [(p^*)^{l, m} + (p^*)^{l+1, m} + (p^*)^{l+1, m+1} + (p^*)^{l, m+1}] \quad (12-118)$$

The next step is to compute the contravariant components $u_\xi = mU$ and $v_\xi = mV$ at the dot-point:

$$(u_\xi)^{l+1/2, m+1/2} = m^{l+1/2, m+1/2} U^{l+1/2, m+1/2} \quad (12-119a)$$

$$(v_\xi)^{l+1/2, m+1/2} = m^{l+1/2, m+1/2} V^{l+1/2, m+1/2} \quad (12-119b)$$

Because the Jacobian-mass weighted contravariant wind components are needed for the mass consistent interpolation, we estimate these quantities at the square-point (flux point) for \hat{x}^1 -direction and at the triangle-point (flux point) for \hat{x}^2 -direction, respectively:

$$\left(\frac{\rho J_\xi}{m^2} u_\xi\right)^{l+1/2, m+1} \cong \frac{1}{4} \left[\left(\frac{\rho J_\xi}{m^2}\right)^{l, m+1} + \left(\frac{\rho J_\xi}{m^2}\right)^{l+1, m+1} \right] [(u_\xi)^{l+1/2, m+1/2} + (u_\xi)^{l+1/2, m+3/2}] \quad (12-120a)$$

$$\left(\frac{\rho J_\xi}{m^2} v_\xi\right)^{l+1, m+1/2} \cong \frac{1}{4} \left[\left(\frac{\rho J_\xi}{m^2}\right)^{l+1, m} + \left(\frac{\rho J_\xi}{m^2}\right)^{l+1, m+1} \right] [(v_\xi)^{l+1/2, m+1/2} + (v_\xi)^{l+3/2, m+1/2}] \quad (12-120b)$$

Both of these parameters, together with the contravariant wind components u_ξ and v_ξ at the DOT points, are stored in the MET_DOT_3D file.

12.4.3.2 Vertical Wind Component

In most meteorological models with terrain-influenced coordinates, the contravariant vertical velocity components are not computed directly because of the complex representation of the divergence term in the generalized coordinate system. In the generalized coordinate system, the prognostic equation for the vertical component contains Christoffel-symbols-of-the-second-type terms that make the equation not only complicated but also make conservation of momentum or kinetic energy difficult (Byun, 1999a). To circumvent this difficulty, some meteorological models use the prognostic equations of motion for the true vertical wind component.

For the MM5 hydrostatic application, the terrain-influenced hydrostatic pressure coordinate allows diagnostic computation of the contravariant vertical velocity. The continuity equation for air density becomes a diagnostic equation for this application. Here, the expressions are written with the normalized vertical coordinate, which increases with geometric height, $\xi \equiv 1 - \sigma_{\tilde{p}}$. By selecting the integration limits as $\xi = 0$ to 1, (i.e., $\sigma_{\tilde{p}s} = 1$ to $\sigma_{\tilde{p}T} = 0$) and using the boundary conditions at the top and bottom $\dot{\xi} = \hat{v}^3 = 0$, the tendency term can be computed with:

$$\frac{\partial(\rho J_\xi)}{\partial t} = \frac{\partial \tilde{p}^*}{\partial t} = \int_0^1 \left[\tilde{p}^* \frac{Q_\rho}{\rho} - m^2 \nabla_\xi \cdot \frac{\tilde{p}^* \hat{\mathbf{V}}_\xi}{m^2} \right] d\xi \quad (12-121)$$

This equation predicts time rate change of the hydrostatic pressure component whose vertical gradient is in balance with gravitational acceleration. In the geometric height coordinate, this equation does not exist. However, the height coordinate does not require surface pressure tendency to close the system because the coordinate is time independent. Because the hydrostatic pressure coordinate $\xi \equiv 1 - \sigma_{\tilde{p}}$ is a material coordinate, the mass continuity equation can also be used to estimate contravariant vertical velocity component by integrating the wind divergence term either from the bottom to a level ξ or from the top to ξ .

$$\dot{\xi} = \frac{1}{\rho J_\xi} \int_0^\xi \left[J_\xi Q_\rho - m^2 \nabla_\xi \cdot \frac{\rho J_\xi \hat{\mathbf{V}}_\xi}{m^2} \right] d\xi - \frac{\xi}{\rho J_\xi} \frac{\partial(\rho J_\xi)}{\partial t} \quad (12-122a)$$

$$\dot{\xi} = \frac{1}{\rho J_\xi} \int_{\xi_T}^\xi \left[J_\xi Q_\rho - m^2 \nabla_\xi \cdot \frac{\rho J_\xi \hat{\mathbf{V}}_\xi}{m^2} \right] d\xi - \frac{(\xi - \xi_T)}{\rho J_\xi} \frac{\partial(\rho J_\xi)}{\partial t} \quad (12-122b)$$

where $\xi_T = 1$.

For other coordinates that do not have diagnostic relations, the contravariant vertical velocity component should be estimated using standard coordinate transformation

$$\dot{\xi} = \hat{v}^3 = \frac{\partial \xi}{\partial t} + (-m \mathbf{V}_\xi \cdot \nabla_\xi h_T + w) \left(\frac{\partial \xi}{\partial z} \right) \quad (12-123)$$

where h_T is the height of the coordinate surface and w is the regular vertical component of wind. For nonhydrostatic MM5 applications, $\xi \equiv 1 - \sigma_{p_o}$ is the corresponding vertical coordinate in CMAQ. Equation 12-122a can be rewritten as:

$$\dot{\xi} = -\dot{\sigma}_{p_o} = \left[\frac{\sigma_{p_o}}{p_o^*} \frac{\partial p_o^*}{\partial \hat{x}^1} \right] (mU) + \left[\frac{\sigma_{p_o}}{p_o^*} \frac{\partial p_o^*}{\partial \hat{x}^2} \right] (mV) + \frac{\rho_o g}{p_o^*} w \quad (12-124)$$

Like the horizontal momentum components, we need the Jacobian-mass weighted contravariant vertical wind for the mass consistent interpolation. The quantity is computed with the thickness-weighted density as:

$$\left(\frac{\rho J_\xi}{m^2} \dot{\xi} \right)^{k+1/2} \equiv \left[f_z^{k+1/2} \left(\frac{\rho J_\xi}{m^2} \right)^k + (1 - f_z^{k+1/2}) \left(\frac{\rho J_\xi}{m^2} \right)^{k+1} \right] \cdot \dot{\xi}^{k+1/2} \quad (12-125)$$

where $f_z^{k+1/2} = (z_F^{k+1/2} - z_H^k) / (z_H^{k+1} - z_H^k)$. Note that $\left(\frac{\rho J_\xi}{m^2} \dot{\xi} \right)$ is defined at the layer interfaces. It is zero at the earth's surface (no-penetration boundary condition) and therefore not included in the

output. It also vanishes at the top of the modeled atmosphere. The quantity $\left(\frac{\rho J_{\xi}}{m^2} \dot{\xi}\right)$ is stored in the MET_CRO_3D file from $k=1$ to K (i.e., $NLAYS$) with the variable name (WHAT_JD).

12.4.4 Mass Consistent Temporal Interpolation of Meteorological Parameters

In the CCTM, the temporal interpolations of meteorological data are needed because the output frequency of the meteorological data is usually much coarser than the synchronization time step of the chemistry-transport model. Consistency in meteorological parameters such as, Jacobian, density of air (total), density of water vapor, entropy (or temperature), and pressure are important for the science modules in the CCTM.

Here, we recommend interpolation schemes for density and velocity fields that maintain mass consistency. First, the Jacobian and density at a time $t_{\alpha} = (1 - \alpha)t_n + \alpha t_{n+1}$ between the two consecutive output time steps, t_n and t_{n+1} , are expected to be interpolated with:

$$(J_{\xi})_{\alpha} = (1 - \alpha)(J_{\xi})_n + \alpha(J_{\xi})_{n+1} \quad (12-126)$$

$$(\rho J_{\xi})_{\alpha} = (1 - \alpha)(\rho J_{\xi})_n + \alpha(\rho J_{\xi})_{n+1} \quad (12-127)$$

where $0 \leq \alpha \leq 1$. The Models-3 I/O API provides a convenient function call (INTERP3) for the linear interpolation of grid variables. The premise used here is that the Jacobian is a fundamental quantity that determines the coordinate system. Density of water vapor (ρ_v) and entropy should follow the same interpolation rule (Equation 12-127). Then densities and entropy at t_n are computed with

$$(\rho)_{\alpha} = \frac{(\rho J_{\xi})_{\alpha}}{(J_{\xi})_{\alpha}}; (\rho_v)_{\alpha} = \frac{(\rho_v J_{\xi})_{\alpha}}{(J_{\xi})_{\alpha}}; (\zeta)_{\alpha} = \frac{(\zeta J_{\xi})_{\alpha}}{(J_{\xi})_{\alpha}} \quad (12-128)$$

It is obvious that the functional form of the Jacobian (which depends on a vertical coordinate) changes the characteristic of density interpolation. For nonhydrostatic MM5 runs, where the Jacobian is constant with time, the density is simply interpolated linearly with time.

When the density tendency term is available from the meteorological model, or can be computed from diagnostic relations for certain choice of vertical coordinate system, one can use a piecewise cubic spline interpolation method for (ρJ_s) :

$$(\rho J_s)_{\alpha} = a\alpha^3 + b\alpha^2 + c\alpha + d \quad (12-129)$$

where $a = \Delta t \left(\frac{\partial(\rho J_s)}{\partial t} \right)_{n+1} + \Delta t \left(\frac{\partial(\rho J_s)}{\partial t} \right)_n - 2[(\rho J_s)_{n+1} - (\rho J_s)_n]$

$$b = 3[(\rho J_s)_{n+1} - (\rho J_s)_n] - 2\Delta t \left(\frac{\partial(\rho J_s)}{\partial t} \right)_n - \Delta t \left(\frac{\partial(\rho J_s)}{\partial t} \right)_{n+1}$$

$$c = \Delta t \left(\frac{\partial(\rho J_s)}{\partial t} \right)_n$$

$$d = (\rho J_s)_n$$

The density of water vapor (ρ_v) and entropy should be interpolated with the same method. The density of dry air from the total air density can be obtained by subtracting ρ_v from ρ . The interpolated temperature is computed with:

$$T = T_{oo} \exp \frac{\zeta + \rho_d R_d \ln(\rho_d / \rho_{do}) + \rho_v R_v \ln(\rho_v / \rho_{vo})}{\rho_d C_{vd} + \rho_v C_{vv}} \quad (12-130)$$

and entropy can be computed with Equation 12-99. The interpolated pressure is computed with the ideal gas law,

$$p = (\rho_d R_d + \rho_v R_v) T \quad (12-131)$$

Next, wind components multiplied with the Jacobian-weighted density are interpolated linearly and the interpolated wind components are obtained by dividing the results with $(\rho J_s)_\alpha$:

$$(\rho J_s \hat{\mathbf{V}}_s)_\alpha = (1 - \alpha)(\rho J_s \hat{\mathbf{V}}_s)_n + \alpha(\rho J_s \hat{\mathbf{V}}_s)_{n+1} \quad (12-132a)$$

$$(\rho J_s \hat{v}^3)_\alpha = (1 - \alpha)(\rho J_s \hat{v}^3)_n + \alpha(\rho J_s \hat{v}^3)_{n+1} \quad (12-132b)$$

$$(\hat{\mathbf{V}}_s)_\alpha = \frac{(\rho J_s \hat{\mathbf{V}}_s)_\alpha}{(\rho J_s)_\alpha} \quad (12-133a)$$

$$(\hat{v}^3)_\alpha = \frac{(\rho J_s \hat{v}^3)_\alpha}{(\rho J_s)_\alpha} \quad (12-133b)$$

When density and wind data are not collocated, the above procedure may incur spatial interpolation errors.

12.4.5 Optional Conversion of Nonhydrostatic Data to Hydrostatic Meteorological Data for MM5

There may be a special situation when a hydrostatic CTM run is desired while the MM5 run is made with the nonhydrostatic option. In such a case one may want to redefine the nonhydrostatic coordinate into hydrostatic one while keeping the profile data as provided. In spite of many theoretical problems with this kind of data conversion, MCIP provides an option to convert the

nonhydrostatic coordinate into the hydrostatic pressure coordinate. Use of this option is not recommended for scientifically rigorous computations. However, this is a useful option for certain purposes such as code development and testing of a hydrostatic CTM.

Nonhydrostatic and hydrostatic coordinates can be compared in terms of the atmospheric pressure. Pressure in a hydrostatic MM5 run is defined in Equation 12-93 while the same in a hydrostatic MM5 is defined in Equation 12-94. Then, the difference in the nonhydrostatic and hydrostatic pressures is:

$$p^* = p_o^* - \sigma^{-1}(p - \tilde{p}) + \sigma^{-1}p_p \quad (12-134)$$

If we force the hydrostatic pressure to be that of nonhydrostatic coordinate, i.e., $p \approx \tilde{p}$ at the surface, the time dependent surface pressure, p_s^* , can be estimated with:

$$p^* \approx p_o^* + p_p(\sigma_H^1) \quad (12-134')$$

where $\sigma_F^{1/2} = \sigma_s = 1$ is used. Here, the perturbation pressure at the surface is assumed to be that of layer 1 because the real surface perturbation pressure is not provided by the nonhydrostatic MM5. One can redefine the vertical coordinate to be hydrostatic with the time dependent surface pressure. The difficulty of converting nonhydrostatic meteorology data into hydrostatic data is not in the estimation of pressure surfaces, but rather in the representativeness of profile data because of the change in the layer definitions.

12.5 Operation of MCIP

Because MCIP is a Models-3 conformant processor, it needs to be compiled and executed using a Models-3 build command (m3bld) with a configuration file. It requires the grid-domain object include files to define output domain and resolution. In most cases, the user does not need to define input data domains and resolutions because reader modules can extract the information from file headers. MCIP code structure, compilation and execution procedures are discussed below. Additional operational information for preparing MCIP through Models-3 system framework can be found in Chapter 7 of the EPA Third-Generation Air Quality Modeling System User Manual. Also, the User Manual Tutorial for the initial public release of Models-3 provides step-by-step instructions for running MCIP with a set of sample examples.

12.5.1 MCIP Modules

MCIP code is archived with CVS (Concurrent Version System) (Cederqvist, 1993) in the Models-3/CMAQ system. Currently, eleven module classes are defined for MCIP. The classification makes it convenient to customize MCIP code for special situations. For example, when different meteorological inputs and process options are needed to link with the CCTM, appropriate modules from different classes can be used. Refer to Table 12-9 for the details of module descriptions and associated source code.

12.5.2 Building MCIP

The MCIP code conforms to the Models-3 coding standard. It is designed to be compiled using m3bld with a configuration file. Refer to Appendix 12C for a sample MCIP configuration file. The user needs to retrieve the source code (main program, associated subroutines for selected modules, and include files) appropriate to the user's choice of optional modules through the CVS system. There are four kinds of include files for this processor. Three include file types, Models-3 I/O API include files, MCIP's global include files, and MCIP module specific include files, are fixed. The fourth include file type describes dimensional information of the input meteorology data and, as an exception, must be edited to match the number of vertical layers in the input.

Therefore the parameter KMAX in MCIPPARM.EXT may need to be changed to match the dimensions of working arrays. Horizontal domain information is obtained from the header of MM5 files automatically. MCIP expects that include files for the CTM grid/domain domain (HGRD.EXT, VGRD.EXT, COORD.EXT), for which the data will be extracted, are provide by the user. Vertical collapsing is done automatically when the number of layers in VGRD.EXT is less than the number of layers in input data and the coordinate interface values match as shown in Table 12-5. When a few lowest input model layers are collapsed into one for the output, only diagnostic option can be used because the surface flux values and aerodynamic resistance passed through are no longer valid due to the change in the thickness of the lowest layer. The M3DDEP option must not be used when collapsing the lowest model layers and doing so will be violating the parameteric values passed through from the meteorological model.

Table 12-9. MCIP Module Definitions and Associated Source Code

Class	Module	Description	Source Code
driver	mcip	controls main computational flow	mcip.F, initx.F
input	mm5	reads in MM5 output files	getmet_mm5.F, readmm1.F, readmm2.F, getgist.F, MM5INPUT.EXT, MM5HEADER.EXT
	m3	reads in MCIP output files	getmet_m3.F
	fakemet	generates meteorology fields for idealized flow field study	getmet_m3fake.F
	rams	reads in RAMS I/O API output files	<i>not available</i>
landuse	m3radm	reads in landuse data in RADM dry deposition category	getluse.F
pbl	pblpkg	computes PBL parameters	pblpkg.F, pblpwr.F, sfcflux.F, slflux.F
drydep	radmdd	computes dry deposition velocities using Wesely's RADM method	radmdry.F, DDEPSPC.EXT
	cmaqdd	computes dry deposition velocities using Pleim's CMAQ method	<i>not available</i>
cloud	radmkuo	computes cloud parameters using convective column assumption	bcl DPR_ak.F
solar	solar_px	computes solar radiation using the algorithm implemented in MM5-PX version	solar.F, transm.F
met3d	m3sup	computes supplemental three-dimensional variables needed for CMAQ	layht.F, verthat.F, vertnhy.F, verthyd.F, jacobi.F, met3dsup.F
output	stnd	generates MCIP output for standard variable lists	comheader.F, gridout.F, metcro.F, metdot.F
util	util	collection of utility subroutines	bilin2d.F, bilin3d.F, cvbdx.F, collapx.F, cvmgp.F, cvmgz.F, ratint.F, errmsg.F, sanity.F
icl	icl	MCIP specific include files	CONST_mete.EXT, CONST_pbl.EXT, FILES3_MCIP.EXT, GROUTCOM.EXT, INFILES_MCIP.EXT, LRADMDAT.EXT, MCIPCOM.EXT, MCIPPARM.EXT, MCOUTCOM.EXT, MDOUTCOM.EXT

12.5.3 Executing MCIP

12.5.3.1 Run Script Command File

As with other interfaces, an execution run script is used to define key environmental variables prescribing run-time characteristics and linkage between logical file names specified in the codes and actual files for input and output. A sample script for MCIP execution can be retrieved from the CVS archive and edited for the user's particular application. The user may modify environmental variables for choosing different processing options and for defining input and output files. Refer to the APPENDIX D for a sample MCIP run script. For processing MM5 output, MCIP may not need to be co-resident with MM5 if its output files are in IEEE binary format. MCIP can be run on any UNIX computer for processing meteorological data in Models-3 I/O API format.

Input parameters METROW, METCOL, and METLAY are defined through the UNIX environmental variable list. These are used to check if the input meteorology data have correct dimensions as expected. Within MCIP, the actual values will be picked up from header information of MM5 data file. When offset values (I0, J0) are inconsistent with the information in MM5 header and in COORD.EXT, MCIP suggests a new set of (I0, J0) or (XORIG, YORIG) values. Make sure to set NDEP to correspond to the number of lowest input layers being collapsed into the lowest output model layer, so aerodynamic resistances are computed accordingly.

12.5.3.2 Input Files for MM5 Data Processing

Logical names of input files are described below:

- MMOUT_DOMAIN#: This standard MM5 file contains gridded hourly (or sub-hourly) two- and three-dimensional meteorological data covering the entire MM5 domain.
- MDL3_DOMAIN#: This is optional EPA added MM5 output that contains file contains PBL parameters needed when the pass-through option is chosen.
- LAND_CRO_2D_##KM: This is LUPROC output that contains 11-category fractional land-use data covering the entire MM5 domain. If USGS North American land/vegetation characteristic data base used as input to LUPROC is not enough to cover the desired domain, dominant landuse file LANDUSE_DOMAIN# from TERRAIN, a preprocessor for MM5 system, can be used.

12.5.3.3 Input Files for I/O API Meteorological Data Processing

MCIP can be used to extract meteorology data for a smaller window domain, to collapse number of layers, or to process meteorological data already in I/O API format further. It treats gridded input meteorological data as pseudo profiles for temperature, moisture and wind components. Required I/O API meteorological inputs for this option are; GRID_CRO_2D, GRID_DOT_2D, MET_CRO_2D, MET_CRO_3D, and MET_DOT_3D files. Because it does not use boundary files as its input, the output domain can be as large as (NCOLS-2)x(NROWS-2) for windowing or layer collapsing process. This option can be used to generate interpolated meteorology data for higher resolution grid than the original input as well.

Table 12-10. MCIP Environmental Variables

Environmental Variables	Description	Note
METLAY	number of layers in input meteorology data	should be larger than or equal to CTM NLAYS
METCOL	column (east-west) direction cell dimension in input meteorology data	should be larger than CTM NCOLS
METROW	row (south-north) direction cell dimension in input meteorology data	should be larger than CTM NROWS
I0	location of CTM domain origin offset in row direction = ROW_OFFSET	offset should be counted based on the input grid definition
J0	location of CTM domain origin offset in column direction = COL_OFFSET	offset should be counted based on the input grid definition
LUTYPE	file type for landuse data	<u>1: TERRAIN binary 13 category</u> <u>2: preprocessed ASCII 11 category</u> <u>3: MM5 dominant landuse category</u> <u>4: use landuse in GRIDCRO2D</u> <u>5: use USGS I/O API landuse file</u>
IOLUSE	location of CTM domain origin offset in row direction w.r.t. landuse data origin	offset should be counted based on the input grid definition. For LUTYPE 4 & 5, IOLUSE is not used
JOLUSE	location of CTM domain origin offset in column direction w.r.t. landuse data origin	offset should be counted based on the input grid definition. For LUTYPE 4 & 5, JOLUSE is not used
LCALCPBL	flag for estimating PBL parameters of not	<u>TRUE: re-compute PBL parameters</u> <u>FALSE: pass through from MM5</u>
LSLFLUX	flag for similarity algorithms	<u>TRUE: use surface layer similarity</u> <u>FALSE: use PBL similarity</u>
LM3DDEP	flag for dry deposition algorithm	<u>TRUE: use CMAQ dry deposition</u> <u>FALSE: use RADM dry deposition</u>

Table 12-10. MCIP Environmental Variables (continued)

Environmental Variables	Description	Note
LWIND	flag for wind field correction	0 (default): no correction +/- 1,2,3 wind field correction options (TBD)
LCALCCLD	flag for cloud algorithm	TRUE: compute cloud parameters FALSE: pass through from MM5
LHYDOUT	flag for hydrostatic output	TRUE: forces hydrostatic data output with approximations FALSE: pass through from MM5
CRO_FTYPE DOT_FTYPE	flag for I/O API file type	1 (default): time dependent 0 (special): time independent
LSANITY	flag for checking ranges of output parameters	TRUE: check FALSE: do not check
BMAX	Maximum boost rate for urban area	2 (default): 100% increase when urban and water areas are coexisting
JUDATE	Julian date for the start time	(yyyyddd)
HSTRT	start hour	(hh)
HTOSKIP	number of hours to skip MCIP process	(hh)
HTORUN	number of hours to run	(hhh)
NDEP	number of deposition layers	1 (default)
GRDNAM	grid/domain name for MCIP output files	
EXECUTION_ID	user defined execution ID	
SCENFILE	user defined file path	
IOAPI_CHECK_HEADERS	flag for checking I/O API file headers	FALSE (default)

Table 12-11. MCIP File Linkage

Environmental Variables	Description	Note
MM51	Input filename for MM51 data file	for mm5 input module
MM52	Input filename for MM52 data file	for mm5 input module
LU13	Input filename for TERRAIN binary landuse	applicable for LUTYPE = 1
LUSE	input filename for I/O API landuse file	applicable for LUTYPE = 4 or 5
GRID_CRO_2D	input filename for GRID_CRO_2D	for m3 input module
GRID_DOT_2D	input filename for GRID_DOT_2D	for m3 input module
MET_CRO_2D	input filename for MET_CRO_2D	for m3 input module
MET_CRO_3D	input filename for MET_CRO_3D	for m3 input module
MET_DOT_3D	input filename for MET_DOT_3D	for m3 input module
GRID_BDY_2D_G1	output filename for GRID_BDY_2D	
GRID_BDY_3D_G1	output filename for GRID_BDY_3D	
GRID_CRO_2D_G1	output filename for GRID_CRO_2D	
GRID_CRO_3D_G1	output filename for GRID_CRO_3D	
GRID_DOT_2D_G1	output filename for GRID_DOT_2D	
MET_CRO_2D_G1	output filename for MET_CRO_2D	
MET_CRO_3D_G1	output filename for MET_CRO_3D	
MET_DOT_3D_G1	output filename for MET_DOT_3D	

12.5.4 Defining Grid and Domain for MCIP

12.5.4.1 MM5 Grid and Domain Definitions

MM5 may output as many as nine grid domains (one coarse grid and up to eight nested grid domains) per MM5 execution. The MM5 developers took the approach of compiling MM5 with the appropriate dimensions for each study being performed. On the other hand, MCIP processes output meteorological data one grid domain at a time. It needs to be compiled explicitly for each grid domain. For multiple scale MM5 model runs, usually MM5 users have to define all the multi-level nest domains together with the coarse “mother” grid. The complication in defining MM5 domains as the Models-3 domain objects is caused by somewhat inauthentic use of the left-hand coordinate system and dot-point grid/domain definitions in MM5. For the details on how to define MM5 domains, users are recommended to read MM5 User’s Guide. In the following, we use a set of multi-level MM5 domains listed in Table 12-12 as the examples of the discussion.

Table 12-12. An Example Set of Multi-level Nesting MM5 Domains
(Note that (I, J) in MM5 corresponds to (ROW, COL) in CMAQ system.)

MM5 Domain No. (N)	Resolution ($\Delta x = \Delta y$)	Dimensions (IX, JX) = (ROWS+1, COLS+1)	Origin Relative to Base Grid (I_11, J_11)	Origin Relative to Immediate Parent grid ($ROW_{offset} + 1, COL_{offset} + 1$)
1	108km	(41,61)	(1,1)	(1,1)
2	36km	(67,82)	(9,24)	(9,24)
3	12km	(82,100)	(19.333333,35.333333)	(32,35)
4	04km	(100,82)	(21.444444,41.555555)	(20,57)

a) Definitions for MM5 108 km mother grid (N=1)

In MM5, the grid is defined with the number of dot points. Therefore, to use MM5's grid definitions, for Models-3/CMAQ's cross-point grid definitions, we need to use following

$$NCOLS = JX - 1 = 61 - 1 = 60 \quad (12-138a)$$

$$NROWS = IX - 1 = 41 - 1 = 40. \quad (12-138b)$$

For this grid, no "parent grid" is defined. Origins should be defined with the formula that is specific to MM5's method of grid/domain definition. Note that we require the MM5 mother domain's number of cells in horizontal directions (i.e., NCOLS and NROWS) to be even numbers, so that the dimensions of the four quadrants relative to the center of the coordinates are identical (Refer to Figure 12-9). The origin of the coarse MM5 grid is defined with

$$(x_{orig}, y_{orig}) = \left(-\frac{N_{cols}}{2} * \Delta x, -\frac{N_{rows}}{2} * \Delta y \right) \quad (12-139)$$

Because it is the mother grid of the grid family, offsets should be set to zero:

$$(COL_{offset}, ROW_{offset}) = (0, 0) \quad (12-140)$$

Currently this domain is defined with resolution of 108km (see Table 12-12).

b) Definitions for MM5 36 km first-level nest grid/domain (N=2)

For this grid, the MM5 108km domain defined above is used as the "parent grid." For the nested domains, NCOLS and NROWS can be either even or odd numbers:

$$NCOLS = JX - 1 = 67 - 1 = 66 \quad (12-141a)$$

$$NROWS = IX - 1 = 82 - 1 = 81. \quad (12-141b)$$

Because the left-most and bottom corner of the nest 36km domain is defined with $(I_{1,1}, J_{1,1})$ in MM5, we need to convert this information into $(COL_{offset}, ROW_{offset})$ using following equation:

$$(COL_{offset}, ROW_{offset}) = (J_{1,1} - 1, I_{1,1} - 1) \quad (12-142)$$

Note that MM5 uses left-hand coordinate system, so that the index positions for $(I_{1,1}, J_{1,1})$ are reversed with those for the Models-3/CMAQ's $(COL_{offset}, ROW_{offset})$. In the following case, the general equation for computing the offset numbers from $(I_{1,1}, J_{1,1})$ of the MM5 domains will be presented. The coordinates of the origin is computed with:

$$(x_{orig}, y_{orig}) = (x_{orig}^{parent} + COL_{offset} \Delta x^{parent}, y_{orig}^{parent} + ROW_{offset} \Delta y^{parent}) \quad (12-143)$$

c) Definitions for MM5 12 km and 4 km nest grid/domains (N=3, 4)

For the third, 12km domain (N=3), we have:

$$\text{NCOLS} = \text{JX} - 1 = 100 - 1 = 99 \quad (12-144a)$$

$$\text{NROWS} = \text{IX} - 1 = 82 - 1 = 81 \quad (12-144b)$$

and MM5 36km domain is used as the parent grid. Also, for the fourth 4 km domain (N=4), we have:

$$\text{NCOLS} = \text{JX} - 1 = 82 - 1 = 81 \quad (12-145a)$$

$$\text{NROWS} = \text{IX} - 1 = 100 - 1 = 99 \quad (12-145b)$$

and MM5 12km domain is used as the parent grid. Usually, the offset values will be known to the Models-3/CMAQ users.

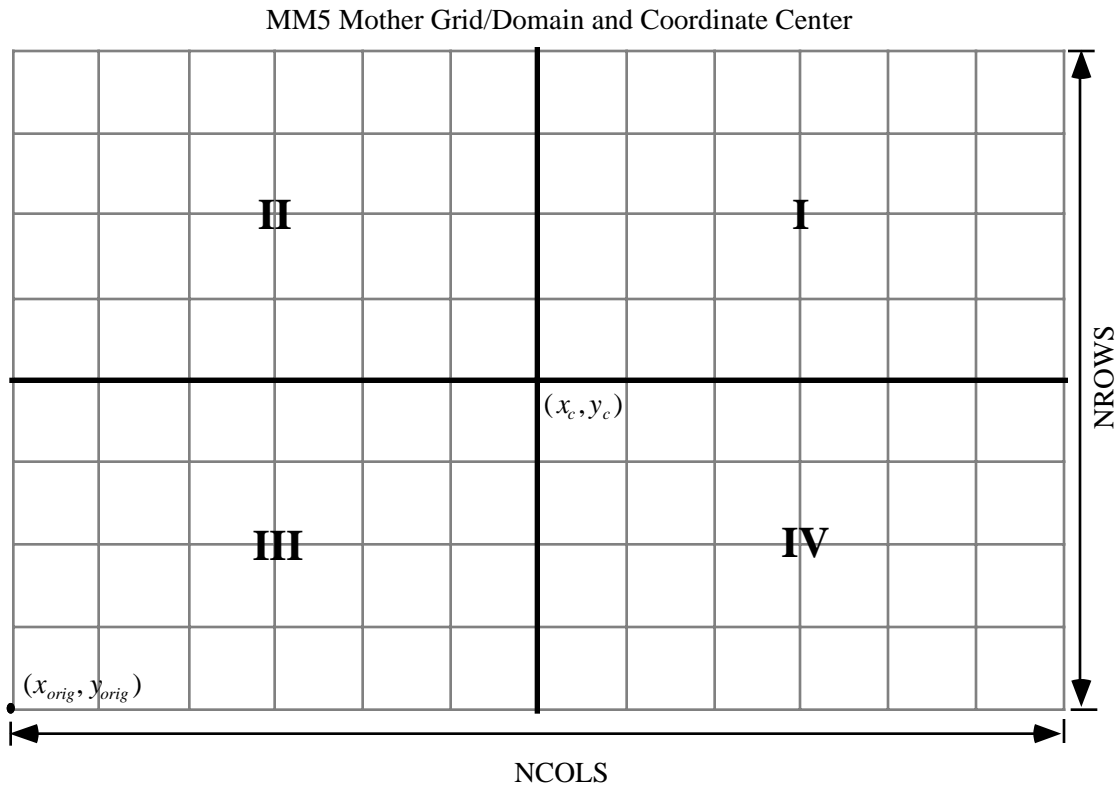


Figure 12-10. A Schematic of the MM5 Mother Grid Definitions.

Because MM5's mother grid is defined from the coordinate center and grows outward, the numbers of columns and rows for each quadrant relative to the coordinate center should be the same, i.e., NCOLS and NROWS for the MM5 mother grid should be even numbers. In case the offset information is not known a priori, one needs to compute the offset values using the header

information in the MM5 output files. To use the information correctly, we need to know how the MM5 nest domain's left-most and bottom corner $(I_{1,1}, J_{1,1})$ is defined. In MM5, all the nest domains are defined relative to the mother grid, and $(I_{1,1}, J_{1,1})$ provides the offset information of the nest domains in terms of the mother grid's resolution. The formula linking a nest MM5's domain $(I_{1,1}, J_{1,1})$ and Models-3/CMAQ's offset values $(COL_{offset}, ROW_{offset})$ are given for $N \geq 2$ as:

$$(J_{1,1}, I_{1,1})_N = \left(\left[1 + \sum_{k=2}^N \frac{(COL_{offset})_k}{(\Delta x^{parent} / \Delta x)^{k-2}} \right], \left[1 + \sum_{k=2}^N \frac{(ROW_{offset})_k}{(\Delta y^{parent} / \Delta y)^{k-2}} \right] \right) \quad (12-146)$$

where $(\Delta x^{parent} / \Delta x) = 3$ for the current MM5 application example. Because our objective is to help users to find out $(COL_{offset}, ROW_{offset})$ for the nest grid, we need to rewrite Equation 12-146 for $(COL_{offset}, ROW_{offset})$. Assuming we know all the coarser grid/domains offset values, $(COL_{offset}, ROW_{offset})$ for the current nesting level $N \geq 2$ can be found as:

$$(COL_{offset})_N = (\Delta x^{parent} / \Delta x)^{N-2} \left[(J_{1,1})_N - 1 - \sum_{k=2}^{N-1} \frac{(COL_{offset})_k}{(\Delta x^{parent} / \Delta x)^{k-2}} \right] \quad (12-147a)$$

$$(ROW_{offset})_N = (\Delta y^{parent} / \Delta y)^{N-2} \left[(I_{1,1})_N - 1 - \sum_{k=2}^{N-1} \frac{(ROW_{offset})_k}{(\Delta y^{parent} / \Delta y)^{k-2}} \right] \quad (12-147b)$$

Although Equations 12-147 a and b look somewhat complicated, one can readily compute offset numbers for Models-3 CMAQ's grid/domain definitions for the example set of domains defined in Table 12-11 as follows:

$$\left[(COL_{offset}), (ROW_{offset}) \right]_{N=2} = [(24 - 1), (9 - 1)] = [23, 8] \quad (12-148a)$$

$$\begin{aligned} \left[(COL_{offset}), (ROW_{offset}) \right]_{N=3} &= \left[3 \left[\left(35 \frac{1}{3} - 1 \right) - 3^0 * 23 \right], 3 \left[\left(19 \frac{1}{3} - 1 \right) - 3^0 * 8 \right] \right] \\ &= [34, 31] \end{aligned} \quad (12-148b)$$

$$\begin{aligned} \left[(COL_{offset}), (ROW_{offset}) \right]_{N=4} &= \left[3^2 \left[\left(41 \frac{5}{9} - 1 \right) - \frac{23}{3^0} - \frac{34}{3} \right], 3^2 \left[\left(21 \frac{4}{9} - 1 \right) - \frac{8}{3^0} - \frac{31}{3} \right] \right] \\ &= [56, 19] \end{aligned} \quad (12-148c)$$

Most of the time, the above MM5 domain definitions are provided by the MM5 modelers and Models-3/CMAQ users do not have to re-compute them.

12.5.4.2 CMAQ Grid Definitions

The horizontal grid structure used for the MM5 serves as the parent grid for the CCTM domains. To define a CCTM grid, number of cells to be excluded from the parent domain must be

determined. It is recommended that the CCTM grid be smaller than its parent MM5 grid by at least 4 grid cells (preferably by 6 grids) to avoid the possible numerical reflection problems at boundaries of MM5 domain. Once the offset values are known, (x_{orig}, y_{orig}) of the nest domain can be computed using Equation 12-143. Refer to Appendix 12B for other examples of other CCTM nest domain definitions.

12.5.5 Extension of MCIP for Other Meteorological Models

The current release version of MCIP can only process MM5 output in binary format or previous MCIP output in I/O API format. To realize the one-atmosphere concept for meteorological and air quality modeling, CMAQ utilizes generalized coordinates. One advantage of the generalized coordinate system is that a single CTM can adapt to any of the coordinate systems and dynamics commonly used in meteorological modeling. Because most meteorological models are not originally designed for air quality studies, they lack characteristics that are required for air quality modeling. Consistencies in dynamic descriptions of atmosphere, physical parameterizations, and numerical algorithms, where applicable, in meteorological and chemistry-transport models are critical in determining the quality of air pollutant simulations. This issue becomes more critical with high resolution air quality study where nonhydrostatic meteorological models must be used.

MCIP is the key processor allowing the consistent linkage between meteorological models and CMAQ. Currently, different meteorological models are used by different atmospheric modeling groups forming their own respective user communities. It is because these meteorological models are applicable for a limited range of spatial and temporal scales. To expand the user base of the Models-3 CMAQ system and to promote the one-atmosphere community modeling paradigm, it is essential to continuously develop MCIP modules for several popular mesoscale meteorological models such as RAMS, ARPS, HOTMAC, and others.

To build a version of MCIP for processing a set of meteorological model output, several issues involved with different dynamics and coordinates must be considered. They are; (1) compatibility of governing set of equations and state variables used, (2) scale limitations in subgrid scale parameterizations such as cloud, turbulence, and surface exchange processes, and (3) consistency in numerical algorithms and discretization methods. Before designing MCIP modules for other meteorological model, developers should identify the structure, format, and frequency of data as well as their impact on the processing structure of MCIP. MCIP expects time dependent meteorological data in a structured grid system as the input. As this moment, there is no provision for handling irregularly spaced data structure either from observations or from a meteorological modeling system with unstructured adaptive (fixed or dynamic) grid structure, such as the one used in OMEGA system (Bacon et al., 1996). If there is need for including these data, object analysis tools must be used to prepare data in a structured grid system.

The essential information related to the coordinates and dynamic assumptions used in meteorological models is captured in MCIP. Dynamic and thermodynamic state variables are recast into the fully compressible system as described in Chapter 5 of this volume.

It is important to know the processing sequence and associated data structures used in the current MCIP code. Major processing steps in MCIP can be summarized as follows: (1) Grid, coordinate, and information on atmospheric dynamics are used to compute Jacobian and layer heights; (2) State

variables in meteorological models are recast into density and entropy; (3) Contravariant wind components are computed; (4) necessary two-dimensional parameters are diagnosed; and (5) Some of two- and three-dimensional parameters are passed through. Figure 12-11 shows corresponding data structures used at different phases. Input phase uses arrays with dimensions covering the full meteorology domain ('F-arrays'), processing phase uses arrays for extended domain covering both the CMAQ and boundary domains ('X-arrays'). During the output phase, the information in X-arrays are separated into the CMAQ and boundary domains for respective data types described in Table 12-3.

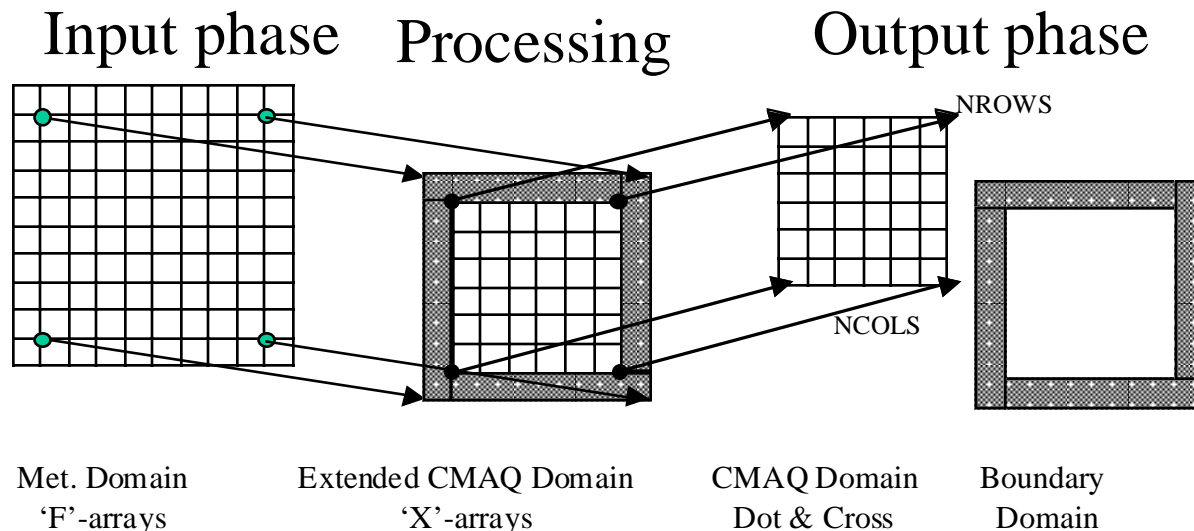


Figure 12-11. Data Structures Corresponding to Input, Processing, and Output Phases of MCIP Processing

12.6 Concluding Remarks

MCIP is a key processor linking meteorological models to the CMAQ modeling system. Its major roles are:

1. To read meteorological data from a meteorological model and converts them in Models-3 I/O API format.
2. To provide all the necessary meteorological parameters for air quality simulations. When necessary, PBL parameters and other derived quantities are computed using gridded meteorology data and high-resolution fractional land use information.
3. To support multiscale generalized coordinate implementation of the CCTM.

Current implementation of MCIP is mainly for linking MM5 output to CCTM. Reader modules to Regional Atmospheric Modeling System (RAMS) (Pielke et al., 1992), will be added. Users who wish to link other meteorological models may need to modify and introduce appropriate input modules.

12.7 References

- Alduchov, O. A. and R. E. Eskridge, 1996: Improved Magnus form approximation of saturation pressure. *J. Appl. Meteorol.*, **35**, 601-609.
- Anthes, R. A., E. Y. Hsie and Y.H Kuo, 1987: Description of the Penn State/NCAR Mesoscale Model version 4 (MM4). NCAR Technical Note, NCAR/TN-282+STR, National Center for Atmospheric Research, Boulder, CO. 66pp.
- Avissar, R., P. Avissar, Y. Hahrer, and B. A. Bravdo, 1985: A model to simulate response of plant stomata to environmental conditions. *Ag. and Forest Meteorol.*, **34**, 21-29.
- Bacon, D. P., Z. Boybeyi, P.R. Boris, T. J. Dunn, M. Hall, R. A. Sarma, S. Young, and J. Zack, 1996: An overview of the operational Multi-scale Environmental model with Grid Adaptivity. *Proc. of the 15th Conf. on Wea. Anal. and Forecasting*, Norfolk, VA, August 19-23, 1996, American Meteorological Soc., Boston, MA.
- Ball, J. T., I. E., Woodrow, and J. A. Berry, 1987: A model predicting stomatal conductance and its contribution to the control of photosynthesis under different environmental conditions. In *Progress in photosynthesis Research, Vol. IV* (ed. J. Biggins), pp. 221-234. Martinus Nijhof Publishers, Dordrecht.
- Betts, A. K., 1973: Non-precipitating cumulus convection and its parameterization. *Quart. J. Roy. Meteorol. Soc.* **99**, 178-196.
- Binkowski, F.S. and U. Shankar, 1995: The Regional Particulate Model. 1. Model description and preliminary results. *J. Geophys. Res.*, **100 D12**, 26191-26209.
- Blackadar, A. K., 1978: Modeling pollutant transfer during daytime convection, *Preprints, Fourth Symposium on Atmospheric Turbulence, Diffusion, and Air Quality*, Reno, Am. Meteor. Soc., 443-447.
- Brost R. A. and J. C. Wyngaard, 1978: A model study of the stably stratified planetary boundary layer. *J. Atmos. Sci.*, **35**, 1427-1440.
- Businger J. A., J. C. Wyngaard, Y. Izumi, and E. F. Bradley, 1971: Flux profile relationships in the atmospheric surface layer, *J. Atmos. Sci.*, **28**, 181-189.
- Byun, D. W., 1990: On the analytical solutions of flux-profile relationships for the atmospheric surface layer, *J. Appl. meteorol.*, **29**, 652-657.
- Byun, D. W., 1991: Determination of similarity functions of the resistance laws for the planetary boundary layer using surface-layer similarity functions, *Boundary Layer Meteorol.*, **57**, 17-48.
- Byun, D.W., 1999a: Dynamically consistent formulations in meteorological and air quality models for multiscale atmospheric applications: I. Governing equations in generalized coordinate System. *J. Atmos. Sci.*, (in print)

- Byun, D.W., 1999b: Dynamically consistent formulations in meteorological and air quality models for multiscale atmospheric applications: II. Mass conservation issues. *J. Atmos. Sci.*, (in print)
- Byun, D. W., and R.L. Dennis, 1995: Design artifacts in Eulerian air quality models: Evaluation of the effects of layer thickness and vertical profile correction on surface ozone concentrations. *Atmospheric Environment*, **29**, No. 1, 105-126.
- Carson, D. J., 1973: The development of a dry inversion-capped convectively unstable boundary layer. *Quart. J. Roy. Meteorol. Soc.* **99**, 450-467.
- Cederqvist, P., 1993: *Version Management with CVS*, Signum Support AB, Linkoping, Sweden. 168pp.
- Chang, J.S., R.A. Brost, I.S.A. Isaksen, S. Madronich, P. Middleton, W.R. Stockwell, and C.J. Walcek, 1987: A three-dimensional Eulerian acid deposition model: Physical concepts and formulation, *J. of Geophys. Res.*, **92**, 14,681-700.
- Chang, J.S., P.B. Middleton, W.R. Stockwell, C.J. Walcek, J.E. Pleim, H.H. Lansford, S. Madronich, N.L. Seaman, D.R. Stauffer, F.S. Binkowski, D. Byun, J.N. McHenry, H. Hass, and P.J. Samson, 1990: The Regional Acid Deposition Model and Engineering Model, NAPAP report 4.
- Coats, C. J., cited 1996: The EDSS/Models-3 I/O Applications Programming Interface. MCNC Environmental Programs, Research Triangle Park, NC. [Available on-line from <http://www.iceis.mcnc.org/EDSS/ioapi/H.AA.html>.]
- Collatz, G. J., C. Grivet, J. T. Ball, and J. A. Berry, 1991: Physiological and environmental regulation of stomatal conductance, photosynthesis and transpiration: a model that includes a laminar boundary layer. *Ag. and Forest Meteorol.*, **54**, 107-136.
- Driedonks, A. G. M., 1981: Dynamics of the well-mixed atmospheric boundary layer. De Bilt KNMI Sci. Rep. WR 81-2, 189pp.
- Dudhia, J., 1989: Numerical study of convection observed during the Winter Monsoon Experiment using a mesoscale two-dimensional model. *J. Atmos. Sci.*, **46**, 3077-3107.
- Dudhia, J., 1993: A nonhydrostatic version of the Penn State-NCAR mesoscale model: Validation tests and simulation of an Atlantic cyclone and cold front, *Mon. Wea. Rev.*, **121**, 1493-1513.
- Erisman, J. W., A. van Pul, and P. Wyers, 1994: Parameterization of surface resistance for the quantification of atmospheric deposition of acidifying pollutants and ozone. *Atmos. Environ.* **28**, 2595-2607.
- Fowler, D., 1978: Dry deposition of SO₂ on agricultural crops, *Atmos. Environ.*, **12**, 369-373.
- Fritsch, J.M., and C.F. Chappell, 1980: Numerical prediction of convectively driven mesoscale pressure systems, 1, Convective parameterization, *J. Atmos. Sci.*, **37**, 1722-1733.

- Geleyn, J.-F., A. Hense, and H.-J. Preuss, 1982: A comparison of model-generated radiation fields with satellite measurements. *Beitr. Phys. Atmos.*, **55**, 253-286.
- Grell, G.A., J. Dudhia, and D.R. Stauffer, 1994: A Description of the Fifth-Generation PENN STATE/NCAR Mesoscale Model (MM5), NCAR Technical Note, NCAR/TN-398+STR, National Center for Atmospheric Research, Boulder, Colorado, 138pp
- Haagenson, P. L., J. Dudhia, D. R. Stauffer, and G. A. Grell, 1994: The Penn State-NCAR mesoscale model (MM5) source code document, *NCAR/TN-392+STR*, National Center for Atmospheric Research, Boulder, Colorado.
- Hack, J. J., B. A. Boville, B. P. Briegleb, J. T. Kiehl, P. J. Rasch, and D. L. Williamson, 1993: Description of the NCAR community climate model (CCM2). NCAR Tech. Note, NCAR/TN-382+STR, 120 pp. [Available from the National Center for Atmospheric Research, P.O. Box 3000, Boulder, CO 80307.]
- Hess, G. D., 1992: Observations and scaling of the atmospheric boundary layer. *Aus. Meteorol. Mag.* **41**, 79-99.
- Högström, U., 1988: Non-dimensional wind and temperature profiles in the atmospheric surface layers: a re-evaluation. *Boundary-Layer Meteorol.*, **42**, 55-78.
- Holtslag, A. A., E. I. F. de Bruin, and H.-L. Pan, 1990: A high resolution air mass transformation model for short-range weather forecasting. *Mon. Weather Rev.*, **118**, 1561-1575.
- Holtslag, A.A.M., E.V. Meijgaard, and W.C. DeRooy, 1995: A comparison of boundary layer diffusion schemes in unstable conditions over land, *Boundary-Layer Meteorol.*, **76**, 69-95.
- Jarvis, P. G., 1976: The interpretation of the variation of leaf water potential and stomatal conductance found in canopies in the field. *Phil. Trans. Royal Meteorol. Soc. of London, Series B*, **273**, 593-610.
- Jacquemin B. and J. Noilhan, 1990: Sensitivity study and validation of a land surface parameterization using the HAPEX-MOBILHY data set. *Bound.-Layer Meteorol.*, **52**, 93-134.
- Jaung, H.-M. H., 1992: A spectral fully compressible nonhydrostatic mesoscale model in hydrostatic sigma coordinates: Formulations and preliminary results. *Meteor. Atmos. Phys.*, **50**, 75-88.
- Kain, J. S., and J. M. Fritsch, 1993: Convective parameterization for mesoscale models: The Kain-Fritsch scheme. *The representation of cumulus in mesoscale models.*, K.A. Emanuel and D.J. Raymond, Eds., Amer. Meteor. Soc., 246pp.
- Lo, A. K., 1993: The direct calculation of fluxes and profiles in the marine surface layer using measurements from a single atmospheric level. *J. Appl. Meteorol.*, **32**, 1890-1990.

- Lo, A. K., 1995: Determination of zero-plane displacement and roughness length of a forest canopy using profiles of limited height. *Boundary-Layer Meteorol.*, **75**, 381-402.
- Madronich, S., 1987: Intercomparison of NO₂ photodissociation and UV radiometer measurements, *Atmos. Environ.*, **21**, 569-578.
- Mason, P.J., 1987: The formation of areally-averaged roughness lengths. *Q.J.R. Meteorol. Soc.*, **106**, 351-366.
- Mesinger, F. and A. Arakawa, 1976: Numerical methods used in atmospheric models. In: Global Atmospheric Research Programme (GARP), Joint Organization Committee, GARP Publication Series, No. 17, Aug., 1976: [Available from WMO Secretariat, Geneva].
- Mihailovic, D. T., R. A. Pielke, B. Rajkovic, L. J. Tsengdar, and M. Jeftic, 1993: A resistance representation of schemes for evaporation from bare and partly plant-covered surfaces for use in atmospheric models. *J. Appl. Meteorol.*, **32**, 1038-1054.
- Noilhan, J. and S. Planton, 1989: A simple parameterization of land surface processes for meteorological models. *Mon. Wea. Rev.*, **117**, 536-549.
- Ooyama, K. V., 1990: A thermodynamic foundation for modeling the moist atmosphere. *J. Atmos. Sci.*, **47**, 2580-2593.
- Padro, J., G. den Hartog, and H. H. Neumann, 1991: An investigation of the ADOM dry deposition module using summertime O₃ measurements above a deciduous forest, *Atmos. Environ.*, **25A**, 1689-1704.
- Paulson, C. A., 1970: The mathematical representation of wind speed and temperature profile in the unstable atmospheric surface layer. *J. Appl. Meteor.*, **9**, 857-861.
- Pielke, R. A., W. R. Cotton, R. L. Walko, C. J. Tremback, M. E. Nicholls, M. D. Moran, D. A. Wesley., T. J. Lee, and J. H. Copeland, 1992: A comprehensive meteorological modeling system—RAMS. *Meteor. Atmos. Phys.*, **49**, 69-91.
- Pleim, J. , A. Venkatram, and R. Yamartino, 1984: ADOM/TADAP Model Development Program, Volume 4, The Dry Deposition Module. ERT P-B980-520, Prepared for OME, AES of Canada and the Umweltbundesamt, Germany.
- Pleim, J. E. and A. Xiu, 1995: Development and testing of a surface flux and planetary boundary layer model for application in mesoscale models, *J. Appl. Meteor.*, **34**, 16-32.
- Pleim, J. E. , A. Xiu, P. L. Finkelstein, and J. F. Clarke, 1997: Evaluation of a coupled land-surface and dry deposition model through comparison to field measurements of surface heat, moisture, and ozone fluxes, Proceedings of the 12th Symposium on Boundary Layers and Turbulence, July 28-August 1, 1997, Vancouver, BC.
- Pleim, J. E., J. F. Clarke, P. L. Finkelstein, E. J. Cooter, T. G. Ellestad, A. Xiu, and W. M. Angevine, 1996: Comparison of measured and modeled surface fluxes of heat, moisture and

- chemical dry deposition. In: Air Pollution Modeling and its Application XI, Ed: Gryning and Schiermeier, Plenum Press, New York.
- Rochette, P., Desjardins, R. L., Dwyer, L. M., Stewart, D. W., Pattey, E., and Dubé, P. A., 1991: Estimation of maize canopy conductance by scaling up leaf stomatal conductance. *Ag. and Forest Meteorol.*, **54**, 241-262.
- Schumann, U., 1989: Large-eddy simulation of turbulent diffusion with chemical reactions in the convective boundary layer. *Atmos. Environ.*, **23**, 1713-1727.
- Seaman, N. L., D. R. Stauffer, and A. M. Lario-Gibbs, 1995: A multiscale four-dimensional data assimilation system applied in the San Joaquin Valley during SARMAP. Part I: Modeling design and basic performance characteristics, *J. Appl. Meteor.*, **34**, 1739-1761.
- Seaman, N. L., and D. R. Stauffer, 1995: Simulation of the thermal structure of the San Joaquin Valley during SJVAQS/AUSPEX/SARMAP using MM5 with four-dimensional data assimilation, paper presented at the AWMA conference, Regional Photochemical Measurement and Modeling Studies, November 8-12, San Diego, Calif., 1993.
- Sellers, P. J., Y. Mintz, Y. C. Sud, and A. Dalcher, 1986: A simple biosphere model (SiB) for use within general circulation models. *J. Atmos. Sci.*, **43**, 505-531.
- Sellers, P. J., R. E. Dickinson, D. A. Randall, A. K. Betts, F. G. Hall, J. A. Berry, G. J. Collatz, A. S. Denning, H. A. Mooney, C. A. Nobre, N. Sato, C. B. Field, and A. Henderson-Sellers, 1997: Modeling the exchanges of energy, water, and carbon between continents and the atmosphere. *Science*, **275**, 502-509.
- Sheih, C.M., M.L. Wesely, and B. B. Hicks, 1979: Estimated dry deposition velocities of sulfur over the eastern United States and surrounding regions, *Atmos. Environ.*, **13**, 1361-1368.
- Sirois, A., and L.A. Barrie, 1988: An estimate of the importance of dry deposition as a pathway of acidic substances from the atmosphere to the biosphere in eastern Canada, *Tellus*, **40B**, 59-80.
- Slinn, W. G. N., L. Hasse, B. B. Hicks, A. W. Hogan, D. Lal, P. S. Liss, K. O. Munnice, G. A. Sehmel, and O. Vittori, 1978: Some aspects of the transfer of atmospheric trace constituents past the air-sea interface. *Atmos. Environ.* **12**, 2055-2087.
- Stauffer, D. R., and N. L. Seaman, 1993: Evaluation of multiscale four-dimensional data assimilation techniques developed and tested in MM5 during SJVAQS/AUSPEX/ SARMAP, paper presented at the AWMA conference, Regional Photochemical Measurement and Modeling Studies, November 8-12, San Diego, Calif., 1993.
- Tesche, T. W., and D. McNally, 1993: Operational evaluation of the SARMAP meteorological model (SMM1) for episode 1: 3-6 August, 1990, Alpine Geophysics, Crested Butte, CO.
- Thorpe, S., cited 1996: PAVE User Guide. MCNC Environmental Programs, Research Triangle Park, NC. [Available on-line from http://www.iceis.mcnc.org/EDSS/pave_doc/SCCS/s.Pave.html.]

- Voldner, E.C., L.A. Barrie, and A. Sirois, 1986: A literature survey of dry deposition of oxides of sulfur and nitrogen with emphasis on long-range transport modelling in North America, *Atmos. Environ.*, **20**, 2101-2123.
- Walcek, C.J., 1987: A theoretical estimate of O₃ and H₂O₂ dry deposition over the northeast United States, *Atmos. Environ.*, **21**, 2649-2659.
- Walcek, C.J., R. A. Brost, J. S. Chang, and M. L. Wesely, 1986: SO₂, sulfate and HNO₃ deposition velocities computed using regional landuse and meteorological data, *Atmos. Environ.*, **20**, 949-964.
- Walcek, C.J., and G.R. Taylor, 1986: A theoretical method for computing vertical distributions of acidity and sulfate production within cumulus clouds, *J. Atmos. Sci.*, **43**, 339-355.
- Warner, J., 1970: On steady-state one-dimensional models of cumulus convection, *J. Atmos. Sci.*, **27**, 1035-1040.
- Wesely, M. L., 1989: Parameterization of surface resistances to gaseous dry deposition in regional-scale numerical models, *Atmos. Environ.*, **23**, 1293-1304.
- Wesely, M. L., and B. B. Hicks, 1977: Some factors that affect the deposition rates of sulfur dioxide and similar gases on vegetation, *J. Air Pollut. Control. Assoc.*, **27**, 1110-1116.
- Wesely, M. L., D. R. Cook, R. L. Hart, and R. E. Speer, 1985: Measurements and parameterization of particulate sulfur dry deposition over grass, *J. Geophys. Res.*, **90**, 2131-2143.
- Wetzel, P. J., and J.-T. Chang, 1988: Evapotranspiration from nonuniform surfaces: a first approach for short-term numerical weather prediction. *Mon. Wea. Rev.*, **116**, 600-621.
- Wojcik, G.S., and J.S. Chang, 1996: An Eulerian modeling study of anthropogenic sulfur budgets and lifetimes for Eastern North America, *submitted to J. Atmos. Chem.*
- Wyngaard, J. and Brost, J.C. and R. A. Brost, 1984: Top-down and bottom-up diffusion of a scalar in the convective boundary layer. *J. Atmos. Sci.*, **41**, 102-112.
- Xue, M., K. Droegemeier, V. Vong, A. Shapiro, and K. Brewster, 1995: ARPS Version 4.0 User's Guide. Center for the Analysis and Prediction of Storms, Univ. of Oklahoma, 380 pp. [Available from Center for the Analysis and Prediction of Storms, Univ. of Oklahoma, Norman, OK 73019].
- Zilitinkevich S. S., 1989: Velocity profiles, the resistance law and the dissipation rate of mean flow kinetic energy in a neutrally and stably stratified planetary boundary layer. *Bound. Layer Met.*, **46**, 367-387.

This chapter is taken from *Science Algorithms of the EPA Models-3 Community Multiscale Air Quality (CMAQ) Modeling System*, edited by D. W. Byun and J. K. S. Ching, 1999.

Appendix 12A MCIP Output Data

MCIP writes the bulk of its two- and three-dimensional meteorology and geophysical output data in a transportable binary format using a tailored Models-3 input/output applications program interface (I/O API) library. Depending on whether the meteorological vertical coordinate is time dependent or not, the temporal characteristics of certain variables that belong to GRID data types and MET data types may differ. For example, when the meteorological coordinate is σ_p , which is time dependent, Jacobian is also time dependent. On the other hand for σ_{po} coordinate, Jacobian is time independent. However we are using a consistent list of meteorological variables for both hydrostatic and nonhydrostatic coordinates for as the standard output. Tables 12A-1 through 12A-6 provide lists of variables in each data type.

Table 12A1. Variables in GRIDCRO2D

Variable Name	Unit	Description
LAT	DEGREES	latitude (south negative)
LON	DEGREES	longitude (west negative)
MSFX2	(M/M)**2	squared map-scale factor (CROSS)
HT	M	terrain elevation
ZZERO	M	roughness length
PSTAR0	Pascal	pressure difference between top and surface
JACOBS0	M	total Jacobian at surface
LUSE_URBA	fraction (0-1)	landuse for URBAN_LAND
LUSE_AGRI	fraction (0-1)	landuse for AGRICILTURE
LUSE_RANG	fraction (0-1)	landuse for RANGE
LUSE_DECI	fraction (0-1)	landuse for DECIDUOUS_FOREST
LUSE_CONI	fraction (0-1)	landuse for CONIFEROUS_FOREST
LUSE_MIXF	fraction (0-1)	landuse for MIXFOREST_WETLND
LUSE_WATE	fraction (0-1)	landuse for WATER
LUSE_BARR	fraction (0-1)	landuse for BARREN_LAND
LUSE_NONE	fraction (0-1)	landuse for NONFOREST_WETLND
LUSE_MIXA	fraction (0-1)	landuse for MIXAGRI_RANGE
LUSE_DECI	fraction (0-1)	landuse for URBAN_LAND
LUSE_ROCK	fraction (0-1)	landuse for ROCKY_OPENSHRUB

Table 12A2. Variables in GRIDDOT2D

Variable Name	Unit	Description
LAT	DEGREES	latitude (south negative)
LON	DEGREES	longitude (west negative)
MSFD2	(M/M)**2	squared map-scale factor (DOT)

Table 12A3. Variables in GRIDCRO3D

Variable Name	Unit	Description
DENS0	KG/M**3	density of reference atmosphere
ENTRP0	J/K/M**3	entropy density of reference atmosphere
JACOB0F	M	total Jacobian at layer face
JACOB0M	M	total Jacobian at layer middle
TEMP0	K	temperature of reference atmosphere
PRES0	Pascal	pressure of reference atmosphere
X3HT0F	M	height of layer face (top) of reference atmosphere
X3HT0M	M	height of layer middle of reference atmosphere

Table 12A4. Variables in METCRO3D

Variable Name	Unit	Description
JACOBF	M	total Jacobian at layer face
JACOBM	M	total Jacobian at layer middle
DENSA_J	KG/M**2	Jacobian weighted total air density
DENSW_J	KG/M**2	Jacobian weighted density of vapor
ENTRP_J	J/K/M**2	Jacobian weighted entropy of moist air
WHAT_JD	KG/(M*S)	J & Density weighted vertical contra-W
QC	KG/KG	cloud water mixing ratio
QR	KG/KG	rain water mixing ratio
QV	KG/KG	water vapor mixing ratio
TA	K	air temperature
PRES	Pascal	pressure
DENS	KG/M**3	total density of air
WWIND	M/S	true W component of wind
ZH	M	mid-layer height above ground
ZF	M	full-layer height above ground
JDRATE	KG/M**2/S	time rate change of Jacob*Density

Table 12A5. Variables in METDOT3D

Variable Name	Unit	Description
UWIND	M/S	U-comp. of true wind at dot point
VWIND	M/S	V-comp. of true wind at dot point
UHAT_JD	KG/(M*S)	(contra_U*Jacobian*Density) at square pt
VHAT_JD	KG/(M*S)	(contra_V*Jacobian*Density) at triangle pt

Table 12A6. Variables in METCRO2D

Variable Name	Unit	Description
PSTAR	Pascal	pressure difference (PSURF - PTOP)
JACOBS	M	total Jacobian at surface
DENSAS	KG/M**3	air density at surface
WSTAR	M/S	convective velocity scale
RIB	NODIM	bulk Richardson number
PBL	M	PBL height
ZRUF	M	surface roughness length
MOLI	1/M	inverse of Monin-Obukhov length
HFX	WATTS/M**2	sensible heat flux
QFX	WATTS/M**2	latent heat flux
MOLI	1/M	inverse of Monin-Obukhov length
RADYNI	M/S	inverse of aerodynamic resistance
RBNFYI	M/S	inverse of laminar bnd layer resistance
RSTOMI	M/S	bulk stomatal resistance for water
TEMPG	K	skin temperature at ground
TEMP10	K	air temperature at 10 m
TEMP1P5	K	air temperature at 1.5 m
SURF2	EMPTY	surface parameter 1
ALBEDO	NODIM	surface albedo
FSOIL	WATTS/M**2	heat flux in soil layers
GLW	WATTS/M**2	longwave radiation at ground
GSW	WATTS/M**2	solar radiation absorbed at ground
RGRND	WATTS/M**2	solar radiation reaching surface
RNET	WATTS/M**2	net radiation .
RN	CM	accumulated nonconvective hourly precip.
RC	CM	accumulated convective hourly precip.
CFRACH	Fraction	fraction of high cloud
CFRACM	Fraction	fraction of middle cloud
CFRACL	Fraction	fraction of low cloud
CFRAC	Fraction	total cloud fraction
CLDT	M	cloud top layer height
CLDB	M	cloud bottom layer height
WBAR	G/M**3	liquid water content of cloud
VD_XXXX	M/S	dry deposition velocity for species XXXX

Note: List of deposition velocities

VD_SO2 : "M/S" ; deposition velocity for species SO2
 VD_SULF : "M/S" ; deposition velocity for species SULF
 VD_NO2 : "M/S" ; deposition velocity for species NO2
 VD_NO : "M/S" ; deposition velocity for species NO
 VD_O3 : "M/S" ; deposition velocity for species O3
 VD_HNO3 : "M/S" ; deposition velocity for species HNO3
 VD_H2O2 : "M/S" ; deposition velocity for species H2O2
 VD_ALD : "M/S" ; deposition velocity for species ALD
 VD_HCHO : "M/S" ; deposition velocity for species HCHO
 VD_OP : "M/S" ; deposition velocity for species OP
 VD_ORA : "M/S" ; deposition velocity for species ORA
 VD_NH3 : "M/S" ; deposition velocity for species NH3
 VD_PAN : "M/S" ; deposition velocity for species PAN
 VD_HONO : "M/S" ; deposition velocity for species HONO
 VD_CO : "M/S" ; deposition velocity for species CO

Appendix 12B Examples of Nest Domain Definitions for CMAQ system

12B.1 Grid Domain Definitions for the Models-3 CMAQ Tutorial Study

Table 12B-1. Origins for the TUTORIAL MM5 domain, MCIP landuse domain, and CTM domains. Note that (x,y) corresponds to (COL,ROW) in CMAQ. MCIP landuse domain is smaller by one cell around than the original MM5 domain. Also, the CTM domain removes three cells around from the original MM5 domain. Origin is measured from the center of Base 108 km domain located at 90W and 40N.

Resolution ($\Delta x = \Delta y$)	Origin for original MM5 Domain (x_{orig}, y_{orig})	Origin for MCIP Landuse Domain (x_{orig}, y_{orig})	Origin for CTM Domain (x_{orig}, y_{orig})
108km	$(-3996 \times 10^3, -2808 \times 10^3)$	N/A	N/A
36km	$(432 \times 10^3, -432 \times 10^3)$	$(468 \times 10^3, -396 \times 10^3)$	$(540 \times 10^3, -324 \times 10^3)$
12km	$(972 \times 10^3, -36 \times 10^3)$	$(984 \times 10^3, -24 \times 10^3)$	$(1008 \times 10^3, 0 \times 10^3)$
04km	$(1200 \times 10^3, 120 \times 10^3)$	$(1204 \times 10^3, 124 \times 10^3)$	$(1212 \times 10^3, 132 \times 10^3)$

Table 12B-2. Offset Definitions for the Tutorial MM5 Nest Domains

MM5 Domain	Resolution (km)	NCOLS	NROWS	Col. Offset from Parent Domain, D1	Row Offset from Parent Domain, D1	Col. Offset for nest	Row Offset for nest
D1	108	74	52	0	0	0	0
D2	36	36	36	41	22	41	22
D3	12	39	36	47	26.666666	15	11
D4	4	36	36	48.666666	28.111111	19	13

Table 12B-3. Dimensions of Set of MM5, MCIP, and CTM Domains for Each Grid Resolution for the Tutorial Study

Resolution	MM5 NCOLS	MM5 NROWS	MCIP NCOLS	MCIP NROWS	CTM NCOLS	CTM NROWS
108	74	52	N/A	N/A	N/A	N/A
36	36	36	34	34	30	30
12	39	36	37	34	33	30
4	36	36	34	34	30	30

12B.2 Grid Domain Definitions for the Models-3 CMAQ Demonstration Study

Table 12B-4. Origins for the CMAQ demonstration MM5 domain, MCIP landuse domain, and CTM domains. Note that (x,y) corresponds to (COL,ROW) in CMAQ. MCIP landuse domain is smaller by one cell around than the original MM5 domain. Also, the CTM domain removes three cells around from the original MM5 domain. Origin is measured from the center of Base 108 km domain located at 90W and 40N.

Resolution ($\Delta x = \Delta y$)	Origin for original MM5 Domain (x_{orig}, y_{orig})	Origin for MCIP Landuse Domain (x_{orig}, y_{orig})	Origin for CTM Domain (x_{orig}, y_{orig})
108km	(-3996x10 ³ , -2808x10 ³)	N/A	N/A
36km	(-1080x10 ³ , -1728x10 ³)	(-1044x10 ³ , -1692x10 ³)	(-864x10 ³ , -1512x10 ³)
12km	(486x10 ³ , -216x10 ³)	(480x10 ³ , -204x10 ³)	(540x10 ³ , -144x10 ³)
04km	(1140x10 ³ , 24x10 ³)	(1144x10 ³ , 28x10 ³)	(1164x10 ³ , 48x10 ³)

Table 12B-5. Offset Definitions for the CMAQ Demonstration MM5 Nest Domains

MM5 Domain	Resolution (km)	NCOLS	NROWS	Col. Offset from Parent Domain, D1	Row Offset from Parent Domain, D1	Col. Offset for nest	Row Offset for nest
D1	108	74	52	0	0	0	0
D2	36	87	81	27	22	27	10
D3	12	102	84	42.333333	25	43	42
D4	4	87	105	48.555556	27.222222	56	20

Table B6. Dimensions of Set of MM5, MCIP, and CTM Domains for Each Grid Resolution for the CMAQ Demonstration Study

Resolution	MM5 NCOLS	MM5 NROWS	MCIP NCOLS	MCIP NROWS	CTM NCOLS	CTM NROWS
108	74	52	N/A	N/A	N/A	N/A
36	87	81	85	79	75	69
12	102	84	100	82	90	72
4	87	105	85	103	75	93

Appendix 12C Sample MCIP Configuration File

```
// RCS file, release, date & time of last delta, author, state, [and locker]
// $Header: /project/work/rep/MCIP/src/sunOS5/sun_m3_12.cfg,v 1.1.1.1 1997/10/13 17:38:23 yoj
Exp $

// what(1) key, module and SID; SCCS file; date and time of last delta:
// @(#)sun_m3_12.cfg 1.1 /project/mod3/MCIP/doc/bldrun/sunOS5/SCCS/s.sun_m3_12.cfg 14 Jun
1997 15:41:54

// This is a configuration file for
model mcip_m3_12;

// f77_flags "-e -N1200 -fast -O4";
f77_flags "-e -g -C";

// link_flags "-fast -O4";
link_flags "-e -g -C";

libraries "-L${M3TOOLS}/IOAPI/src_lib/SunOS5 -lm3io \
-L${M3TOOLS}/netCDF/SunOS5 -lnetcdf";

// global { verbose | parse_only | compile_all | one_step | clean_up } ...

global verbose;

// shared include files //////////////////////////////////////

// Models-3 I/O API permanent includes
include SUBST_IOPARMS    ${M3TOOLS}/IOAPI/includes/PARMS3.EXT;
include SUBST_IOFDESC    ${M3TOOLS}/IOAPI/includes/FDESC3.EXT;
include SUBST_IODECL     ${M3TOOLS}/IOAPI/includes/IODECL3.EXT;

// Models-3 global constants for this processor
include SUBST_CONST      ${M3MODEL}/ICL/src/fixed/const/CONST.EXT;

// Models-3 grid definitions
include SUBST_HGRD_ID    ${M3MODEL}/ICL/src/grid/D_12_15/HGRD_21X21.EXT;
include SUBST_VGRD_ID    ${M3MODEL}/ICL/src/grid/D_12_15/VGRD.EXT;
include SUBST_COORD_ID   ${M3MODEL}/ICL/src/grid/D_12_15/COORD_21X21.EXT;

// Models-3 I/O API files for this processor
include SUBST_INFILES    ${M3MODEL}/MCIP/src/icl/icl/INFILES_MCIP.EXT;
include SUBST_FILES      ${M3MODEL}/MCIP/src/icl/icl/FILES3_MCIP.EXT;

include SUBST_MET_CONST  ${M3MODEL}/MCIP/src/icl/icl/CONST_mete.EXT;
include SUBST_PBL_CONST  ${M3MODEL}/MCIP/src/icl/icl/CONST_pbl.EXT;
```

```
// MCIP parameters
include SUBST_MPARAM      $M3MODEL/MCIP/src/icl/icl/MCIPPARM.EXT;
include SUBST_MCMMN      $M3MODEL/MCIP/src/icl/icl/MCIPCOM.EXT;
include SUBST_MGOUT      $M3MODEL/MCIP/src/icl/icl/GROUTCOM.EXT;
include SUBST_MCOUT      $M3MODEL/MCIP/src/icl/icl/MCOUTCOM.EXT;
include SUBST_MDOUT      $M3MODEL/MCIP/src/icl/icl/MDOUTCOM.EXT;
include SUBST_LRADM      $M3MODEL/MCIP/src/icl/icl/LRADMDAT.EXT;

////////////////////////////////////

// the mcip driver class
module mcip development;

// the landuse class
module m3radm development;

// the input class
module m3 development;

// the met3d class
module m3sup development;

// the pbl class
module pblpkg development;

// the drydep class
module radmdd development;

// the cloud class
module radmkuo development;

// the util class
module util development;

// the output class
module stnd development;
```

Appendix 12D Sample MCIP Run Script

```

#!/bin/csh -f

# RCS file, release, date & time of last delta, author, state, [and locker]
# $Header: /project/work/rep/MCIP/src/sunOS5/sun_m3_12.q,v 1.1.1.1 1997/10/13 17:38:23 yoj
Exp $

# what(1) key, module and SID; SCCS file; date and time of last delta:
# @(#)sun_m3_12.q 1.2 /project/mod3/MCIP/doc/bldrun/sunOS5/SCCS/s.sun_m3_12.q 19 Jun 1997
08:26:34

# for Sun Sparc 20, UltraSparc 2
# method: sun_m3_12.q >&! sun_m3_12.log &

# QSUB -r sun_m3_12
# QSUB -eo -o /work/you/your_directory/sun_m3.log
# QSUB -lM 8Mw
# QSUB -lT 1800

date; set timestamp; cat sun_m3_12.cfg; echo " "; set echo

setenv M3HOME /home/models3
setenv M3DATA $M3HOME/datasets

#-----
# set executable
#-----
set EXEC = mcip_m3_12

#-----
# set base directory
#-----
#set BASE = /work/you/your_directory
set BASE = $cwd

#-----
# set working directories
#-----
set MCIPDIR = $BASE
set OUTDIR = $cwd

#-----
# set input data directories
#-----
set DATADIR = $M3HOME/datasets/nostudies

#-----

```

```

# (METROW,METCOL,METLAY) is (ROWS, COLS, LAYS) for MM5 data
#-----
setenv METROW 25
setenv METCOL 25
setenv METLAY 15

#-----
# (I0, J0): The left bottom loc. of CTM domain in MET terms
#           In CTM terms, I0 = ROW_OFFSET, J0 = COL_OFFSET
#-----
setenv I0 1
setenv J0 1

#-----
# LUTYPE: Filetype for Landuse data:
#           1: BINARY 13 category directly from TERRAIN
#           2: Preprocessed ASCII 11 category
#           3: Use MM5 internal dominant landuse category
#           4: Use M3 landuse fractions available in GRIDCRO2D
#-----
setenv LUTYPE 4

#-----
# (IOLUSE, JOLUSE): The left bottom loc. of CTM domain in
#                   LAND USE DATA GRID terms
#-----
setenv IOLUSE 1
setenv JOLUSE 1

#-----
# If LCALCPBL is: TRUE,  Recompute PBL values
#                 FALSE, Read PBL values from MM52
#-----
setenv LCALCPBL T

#-----
# If LSLFLUX is:  TRUE,  Use only surface layer similarity
#                 FALSE, Use PBL similarity
#-----
setenv LSLFLUX F

#-----
# If LM3DDEP is:  TRUE,  Use Models-3 D. Dep routine
#                 FALSE, Use RADM D. Dep. routine
#-----
setenv LM3DDEP F

#-----
# If LCALCLD is:  TRUE:  Recompute CLOUD values

```



```

#                 FALSE: Read CLOUD values from MM52
#-----
setenv LCALCCLD T

#-----
# If LSANITY is:  TRUE:  check range of output parameters
#                 FALSE: do not check range of paramters
#-----
setenv LSANITY T

#-----
# JUDATE :  INITIAL JULIAN STUDY DATE (YYDDD)
# HSTRT  :  STARTING HOUR OF JUDATE FOR STUDY
# HTORUN :  NUMBER OF HOURS TO USE FROM MM5
# HTOSKIP:  NUMBER OF HOURS TO SKIP FIRST
#-----
# 88218 00 0 2  ! John's data
# 88216 12 0 49 ! Dave's data
# 88214 12 10 108 ! Daewon's data
setenv JUDATE 88209
setenv HSTRT 00
setenv HTOSKIP 00
setenv HTORUN 25
#setenv HTORUN 108

#-----
# input file linkage
# MM51:  Filename for MM51 datafile
# MM52:  Filename for MM52 datafile (NA if none)
# LU13:  Filename for LU13 datafile (binary from TERRAIN)
#-----
#setenv MM51 $INDIR/MM51_es80
#setenv MM52 $INDIR/MM52_es80
#setenv LU13 $INDIR/LU80
#setenv LUSE $DATADIR/LU11_80
#setenv LUSE /work/bdx/metpp/newmcip/input/LU11_80

#-----
# number of iterations for vertical wind correction
# (Use 0, +/- 1,2,3,..)
#-----
setenv IWIND 0

#-----
# number of deposition layers (default = 1)
# (for layer collapsing, it could be 2, or 3)
#-----
setenv NDEP 1

```

```

#-----
# GRDNAM:  Grid Name (User Defined)
#-----
setenv GRDNAM TUTOR12

#-----
# EXECUTION_ID      (User Defined)
#-----
setenv EXECUTION_ID MCIP_BETA

#-----
# SCENFILE:  file path(User Defined)
#-----
#setenv SCENFILE    $BASE/

#-----
# If IOAPI_CHECK_HEADERS is:  TRUE,  Check the headers
#                               FALSE, Do NOT check headers
#-----
setenv IOAPI_CHECK_HEADERS F
#setenv LOGFILE mcip.log

#-----
# Remove any previously generated output files
#-----
#/bin/rm GRID_* MET_*
#/bin/rm ../output/GRID_* ../output/MET_*

#-----
# Set up input files
#-----

setenv GRID_CRO_2D  $DATADIR'/GRIDCRO2D_TUT12'
setenv GRID_DOT_2D  $DATADIR'/GRIDDOT2D_TUT12'
setenv MET_CRO_2D   $DATADIR'/METCRO2D_TUT12'
setenv MET_CRO_3D   $DATADIR'/METCRO3D_TUT12'
setenv MET_DOT_3D   $DATADIR'/METDOT3D_TUT12'

#-----
# Set up output files
#-----

setenv GRID_BDY_2D_G1 $OUTDIR'/GRIDBDY2D_tut12'
setenv GRID_BDY_3D_G1 $OUTDIR'/GRIDBDY3D_tut12'
setenv GRID_CRO_2D_G1 $OUTDIR'/GRIDCRO2D_tut12'
setenv GRID_CRO_3D_G1 $OUTDIR'/GRIDCRO3D_tut12'
setenv GRID_DOT_2D_G1 $OUTDIR'/GRIDDOT2D_tut12'
setenv MET_BDY_2D_G1  $OUTDIR'/METBDY2D_tut12'
setenv MET_BDY_3D_G1  $OUTDIR'/METBDY3D_tut12'

```

```
setenv MET_CRO_2D_G1 $OUTDIR'/METCRO2D_tut12'  
setenv MET_CRO_3D_G1 $OUTDIR'/METCRO3D_tut12'  
setenv MET_DOT_3D_G1 $OUTDIR'/METDOT3D_tut12'
```

```
#-----  
# Execute MCIP  
#-----  
#cdbx "$EXEC -g -x"; exit  
# ja  
#/opt/SUNWspro/bin/debugger "$MCIPDIR/$EXEC"; exit  
$MCIPDIR/$EXEC  
# ja -cshlt  
  
exit()  
#-----  
# Move output to proper directory  
#-----  
#/bin/mv GRID* ../output1/  
#/bin/mv MET* ../output1/
```